frontiers | Frontiers in Nuclear Engineering

TYPE Review
PUBLISHED 20 January 2025
DOI 10.3389/fnuen.2024.1433247

OPEN ACCESS

EDITED BY
Bernd Grambow,
UMR6457 Laboratoire de Physique Subatomique et des Technologies Associées (SUBATECH), France

REVIEWED BY
Axel Liebscher,
Federal Company for Radioactive Waste Disposal, Germany
Michael Ojovan,
Imperial College London, United Kingdom

*CORRESPONDENCE
Diederik Jacques,
djacques@sckcen.be

This is Part 1 of Report Assessment of the chemical evolution at the disposal cell scale Part 2 link: https://doi.org/10.3389/fnuen.2024.1433257

RECEIVED 15 May 2024
ACCEPTED 01 August 2024
PUBLISHED 20 January 2025

CITATION
Neeft E, Deissmann G and Jacques D (2025) EURAD State-of-the-Art Report: ACED assessment of the chemical evolution at the disposal cell scale—part I—processes at interfaces and evolution at disposal cell scale. *Front. Nucl. Eng.* 3:1433247.
doi: 10.3389/fnuen.2024.1433247

EURAD State-of-the-Art Report: ACED assessment of the chemical evolution at the disposal cell scale—part I—processes at interfaces and evolution at disposal cell scale

Erika Neeft[1], Guido Deissmann[2] and Diederik Jacques[3]*

[1]Central Organisation for Radioactive Waste (COVRA), Nieuwdorp, Netherlands, [2]Forschungszentrum Jülich GmbH, Jülich, Germany, [3]Belgian Nuclear Research Centre (SCK CEN), Mol, Belgium

Within the framework of the European Joint Programme on Radioactive Waste Management, the work package ACED–Assessment of chemical evolution of intermediate level (ILW) and high level (HLW) waste at disposal cell scale–used combined experimental and modelling methods in a multi-scale approach with process integration to improve the long-term modelling and assessment of the chemical evolution at the disposal cell scale. Part I provides the relevance of the assessment of the chemical evolution for safety, performance, and optimization. It further describes the main characteristics of disposal cells for ILW and vitrified HLW waste in European disposal programmes. From that, a number of interfaces between different types of material are identified that are highly relevant for many national disposal programs: glass-steel, steel-concrete, steel-clay, steel-crystalline, concrete-clay, and concrete-crystalline. Based on literature review, the main processes and consequences occurring at these interfaces are described. The key element is the narrative of the evolution at the disposal cell scale based on process understanding. In part II, tools to obtain process understanding–experiments, analogues, modelling–are discussed in detail.

KEYWORDS

radioactive waste disposal, chemical evolution, vitrified waste, cementitious materials, steel, clay, granite

1 Introduction

1.1 Geological disposal of high-level or intermediate-level radioactive waste

The most safe and sustainable option for the end point management of high-level (HLW) and (long-lived) intermediate-level (ILW) radioactive waste is to isolate the waste and contain the radionuclides in a system of engineered barriers and natural barriers. The waste packages are to be emplaced in a deep (several hundreds of meters) repository that is constructed in a stable geological formation (a natural barrier). After closure of this facility, the isolation of the waste and containment of radionuclides is controlled by natural processes (passive safety), i.e., the waste is no longer managed. The depth of the

disposal facility determines the vulnerability of its barriers to climate change. The multiple barriers (see Figure 1) are assumed to be deep enough to neglect climate change for their evolution.

All EU countries need to have a national program to deal with radioactive waste. In general terms, the engineered barrier system consists of a solid waste form in a (backfilled) disposal container that is placed in a sometimes backfilled and/or lined disposal gallery. Several materials coexist in the engineered barrier system such as glass, cementitious materials or bitumen in the waste form, concrete and steel of containers, and cementitious materials or clay (bentonite) as buffer or backfill and concrete or steel as liner material. In addition, different types of host rocks, i.e., the stable geological formation, are envisaged with a clayey or a crystalline type of rock being the most common host rock types in Europe. The geological environment provides isolation of the waste. The effects of climate change in the next million year are included in the depth of the underground facility. For example, surface areas can be covered with ice sheets during ice ages. The erosion potential of streams of melting water associated with the retreat of these ice sheets may be small for crystalline rock due to its hardness but this potential is considered high for clay rock. Clay host formations are therefore below several other geological formations (see Figure 1).

The engineered barriers (see Figure 1) provide containment of the radionuclides in various functions:

- The solid waste form has a very low solubility in order to limit the radionuclide release rates; the solid waste form is in a thin walled container;
- The metal overpack–in which the solid waste form with the container is to be encapsulated - prevents contact between the waste form and groundwater for thousands till hundreds of thousands years after closure of the disposal facility;
- The buffer or backfill can provide beneficial physical and chemical conditions to the overpack to limit corrosion of the overpack.

These functions are just a few examples of safety functions of the engineered barriers and described here in order to introduce the reader into the multiple barrier system. Each barrier can also have multiple functions that contribute to the containment of radionuclides (Chapman and Hooper, 2012). The engineered barriers to contain radionuclides can be different for ILW and HLW. Some safety functions can be time-dependent. The required time depends on the radiotoxicity of the waste. This radiotoxicity decreases by decay of radionuclides. Figure 2 shows that it takes about 25,000 years for vitrified HLW to decrease to the same radiotoxicity as the amount of uranium ore that was originally used to manufacture nuclear fuel.

The americium isotopes are mainly responsible for the radiotoxicity of vitrified HLW and heat generation in the long-term. The ultimate goal of a geological disposal system is long-term (post-closure) safety for people and the environment. To assess the long-term safety and performance, analyses at the disposal system scale as a whole including the engineered barriers, the host rock and the geological environment are required. To scientifically underpin such analysis, many additional aspects are studied experimentally and numerically, ranging from the repository scale (or disposal facility, including mainly engineered barriers) to more detailed scales (e.g., interfaces between materials).

A particular scale between repository scale and detailed scale is the scale that represents the waste packages, the gallery and a few meters of the host rock around the gallery. This scale is called the disposal cell scale in this review paper. The disposal cell scale consists of several different types of materials with different geochemical properties. As such, all these materials will evolve geochemically and also physical and mechanical properties will vary over long time scales. These alterations are driven by chemical gradients between the materials and disequilibrium with their environment. The performance of the engineered barriers will change by these chemical alterations and associated changes in physical and mechanical properties. Ultimately, the prevailing time-dependent geochemical, physical and mechanical conditions of the waste form, other engineered barriers and the host rock will influence radionuclide release, fate and transport.

1.2 The chemical evolution at the disposal cell scale

1.2.1 Why is the chemical evolution relevant?

The chemical evolution at the disposal cell scale, even it is only a part of the repository, forms a highly relevant input to the assessment of many safety- and performance-related aspects such as waste form degradation, material alteration, source term evolution (radionuclide release), and radionuclide speciation, fate, and transport but also to scenarios describing the evolution of the repository. Important aspects to which a scientific-based description of chemical changes contributes are, amongst others:

- Waste package (for HLW consisting of a container/canister encapsulated in an overpack is embedded in a buffer) evolution and integrity–The geochemical conditions in the materials of waste packages and the interactions at different interfaces within a waste package are an important factor in the durability, performance and life time assessment of waste packages. Crucial is the impact of these geochemical transformations on the evolution of porosity (including clogging phenomena), as porosity represents the primary affected physical variable determining radionuclide migration and fluid flow. In addition, elements in the metallic and cementitious components in waste packages will have an influence on the geochemical conditions in other components.
- Radionuclide release–The geochemical evolution influences degradation/corrosion of different waste immobilisation matrices (vitrified waste, cemented waste) and metallic wastes as function of the evolving conditions imposed by different materials and geometrical features. Experimental and modelling studies concerning waste form alteration provide essential information on the mechanisms and kinetics of radionuclide release.
- Near field evolution–Specifically, feedbacks between the transport of reactive species and/or other drivers for geochemical alterations are important. The geochemical evolution is inevitable linked with the Thermal-Hydraulic-Mechanical (THM) processes at the disposal cell scale.

This is relevant with respect to safety assessments, implementation and optimization (specifically within national programs):

- The assessment and quantification of containment of the radionuclides which is one of the principal objectives of a multiple barrier system in a repository, obtained via attributing various safety functions to the system, structures and components (SSCs). It is to be expected that, at least for some SSCs, geochemical changes will be relevant, i.e., they affect a given safety function of a SSC in its foreseen timeframe. Differences in chemical conditions between different materials induce diffusive transport, changing geochemical conditions and, most likely, geochemical alterations of the barriers. These alterations may influence the lifetime of a barrier, including the waste package, and change the mobility of radionuclides as they effect solubility and sorption.
- The quantification of safety margins and the decrease in conservatism and uncertainty.
- To definition of the requirements for materials, including the robustness of allowable tolerances. The specifications, including dimensioning, of the packages and disposal cell(s) can be influenced based on the calculations of the geochemical evolution. The geochemical evolution can be one of the factors for defining acceptance criteria for varying wastes and stabilization materials.

1.2.2 How to assess the geochemical evolution of a disposal cell

Crucial elements to assess the geochemical evolution are a good scientific understanding of processes that will influence the chemical evolution and tools to extrapolate the understanding to relevant time scales. Understanding is mostly based on observations obtained from dedicated experiments (mostly limited in time and scale) or natural analogues (can give information over long time scales). Extrapolation is based on numerical modelling tools. The challenges to assess the chemical evolution at the disposal cell scale are how scientific understanding and knowledge on individual materials or processes and the conceptual and mathematical models can be integrated at a disposal cell scale, and how these complex integrated models can be simplified to obtain model descriptions with a complexity appropriate for a given application in the safety and performance assessments. Crucial points are thus to:

- describe which processes are influencing the chemical evolution at the disposal cell scale (narrative of chemical evolution);
- understand the chemical processes within and at the interface between materials;
- integrate the scientific knowledge into conceptual and mathematical models for simulating the long-term large-scale evolution;
- simplify–abstract these models to allow sensitivity and uncertainty calculations or optimisation.

Furthermore, as processes and features on small scales may affect the chemical evolution at a disposal cell scale, studies at different scales are required. It is important that scales here do not refer to its meaning in some multi-scale studies looking at molecular, pore-, meso- and macro-scale, but to looking at less or more different materials in less or more complex geometries. Assessing the geochemical evolution could study following scales:

- **Interface scale:** The focus of the interface scale is on two materials in contact with each other to obtain information on the geochemical evolution close to an interface in terms of changes in aqueous composition and alteration in solid phase composition at, typically, a detailed small scale.
- **Waste package scale:** The key feature of the waste package scale is that several materials are present in a specific configuration and are interacting with each other under chemical and possible other gradients. Here, interactions with host rocks or other waste packages are not considered. For HLW disposal cells, in which the chemical evolution of the waste package is governed to a very high degree by the integrity of the canister, mainly the small-scale evolution of the system glass, iron corrosion products and part of adjacent backfill material (clay/cement) after canister breaching is of interest to assess the evolution of the glass and cement alteration zones when the materials are in contact via a perforated stainless steel barrier.
- **Disposal cell scale:** The disposal cell scale consists of waste packages and their immediate surrounding being other waste packages or other near field components including the host rock.

To develop integrated models for assessing the chemical evolution at different scales, two main methodological routes are possible being process integration and model abstraction:

- **Process integration:** This concerns the integration of scientific knowledge, conceptual and mathematical models on individual or selected processes into an integrated, usually simplified, model. The integration will increase the understanding of the system behaviour and evolution, helps identifying key processes or parameters, or enables transfer of information from a more detailed scale to a larger scale.
- **Systematic abstraction:** Model complexity is reduced in a systematic way such that (i) an acceptable description of the chemical evolution is preserved during model abstraction, and/or (ii) differences in some key variables of the chemical evolution can be described qualitatively and/or quantitatively. This leads to a better representation of the expected evolution in safety or performance models, thus helping in reducing and quantifying conservatism and uncertainty and thus directly impacts the definition of safety margins.

1.3 Objectives

This two-part overview focusses on process integration and provide the state-of-the-art of building blocks of the geochemical

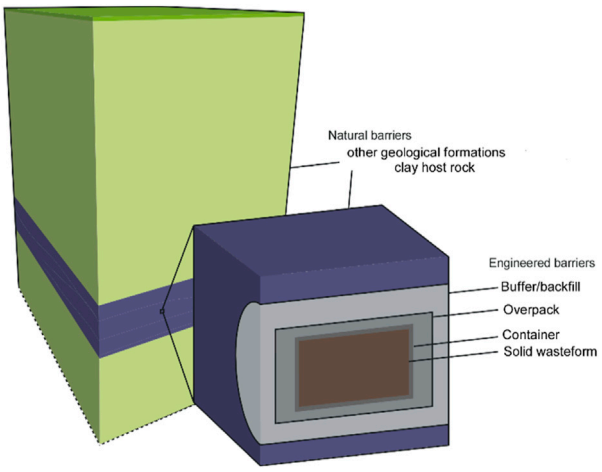

FIGURE 1
The general concept of the multibarrier system for geological disposal of radioactive waste—the waste package (solid waste form, container, overpack), the host rock (blue) and other geological formations (green) (adapted from Chapman and Hooper, 2012).

assessment. The overview focuses solely on waste placed in deep geological repositories with consideration of following waste forms:

- For HLW, only vitrified waste forms, typically originating from reprocessing activities, are considered. This overview does not examine disposal cells with waste packages containing spent fuel.
- For ILW, the focus is on waste that is conditioned in a cementitious matrix. Cementitious waste forms are common conditioning material in many countries (IAEA, 2013; Abdel Rahman et al., 2014; Ojovan and Lee, 2014; Rahman and Ojovan, 2021). However, there exists a large variety of other conditioning matrices including for example, bitumen (Millot et al., 2024), but they are outside the scope of this study. Intermediate level waste have much more origins compared to HLW resulting in a larger variety of waste types. The overview considers here only waste with organics and metallic elements that have been processed with cementitious materials.

The first part describes the various components and characteristics of a disposal cell commonly found in the main European programs (section 2). State-of-the-art scientific knowledge on processes occurring on common interfaces in most disposal cells are discussed in detail in section 3. Based on the information presented in section 2, the following interfaces have been selected: glass-steel, cement/mortar-crystalline, cement/concrete-clay, steel/iron-bentonite, steel/iron-cement/concrete, and steel/iron-crystalline. Based on this scientific understanding, a description is given in section 4 of the space-time evolution of different generic disposal cells. The second part of this overview focusses on how the scientific understanding of processes at different spatial and temporal scales can be obtained and how quantitative assessments can be made. Information is given on experimental studies at laboratory scale or in-situ, on available natural or archaeological analogues, and on coupled reactive transport models for quantitative assessment.

2 Main characteristics of European HLW and ILW disposal cells

The conceptualisations of the chemical evolutions require the radiological, chemical, and physical properties of the engineered barriers and natural barriers and the potential microbial activity in these barriers. The radiological properties determine the classification of waste.

- HLW has a very high activity content and also generates heat in such amounts that special measures for sufficient heat dissipation need to be made during storage and disposal of this waste. Examples of HLW are vitrified waste forms from the reprocessing of spent fuel and spent nuclear fuel. As described in section 1.3, only vitrified HLW is considered in this paper.
- HLW and ILW both require shielding during transport and storage of this waste, but no additional measures for heat dissipation need to be made for ILW. An example of ILW are the compacted metallic parts of spent fuel that arise during the reprocessing process of spent fuel. Also sources with alpha-emitting radionuclides with smaller half-lives than naturally occurring uranium isotopes such as plutonium and americium can be ILW.

HLW and long-lived ILW are disposed of at larger depth than LLW and short-lived ILW. Usually, the depth of the disposal facility is so large that reducing chemical conditions are present in the virgin clayey and crystalline host rock. The diversity in the chemical composition of the waste forms generally decreases with increasing radioactivity of the waste:

- HLW: Spent fuel has currently always uranium oxide as a waste matrix and the HLW arising from reprocessing of this fuel results into a vitrified waste form. The chemical alteration rate of these waste forms is very small and generally well understood for example, by studying natural analogues or modelling (see Part II, Deissmann et al. (2024)). These analogues do however not have complementary materials such as steel that might alter the chemical process on a small scale.
- ILW: The chemical nature of the waste considered in this review is metallic or organic. Radiation resistant resins (organic) are used to absorb radionuclides from water used in operation and maintenance of nuclear reactors. The volume of waste is reduced since the radionuclides are concentrated in these resins and the cleaned water can be re-used. Metallic waste can be compacted Zircaloy hulls from spent nuclear power fuel but also stainless steel that has been neutron irradiated in nuclear plants. There are several reasons why these metallic materials (Zircaloy and stainless steel) have been chosen to use in nuclear plants and one of them is their high corrosion resistance. The chemical alteration rate associated to both resins and these metallic materials can also be very small but only for resins evidence from natural analogues are available.
- LLW: The chemical nature of the waste can also be metallic and organic, but the diversity in organic material arising from nuclear

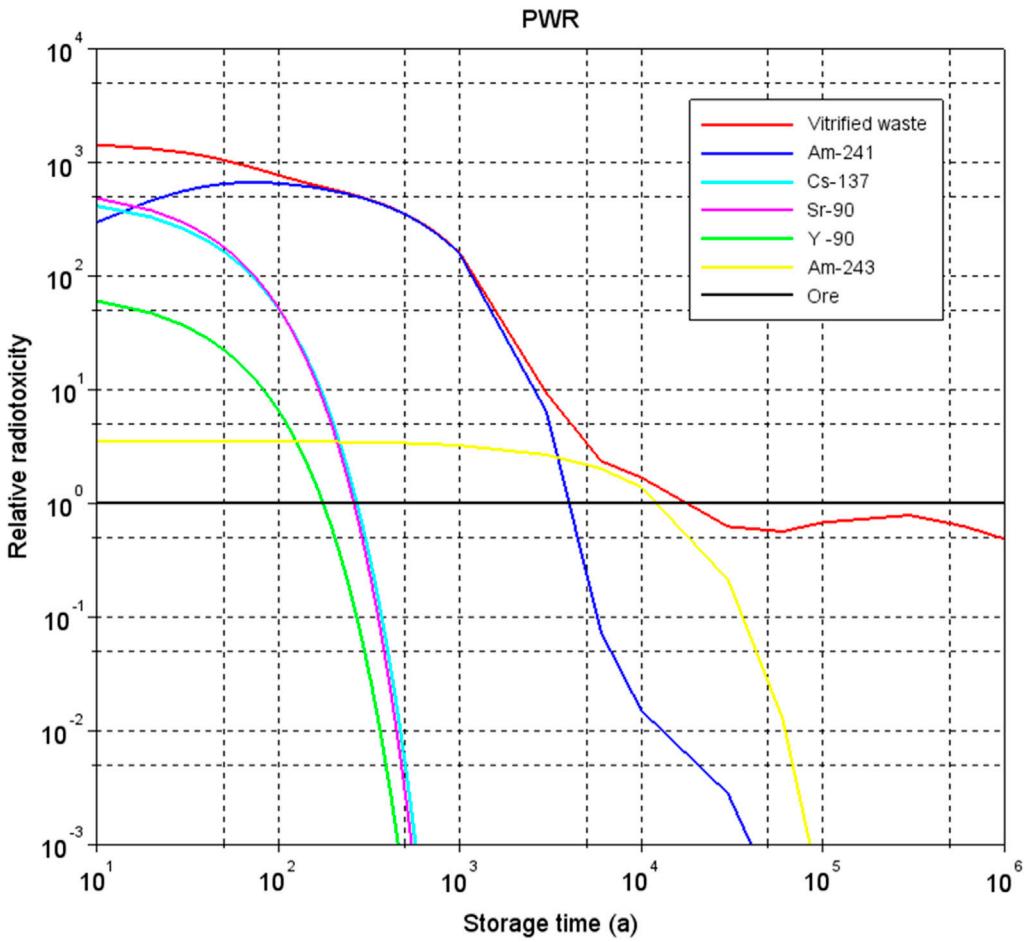

FIGURE 2
Relative radiotoxicity of vitrified HLW from reprocessing of spent nuclear power fuel from a pressurized water reactor (PWR) when all radionuclides are released from the glass and the uranium ore, radiotoxicity of uranium ore to manufacture fuel is here set as 1. Calculations performed by Professor Jan Leen Kloosterman from Delft University of Technology in the Netherlands in 2017.

power plants is generally larger for LLW than for ILW. Exceptions are the waste arisings from research and reprocessing plant dismantling operations; a similar diversity in the chemical nature of the waste forms may be for LLW and ILW. Everything that people use in ordinary life such as cloths, paper (tissues), rubber, steel, aluminium can also become contaminated with radionuclides and become waste. Also LLW is often conditioned into cementitious materials. Substantiation of the chemical alteration process and the prediction of the chemical alteration rate of some specific waste forms is still investigated since degradation of these waste forms can enhance the transport of radionuclides into our living environment.

The waste forms for HLW and ILW (glass, metal) have such a low porosity that the presence of the pores within these waste forms is neglected in the chemical evolution. The alteration rate of these waste forms depends on the physical properties that interface these waste forms. These properties having an impact on the chemical evolution at disposal cell scale are the porosity, the pore size distribution and the presence of cracks in the engineered materials and host rocks. These two properties and the water content in the pores and cracks of these materials determine the potential exchange of chemical species and microbial activity. The potential diffusional pathways of dissolved species in materials increase with increasing saturation degree. The interfacing materials are not in equilibrium and a new precipitated material between the interfacing materials may arise. This new material can also have physical properties that impact the chemical evolution.

Microbial activity enhances chemical processes, for example, the microbially induced corrosion rate of steel is larger than the pure chemically induced steel corrosion rate. Microbes are always present but there is no microbial activity if these microbes are in a dormant phase. The microbial activity depends on various factors that can be generalized (see Figure 3) and these factors need to be taken into account in the selection of (the combination of materials for) the engineered barriers. Preferably, microbial activity is minimized by design, especially for HLW, in order to be able to reduce the uncertainty in the prediction of the chemical evolution. There are also very different types of microbes but the alteration of a material may require specific microbes. Microbes require organic matter as a food source but also other nutrients to build their DNA

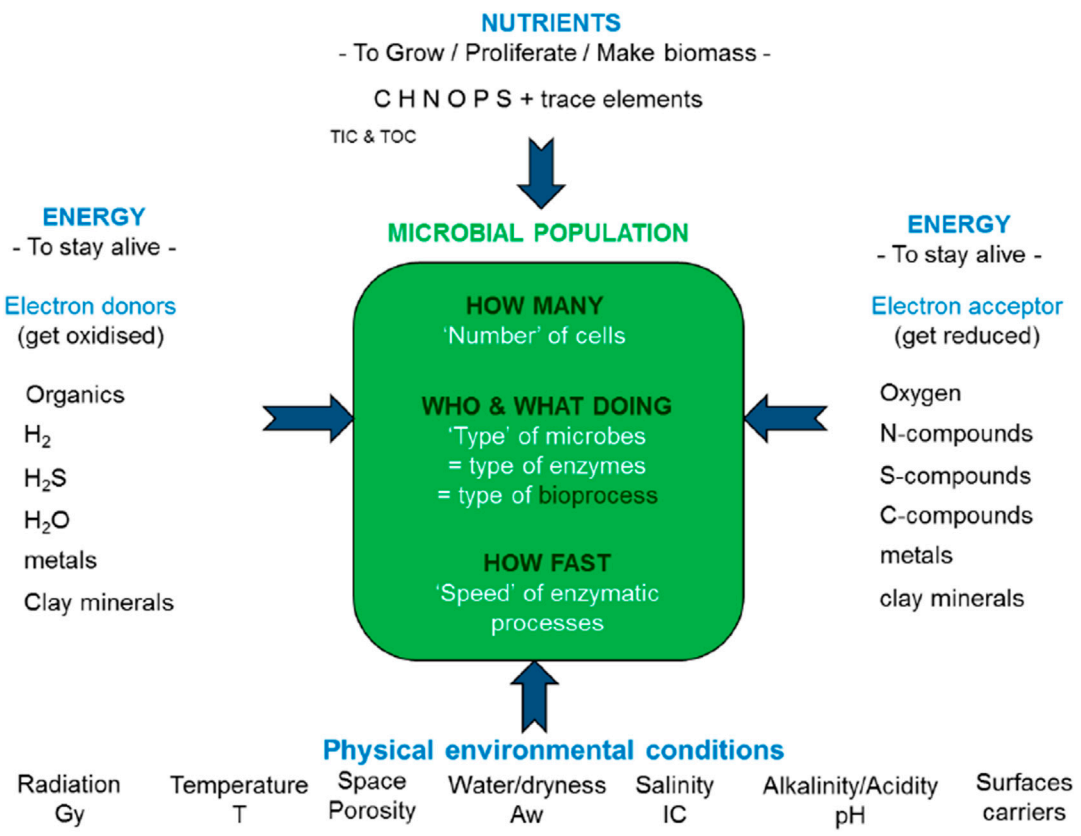

FIGURE 3
Generalized overview of restricting and enhancing parameters for microbial life (Wouters et al., 2016).

and proteins. Organic matter can be present in the waste forms of ILW but not in a HLW waste form.

Radiation There is a wide diversity of values considering the radiation resistance of microbes. It is the hydroxyl radical that is formed during irradiation of water and water containing media that is the most damaging agent since this radical oxidises DNA, RNA, proteins and lipids (Brown, 2013). The upper limit of the radiation dose of microbes is 30 kGy (Wouters et al., 2016). For example, microbes that can enhance corrosion of steel and have been added to steel lose their activity after 100 days irradiation at dose rates of 2.1 Gy per hour, i.e. 5 kGy (Bruhn et al., 2009). Figure 8 shows the expected radiation dose rates for steel interfacing buffers (see Section 4.1). Some elements determining the activity of the microbes are shortly described below.

Temperature The diversity in the denaturation resistance of microbes is large and can range from −20°C till 122°C (Wouters et al., 2016). The optimal activity of sulphate reducing bacteria[1], i.e., bacteria mainly responsible for microbial induced corrosion, is 28°C–30°C, but these bacteria can tolerate a temperature as high as 75°C (Virpiranta et al., 2019). Buffers usually have a limit of 100°C (see Section 2.1.3.3).

Space/porosity A microbial cell should have a certain minimal size in order to harbour all essential proteins and nucleic acids to maintain life. The range in diameters of microbes is between 0.2 µm and 2 µm. The connecting pore throats in clayey host rocks such as Boom Clay are smaller than 10–50 nm. The microbial activity is restricted in space in these clayey rocks not only because they are not mobile but also because the transport of electron donors and acceptors and carbon sources is very slow (Wouters et al., 2016). The best natural analogue to illustrate negligible microbial activity in clays is the Dunarobbe forest in Italy in which 2 million year old trees had been preserved in compacted clay. These trees were protected against microbial degradation and therefore had cellulose contents similar to present-day wood (Lombardi and Valentini, 1996; De Putter et al., 1997)). Manufactured concrete can also have pores with a maximum in diameter till 50 nm but that requires very well engineering. A maximum in 100 nm (0.1 µm) is not uncommon for concrete by which it can also be assumed that the potential microbial activity is limited due to space restriction in concrete. Dormant microbes can become activated when cracks in clayey rock or concrete appear.

Water/dryness Most microbes require water activities larger than 0.9 in order to be active (Swanson et al., 2018), i.e., a relative humidity of 90%. However, there is also a wide diversity in the desiccation resistance of microbes. Sulphate reducing bacteria have been experimentally

1 The presence of FeS is attributed to the presence of sulphate reducing bacteria in soils and although these bacteria are regarded as harmful to steel, archaeological analogues do not confirm this behaviour (Dillmann et al., 2014).

examined to require a minimum in water activity of 0.96 (Stroes-Gascoyne and West, 1997; Stroes-Gascoyne et al., 2007). Lower relative humidities can be present during storage of the waste, in the operational phase of the disposal facility and early in the post-closure phase for HLW disposal cells, when the waste emits heat and drying occurs.

Salinity Salinity has a similar effect as drying, i.e., the water activity is reduced with increasing salinity. A water activity of 0.90 is equal to ≈2.7 M NaCl solution or ≈1.4 M $MgCl_2$ solution (Swanson et al., 2018).

pH Microbial life in high pH environments requires a mechanism to keep a neutral cellular life and a proton motive force across the cell membrane to preserve proteins and produce adenosine triphosphate (ATP), a carrier of energy. The concentration of H^+ is very small at high pH and an upper limit of 12 is generally assumed, although microbial communities have been described also to grow up till a pH of 13.2 (Wouters et al., 2016). These microbes have been found in a lake in which steel slag had been dumped (Roadcap et al., 2006).

Although the HLW and ILW disposal cells have country or program-specific features and specifications, it is possible to group them into different classes with respect to the different components, structures, interfaces etc. The following sections describe this grouping and the main characteristics of the HLW and ILW disposal cells in European countries/programs. The section starts with the characteristics of the waste and the engineered barriers. Construction and operation of the disposal facility can have an impact on the clayey and crystalline host rock and affect both ILW and HLW disposal cells and are described at the end of this section.

2.1 HLW disposal cells

2.1.1 Characteristics of vitrified HLW

Vitrified HLW results from the reprocessing of spent nuclear fuel from which uranium and plutonium have been extracted. The pretreated High-Level Liquid Waste (HLLW) is melted with a glass frit and poured into a stainless steel container (Baehr, 1989). This waste processing ensures that the radionuclides are homogeneously distributed in a borosilicate glass matrix. This matrix contains traces of plutonium and uranium, other actinides that have not been extracted such as americium and fission products. These vitrified waste products have been made in Sellafield (UK) and are still being made in La Hague (France). The largest amount comes from France and therefore frequently, the French abbreviation for this waste product is used: Conteneur Standard de Déchets vitrifiés, CSD-V. The vitrified waste product is made in two batches with each of 200 kg of molten glass (Moncouyoux et al., 1991) – typical dimensions of CSD-V are found in CEA (2009). The thermal power as a function of time and other properties of a CSD-V with a high actinide content can be found in the (Supplementary Materials Section 1). Vitrified waste was also produced in a few other countries United Kingdom and Belgium (Thorpe et al., 2021; Ojovan and Yudintsev, 2023).

The number of cracks that are present within this waste form after pouring into the canister and subsequent cooling may be limited, but a tomographic or X-ray image of a canister with processed waste to deduce the cracks within the waste form has not been found. The experimental studies performed in the nineties for the 3rd framework (RTD) programme to characterize radioactive waste forms have demonstrated that it is possible to produce homogeneous glass blocks by applying appropriate cooling procedures even with non-radioactive simulate HLW, as has been observed with tomograms (Reimers, 1992). Full-scale tests with non-radioactive simulants without appropriate cooling procedures show large glass shrinkage cavities (Moncouyoux et al., 1991) as the inner part solidifies last. Rapid cooling also generates a large number of circumferential cracks due to the stress associated with the large thermal gradient (Reimers, 1992). The temperature of the waste will remain several hundreds of degrees after the vitrified waste form is transferred to the storage facility. The size of the glass specimen and cooling rate are essential in order to determine which experimental results are representative for disposal of waste. The 'so-called' reference blocks with a controlled cooling rate of 2.8°C per hour (Moncouyoux et al., 1991) may therefore provide the best estimate for the determination of a cracking factor but the time at which the package is removed from the casting station at which molten vitrified waste is poured in the canister is an essential feature. This cracking factor (or fracturation factor) is a parameter that is used in performance assessment studies to determine the alteration/dissolution rate of glass and radionuclide release rate. The cracking factor can be best estimated from the actual measured surface area. For the block with the controlled cooling rate of 2.8°C per hour: the outer surface of a glass block would be 1.781 m^2, assuming the surfaces at top and bottom to be flat. After the reference block of 391 kg was taken out of the canister, it was broken into 11 pieces: one weighing 250 kg, another 80 kg and nine pieces with a weight of less than 10 kg. The outer surface was 2.787 m^2 as measured by wrapping all the faces in aluminum foil. The cracking factor then becomes 1.56. Even if the 400 kg poured glass was removed 2.5 h after pouring and left to naturally cooling, the cracking factor only increases till less than one order in magnitude: 14.5 (Moncouyoux et al., 1991). Please note that this cracking factor is smaller than average in cracking factor of 40 obtained from leaching experiments with another experiment with inactive glass blocks at full-scale. This factor is reduced during the leaching experiment until an average in cracking factor of 5 due to alteration of glass by which the small cracks were closed (Ribet et al., 2009).

The presence of radionuclides within glass has some beneficial characteristics to prevent or heal cracks. The thermal power source and the radioactivity work as glass network modifier by producing ionization rays. Cooling (passive) systems are needed in order to store these vitrified waste forms. The thermal power is so large that it can take 65 years in order to have a sufficient heat loss for disposal. The α-decay of actinides present in waste diminishes slightly the glass density and its mechanical properties and appreciably improves, especially its resistance to cracking (Ribet et al., 2009). The evolving helium diffuses through the glass at such a high speed at room temperature that helium implantation below room temperature is necessary to make helium observations within glass using neutron activation analysis (Chamssedine et al., 2010). Consequently, defects generated by stopping the highly energetic alpha particles within the waste form are annealed at room temperature by which helium trapping by defects within the waste form glass does not occur at temperature conditions representative for storage and disposal.

2.1.2 Metal overpack

For disposal, the stainless steel canister with vitrified waste is envisaged to be put in a carbon steel overpack (see Figure 1) in many national programmes (e.g., France, Switzerland, Belgium and Netherlands) (Neeft et al., 2020). This steel has predictable corrosion kinetics; general corrosion is considered the predominant mechanism rather than localised corrosion processes such as pitting. In all programmes, the safety function of the overpack is to prevent contact between the vitrified waste form and groundwater but the required periods for this physical containment are different. These differences are caused by the used safety concepts.

- In the French concept, there should be no contact between pore water and vitrified waste until the temperature of the core of the vitrified waste form is lower than a certain temperature. This temperature is determined by the advances in knowledge about the behaviour of vitrified waste forms and radionuclides in solution. The required period for containment is envisaged to be less than 500 years.
- The temperature of the host rock is considered as a criterion in other programmes for this physical containment, for example, in the Belgian and Dutch programme. The heat dissipation to the host rock should be declined to negligible. If that is achieved, radionuclide migration data obtained in laboratory experiments performed at room temperature or the radionuclide migration data extracted from the site, can be used to calculate the transport of the released radionuclides in the clay formation. The required period for integrity of the steel container and carbon steel overpack is envisaged to be more than 1,000 years.

The Czech and Spanish programmes do not consider vitrified HLW but they do consider these steel overpacks for physical containment of spent nuclear power fuel and spent fuel also generates heat like vitrified waste Such programmes therefore also contributed to understanding of chemical evolution under temperature gradients as long as overpacks are intact. This steel overpack is in contact with an engineered buffer in their programmes and has the same purpose as disposal cells with vitrified waste Many other programmes also envisage an overpack interfacing an engineered buffer (Neeft et al., 2020).

2.1.3 Characteristics of disposal cells with buffer materials

Bentonite and concrete are envisaged as interfacing materials for the carbon steel overpack. Bentonite buffers are considered in the Czech, English, German, Spanish and Swiss programmes and concrete buffers are considered in Belgian and Dutch programmes. These engineered buffers are carefully designed to meet specific criteria. The work performed on bentonite in the Swedish and Finnish programmes has been carefully looked at to extract its characteristics.The bentonite interfaces copper in these Scandinavian programmes instead of steel. In this paper, interfacial reactions between copper and bentonite are not considered, only those between bentonite (clay) and steel.

2.1.3.1 Characteristics of bentonite buffer

Bentonite has a high smectite content of which montmorillonite is the most abundant mineral. These minerals can swell and therefore induce a large impact on the distribution in size of pores, its consequent connecting pore throats and hydraulic conductivity. The smectite content can be 88 wt% as used in the Czech and 75 wt% in the Swiss programme, in which smectite is further specified as Na-montmorillonite in Wyoming MX-80 bentonite (Müller-Vonmoos and Kahr, 1983). Wyoming MX-80 bentonite is also used in the Swedish programme (Wanner et al., 1983). Please note that these clay contents are higher than the clay contents of around 60 wt% in any clay host rock considered in the national programmes (see Supplementary Materials). The bentonite is compacted to an optimum in density and its resulting swelling pressure. The density and swelling pressure should be high enough to reduce microbial activity and resulting swelling pressure, prevent movement (sinking) of the overpack, and limit advective transport (Hedin et al., 2011). There is much evidence indicating that microbial activity will not occur in compacted bentonite with a dry density exceeding 1,600 kg/m^3, either because of low water activity or because of the effect of swelling pressures in excess of 2 MPa on the physiology of the microbes (Johnson and King, 2008). There are a number of interface locations such as placement gaps, contact regions with materials of different densities and contact points with water carrying fractures in the crystalline rock by which the dry density can become smaller than 1,600 kg/m^3 upon expansion of compacted bentonite into a void. The reduction in dry density can stimulate or restore the cultivability of indigenous microbes which would increase the possibility for in-situ microbial activity. Reductions in dry density should therefore be minimized or eliminated by adequate design (Stroes-Gascoyne et al., 2011). The density and resulting swelling pressure should also be low enough to prevent damage to the metal overpack and host rock (Hedin et al., 2011).

Bentonite buffers are usually ‘dry’ emplaced. Dry can mean for bentonite buffers a water content of 17 wt% (e.g., Johannesson et al. (2020) or 10% (e.g;, Atabek et al., 1991). The saturation of these dry blocks with which the buffer is constructed is between 50%–60% (Johnson and King, 2008). The pore water chemistry of this engineered barrier is therefore determined by the inflow of host rock water and establishment of equilibria between dissolved species present in this host rock water and minerals present in bentonite, i.e., there is no initial pore water chemistry as in concrete.

2.1.3.2 Characteristics of concrete

Cementitious materials, a material omnipresent in many disposal systems (Jacques et al., 2021a), are a chemically reactive material in many environments and could be subject to several chemical ageing and processes (Jacques et al., 2021b; Rahman and Ojovan, 2021). Therefore, the characteristics of concrete are of uttermost importance for its long-term chemical durability. The required strength of concrete, environmental class, fluidity during pouring and distribution in size of aggregates have all been defined before fabrication of any cementitious material. The strength of concrete is determined by the strength of aggregates and the attachment of the aggregates with the cementitious phase in concrete. Choices in concrete recipe and type of mixing of ingredients follow from these requirements and available knowledge. This available

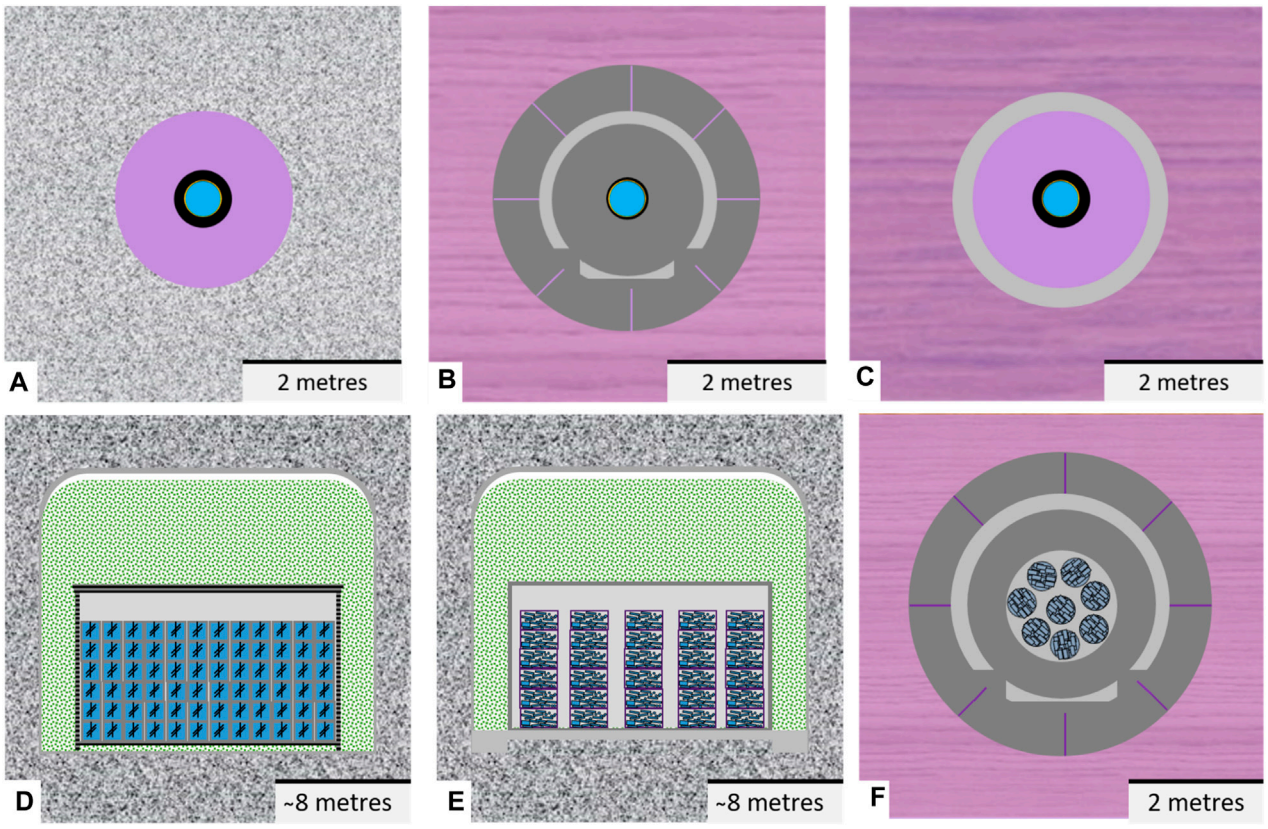

FIGURE 4
(Top) Abstracted disposal cells containing vitrified HLW considered in Europe for the host rocks: crystalline **(A)**, poorly indurated clay **(B)** and indurated clay **(C)**. Blue = vitrified HLW, black = steel overpack, bentonite (purple) or concrete buffer (grey) surrounds the overpack, grout = light grey and purple both clay host rocks. (Bottom) Abstracted disposal cells containing cemented ILW considered in Europe for the host rocks: crystalline **(D, E)** and poorly indurated clay **(F)**. Blue = ILW or cemented ILW, black = steel, green = crushed crystalline rocks, grey = concrete, light grey = mortar or shotcrete and purple = poorly indurated clay.

knowledge is integrated in standards for civil engineering. These standards are regularly updated. The European standard EN 206 divides the potential degradation of concrete or the reinforcement inside the concrete into 18 exposure classes. There are three exposure classes for ranges in dissolved sulphate content, pH, amount of dissolved CO_2, dissolved ammonium and magnesium content. All dissolved species are also present in the pore water of clay and crystalline host rock except for dissolved ammonium, which is characteristic for polluted groundwater. Polluted groundwater may not be relevant for disposal studies. The pH of concrete pore water is high after fabrication of concrete, around 13 (see Supplementary Material Section 2). The ingress of CO_2 can lower the pH of the concrete pore water, which can be detrimental to the steel used for the reinforcement, i.e., ingress of CO_2 may not be detrimental to concrete itself. The resulting calcite precipitation within concrete results in a porosity reduction that can decrease the permeability of concrete. The environmental class determines many requirements. For example, concrete being exposed to the highest magnesium concentration (XA3) requires:

- the smallest water to cement ratio since this ratio has an impact on the permeability of concrete and thereby ingress rate of dissolved magnesium. A small permeability is characteristic for a concrete with a high strength and has the smallest ratio in water to cement;
- the largest cement content in order to buffer the ingress of magnesium;

Superplasticisers are used to achieve a well mixing and processability of cementitious fluid with a reduced water content. There are chemical alterations in which the mechanical strength of fabricated concrete is too early too much decreased in the operational phase of the disposal facility or in the post-closure phase of the disposal system. These alterations can be prevented with a proper choice in cement, content of cement in concrete and a proper choice in combination of cement and aggregates. For example, sulphate resistant cement is used to prevent Delayed Ettringite Formation (DEF). DEF can be caused by:

- an internal sulphate attack, when the temperature during hydration is too high;
- an external sulphate attack by ingress of dissolved sulphate species reacting with tri calcium aluminate (C_3A).

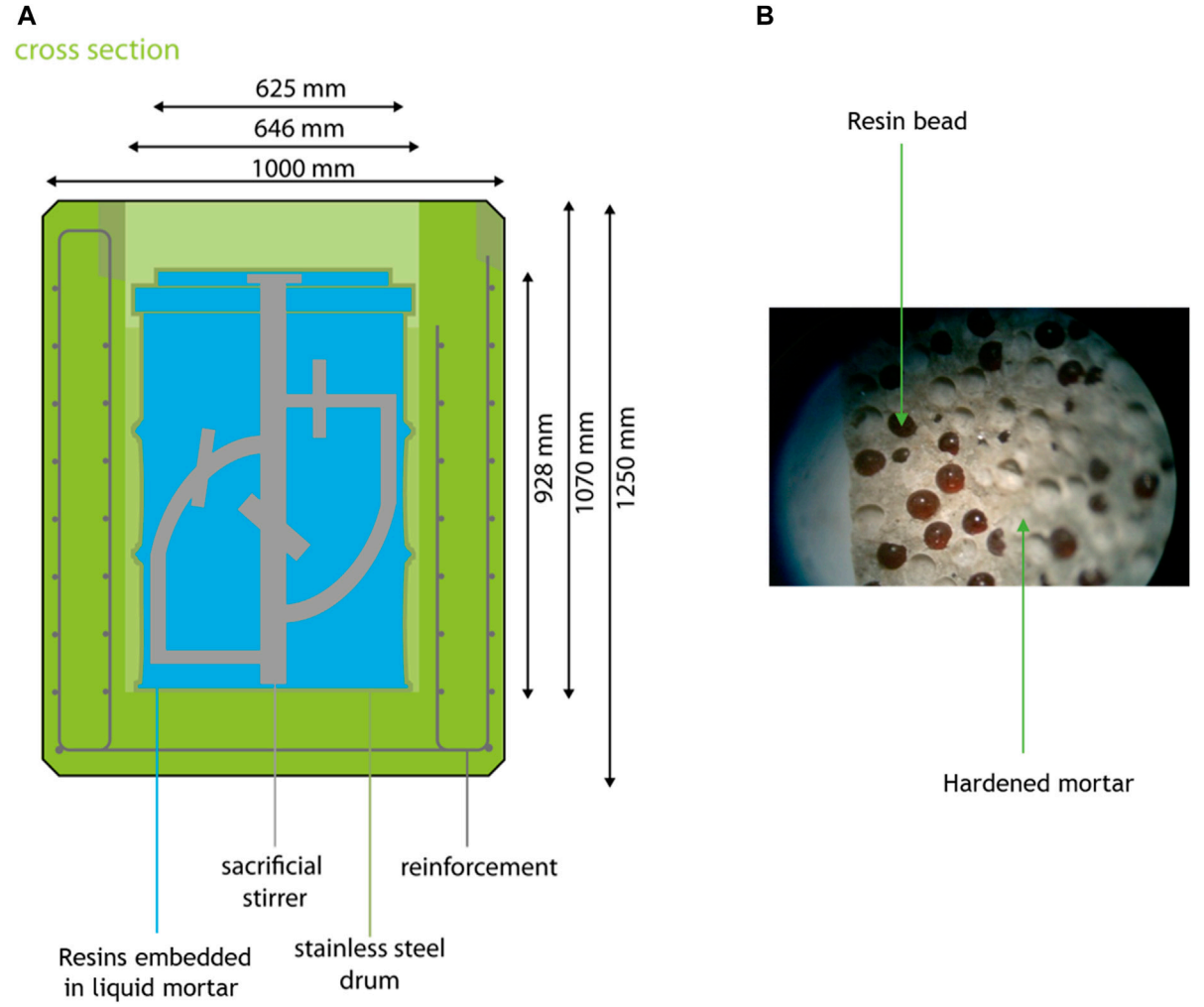

FIGURE 5
(A) Schematics of processed resins (adapted from Verhoef et al. (2016)). Magnetite aggregates are used for the fabrication of the concrete in reinforced concrete container in order to contribute to shielding. **(B)** Detail with the resin beads embedded in a cementitious matrix.

The hardened cement paste between the aggregates is cracked when DEF occurs. Both cases of DEF can be prevented by limiting the C_3A concentration. A Portland cement blended with microsilica, fly ash or slag also reduces the temperature for hydration by which internal sulphate attack is prevented. These blended cements can be called sulphate resistant cements for example, CEM III/B.

Another example of a proper choice to prevent chemical alteration in which the mechanical strength of fabricated concrete is too early too much decreased is using calcite or quartz aggregates instead of aggregates with silica polymorphs that have a higher reactivity with alkalis in the concrete pore water. These silica polymorphs change into silica gels; cracks become present through the reactive siliceous aggregates. The use of blended cements also reduces the probability of the alkali silica reaction (ASR) due its low permeability at an ordinary engineering time scale of about 100 years. Concrete made with blended cements are called low-permeability concretes, due to their more refined pore structure compared to concrete made with Portland cement (Atabek et al., 1991; Atkins et al., 1991; Mulcahy et al., 2017). A porosity between 10 and 15 vol% is a good estimate for the concrete buffer.

2.1.3.3 Characteristics of the bentonite buffer and concrete buffer

Both bentonite and concrete buffers have small connecting pore throats by which two beneficial physical conditions are provided for the durability of the carbon steel overpack:

- the transport of dissolved chemical species is dominated by predictable slow diffusional processes;
- microbial activity is limited.

The corrosion of many metals is determined by the solubility of the metal-oxide that is formed, the diffusion of species through this metal-oxide and the concentration of dissolved species near this metal-oxide. In case of carbon steel, the anaerobic corrosion rate is controlled by the formation of magnetite. These dissolved species have a larger diffusional speed in stagnant groundwater than in these buffer materials, by which the removal speed of these dissolved species is larger. The concentration of dissolved species near the metal-oxide can however also be reduced, if the buffer adsorbs the dissolved species. The microbial corrosion rate is usually larger than

the chemical corrosion rate (e.g., Swanton et al. (2015)), but the initiation of microbial corrosion does not take place when the microbial activity is absent. This absence may be possible by space restriction in both buffers. The high pH for the concrete buffers is also limiting the microbial activity.

Both buffers have a temperature limit of 100 °C in many disposal programmes. One of the reasons for this temperature constraint is to limit degradation or mineral alteration of the bentonite buffer for bounding the uncertainty in the long-term predictability of this buffer. For the concrete buffer, this temperature constraint has been set to limit the formation of a gaseous phase.

Figure 4 shows an abstraction of the disposal cells considered in Europe for the following host rocks: granite (e.g., Czech Republic[2]), poorly indurated clay (e.g., Figure 4B, Belgium and Netherlands with the supercontainer concept (Bel et al., 2006)) and indurated clay (e.g., Switzerland and France, Figure 4). The disposal concept of compacted clay buffer bricks surrounding vitrified waste in granitic host rocks has been studied earlier in Europe (e.g., Atabek et al., 1991) but these studies were without a carbon steel overpack. Please note that the thickness of the carbon steel overpack considered for concrete buffer is thinner (about 3 cm (Neeft et al., 2020)) than considered for this overpack for bentonite buffers (about 14 cm, e.g., in the Swiss programme (Leupin et al., 2016). The reason for this difference in thickness is the higher corrosion rate foreseen for steel interfacing bentonite compared to concrete.

Lining material to support the rock is not needed and used for crystalline host rocks. Pre-fabricated concrete segments are needed to construct a disposal gallery in poorly indurated clay. These hardened segments need to be directly applied against the fast convergence of this clay. There is more time to apply a lining in indurated clay for example, when excavation has been finished. The lining is made by in-situ curing of shotcrete (grout). Grouts are sprayed against the surface of excavated rock in a disposal gallery for indurated clays. Chemical interactions between the cementitious fluid and the clay host rock take place before hardening. Reaction rims between shotcrete and clay may have been formed in order to enhance the bonding of the shotcrete with the clay host rock.

The porosity of the pre-fabricated concrete segments is similar to the concrete buffer, i.e., between 10 and 15 vol%. The porosity for the backfill grout and shotcrete is larger between 25 and 35 vol%.

2.2 ILW disposal cells

2.2.1 Characteristics of ILW

2.2.1.1 Metallic ILW

If further specified, the metallic ILW considered in this review was Zircaloy, stainless steel and carbon steel (Neeft et al., 2020). Metallic radioactive waste is mainly generated by reaction with neutrons and elements within these metals.

Stainless steel and carbon steel arise from the maintenance and dismantling of nuclear reactors. Metallic waste also arises from reprocessing spent fuel from nuclear plants: Compacted waste Standard Residues (Collis Standard de Déchets Compatés: CSD-C). It comprises metal parts from the spent fuel assemblies that have been cut off to extract the spent fuel, then rinsed and dried. A canister of about 170 L internal volume is filled with either hulls or end pieces. The hulls are made of Zircaloy; other metal parts are usually made of Inconel. End pieces are solid stainless steel sections. Drums with other waste arising from reprocessing fuels, such as pumps, stirrers and filters, are primarily made of stainless steel. All drums are compacted to produce pucks that are loaded into CSD-C canisters with similar outer dimensions to those used for vitrified waste, which are welded closed. The void space is about 20% in the canisters. CSD-C canisters can later be encapsulated in concrete containers (see Figure 4). Another example of pure metallic ILW is activated steel (e.g., Stein, 2014). Frequently, however, radioactive steel is processed with organic ILW (e.g., Uras et al., 2021).

2.2.1.2 Organic ILW

If further specified, the organic ILW in this review were spent resins, but the French programme noted a special interest in PVC and cellulose since degradation of both polymers lead to complexing agents for radionuclides (Neeft et al., 2020). The amount of cellulose based material identified in the ILW inventory in the French programme is 25 wt% (Altmaier et al., 2021). Experiments with cellulose have been made and described e.g., in Blanc et al. (2024) and Altmaier et al. (2024) but are not treated in this paper.

Resins purify reactor coolant water and other types of water used during operation and maintenance of nuclear reactors. The most common form of synthetic ion exchange resins is polystyrene divinylbenzene in powdered form with diameters from 5 to 150 μm or in beads from 0.5 to 2 mm. The resins have functional groups that are to be exchanged with a radionuclide in cationic form such as $^{60}CoOH^{+}$ or in anionic form such as $H^{14}CO_3^{-}$. Spent resins are mixed with a waste matrix that can be a cementitious matrix. Figure 5 shows the schematics of this waste with an example showing a detail with the embedding of resin beads in a cementitious matrix (blue). This matrix is fabricated without siliceous aggregates. This type of waste is a so-called homogeneously mixed cemented waste (Uras et al., 2021).

An image of a heterogeneously cemented waste is compacted plutonium contaminated material generated at the Sellafield site in the United Kingdom that contains halogenated plastics (PVC) and non-halogenated plastics, is available in the MIND project from the Horizon 2020 programme. These compacted plastics have been enclosed in an annulus of cement grout (Abrahamsen et al., 2015).

2.2.2 Characteristics of ILW disposal cells

Cementitious materials are used to condition the ILW but can also be used as a backfill. The dimensions of a disposal gallery for ILW are usually larger than those of galleries constructed for disposal of HLW. Figures 4D,E shows an abstraction of the ILW disposal cells considered in Europe for the following host rocks: crystalline (Figure 4d,e, e.g., Sweden) and poorly indurated clay

2 Spent fuel is not reprocessed in the Czech and Spanish programmes; thus, there is no vitrified HLW to be disposed of in Spain and Czech Republic. The HLW disposal cell does have the steel/iron-bentonite and steel/iron-granite interfaces investigated within ACED. The available knowledge from these programmes is therefore relevant for ACED until there is contact between the pore water and the waste form.

(Figure 4f, e.g., Belgium). The ILW disposal cells in crystalline rocks consist of vaults that are lined with shotcrete to stabilise the rock in the operational phase and caissons in which the waste containers are emplaced.

The types of waste drawn in Figures 4D,E are processed spent ion exchange resins with a sacrificial stirrer for each package and metallic waste arising from the maintenance of a nuclear reactor and being mostly steel (both disposed in granitic rock). As an example, processed resins have been drawn within reinforced concrete caissons and metallic waste in unreinforced concrete caissons. The coverage of concrete in well-engineered reinforced concrete depends on the environmental class, for example, 40 mm for the highest environmental class XA3 in the European standard EN 206. For reinforced concrete, the attachment between steel and the cementitious phase is important. Steel rebars have usually ribbons and are commonly oxidised in air before concrete pouring in order to obtain a good attachment between concrete and steel. Gaps between steel and the cementitious phase of concrete may arise due to shrinkage of the cementitious phase during hardening, when polished and smoothend steel is used. Oxygen in air can increase the corrosion rate of steel. The corrosion rate of steel is minimized if steel is exposed to reducing, alkaline conditions, since a passivation layer on the steel surface that limits corrosion is stable at these chemical conditions. Consumption of oxygen by corrosion of steel can deplete oxygen in the vicinity of the steel bar by which aerobic corrosion is followed by a lower anaerobic corrosion rate. High aerobic corrosion rates caused by the insufficient coverage of the steel bar by concrete may result into the spallation of concrete during the operational phase of the disposal facility. Especially if carbonation of the concrete cover has occurred by which the alkaline environment is no longer provided. So far, only cracking of concrete by aerobic corrosion of rebars has been known with characteristic orange-brown corrosion products with minerals such as hematite and lepidocrocite. Anaerobic corrosion of rebars is characterised by dark-brown to black corrosion products with minerals such as magnetite (Argo, 1981).

For granitic rocks, also shotcrete or a grout can be applied sometime after excavation as previously explained for the HLW disposal cells constructed in indurated clay. The caissons are backfilled with cementitious grout after completion of emplacement of waste packages. The empty volume between the caissons and shotcrete is backfilled with crushed granitic rock to control the waterflow in the disposal gallery. Granitic rock is easily available from the excavation activities.

Hardened concrete segments need to be immediately applied after excavation of poorly indurated clay as previously explained for the HLW disposal cells constructed in poorly indurated clay. A cylindrical concrete disposal package containing eight canisters CSD-C is envisaged to be emplaced in this disposal gallery. This gallery is backfilled with mortar.

2.3 Characteristics of host rocks

Usually, the depth of the disposal facility is so large that reducing conditions are dominant for clayey and crystalline host rocks. Determination of the chemistry of the porewater is not always possible by measurements, modelling needs to be used especially for clayey host rocks. The pore water chemistry of the virgin host rock and how this chemistry has been determined and the mineralogy and its impact on the pore water chemistry are described in the Supplementary Materials.

The properties of the host rock in the vicinity of the engineered materials change during excavation of the host rock and may change during the operation of the facility. There will be some fractures generated in the host rock and the size and density of the cracks depends on the excavation technique, size of excavated volume and type of host rock. The disposal galleries to emplace HLW packages are usually smaller in diameter than the disposal galleries to emplace packages containing ILW and the excavation procedure can be different. The outcome of both features is that the Excavation Damaged Zone (EDZ) is smaller for galleries to dispose HLW than for galleries to dispose ILW. The required time to heal or seal these fractures is host-rock dependent.

2.3.1 Crystalline host rocks

2.3.1.1 Construction

Crystalline rock specific excavation procedures have been defined in Finland and Sweden to make galleries to dispose of HLW with an acceptable limited water inflow through fractures to emplace the engineered material bentonite in the operational phase (e.g., Baxter et al., 2018). The water flow from the host rock into the disposal cells needs also to be limited for the post-closure phase to limit ingress of species from shallow and deep ground water (Vieno et al., 2003) and bentonite erosion (Baxter et al., 2018). Excavation of rock to construct disposal galleries is performed by drilling and blasting. Rock support are bolts and shotcrete; the density of applied bolts as well as non-reinforced or reinforced shotcrete is determined by the fracture extent of the rock (e.g., Carlsson and Christiansson, 2007). Shotcrete hardens in-situ and chemical interactions between the cementitious fluid and crystalline host rock can take place before hardening. Reaction rims between shotcrete and crystalline may have been formed in order to enhance the bonding of shotcrete with the crystalline host rock.

2.3.1.2 Operation

Decades of experience is available for operating a disposal facility for LLW and short lived ILW in Hungary, Sweden and Finland. Pumps are needed to keep the disposal facility dry. The main inflow of water into this facility in Sweden is, however through, the access tunnels and not the disposal galleries (Carlsson and Christiansson, 2007; Vahlund and Andersson, 2015). The permeability of the shotcrete lining is smaller than the permeability of the crystalline rock. The same accounts for the bentonite buffer that is emplaced in HLW disposal cells. Consequently, the concrete lining and bentonite buffer acts as a barrier for further transport of water into the facility. Potential healing of fractures can take place by precipitation of minerals, e.g., calcite, chlorite and clay minerals (Drake et al., 2006).

Also, the ingress of dissolved species from the host rock pore water that can alter the cement mineralogy of the lining in ILW disposal cells starts in the operational phase. The shotcrete used for disposal cells in crystalline rock can become atmospherically

carbonated due to ventilation air. The fractures in crystalline rock give a heterogeneous influx of granitic pore water into the shotcrete. The ingress of bicarbonate, sulphate and dissolved magnesium (depending on the host rock geochemistry) may precipitate into minerals that replace the calcium-containing cement minerals. There can therefore be a loss in strength of shotcrete liner in the operational phase since the calcium-containing minerals provide the binding and strength of the shotcrete.

2.3.2 Poorly indurated clay

2.3.2.1 Construction

Special tunnel boring machines are used to construct galleries in poorly indurated clays. Concrete segments are immediately applied after excavation of the clay with these machines. The stability of the lining is caused by the use of a wedge block. The block is emplaced between concrete segments. Concrete interfacing clay in the HLW and ILW disposal cells (Figure 4) is the external diameter of the gallery. The diameter of the excavated clay is slightly larger than the envisaged external diameter of the gallery. This so-called overcut is needed in order to be able to emplace the concrete segments. So far, the EDZ has been measured by the larger hydraulic conductivity compared to virgin clay. The larger hydraulic conductivity is attributed to the presence of cracks. The hydraulic conductivity of clay interfacing the concrete liner is the largest measured hydraulic conductivity. Further away from this interface, the hydraulic conductivity diminishes and approaches the virgin hydraulic conductivity.

The cracks induced by excavation revoke the limitations for microbial activity that were initially present in the virgin host rock. Active microbial communities present in various boreholes demonstrate that only providing space is sufficient to initiate the establishment of an active microbial community (Wouters et al., 2013; Wouters et al., 2016). The smectite content of poorly indurated clay is more than 20 wt% (see Supplementary Material Section 3.1). The dominant process for closure of cracks is self-healing by swelling clay minerals (Bernier et al., 2007). The decrease in hydraulic conductivity by self-healing of cracks will limit the transport of cells and nutrients. This excavation induced microbial activity is therefore envisaged to be only temporarily present.

2.3.2.2 Operation

The concrete segments are usually manufactured with a so-called engineered impermeability; envisaged porosities are between 10% and 15%. This limits the diffusional exchange between the dissolved species in the concrete segments and clay but also dehydration of the clay; the Boom Clay surface - at emplaced concrete segments that had been removed for experimental reasons - felt wet. The flow of water into the disposal facility is so small that ventilation is sufficient to keep the facility dry. The salts that have been deposited at the intrados of the concrete liner especially at joints between concrete segments indicate the preferential flow of clay pore water (Levasseur et al., 2021). The concrete lining acts as a barrier for further transport of water into the facility by which sufficient access of water is present in the operational phase to seal the fractures. The sealing of these cracks takes place by swelling of clay minerals such as smectite. This process can be very fast. No difference in hydraulic conductivity has been found for galleries constructed with an external diameter of 2.5 m (Dizier et al., 2017). The overcut during the construction of the gallery was minimized. In the SELFRAC project from the FP5 programme, the hydraulic conductivity in clay surrounding a gallery with an external diameter of 4.6 m was studied. This gallery was constructed with a larger overcut. After a few months, the hydraulic conductivity at 1.5 m from the interface with concrete was measured to be 3 times larger than the virgin hydraulic conductivity (Bernier et al., 2007) and two times this hydraulic conductivity after 8 years (NIROND, 2013). The virgin vertical hydraulic conductivity is about 1.7×10^{-12} m/s for Boom Clay, i.e., a poorly indurated clay (NIROND, 2013; Levasseur et al., 2021).

Atmospheric carbonation of the concrete segments from the intrados towards the extrados is expected but the small porosity and the engineered water tightness of the concrete segments prevents carbonation. Carbonation of well-engineered buildings at the surface exposed to the atmosphere for more than 100 years have measured carbonation depths smaller than 1 cm (Mallinson and Davies, 1987). This carbonation depth is very small. Above all, carbonation may not necessarily be a problem for the performance of unreinforced concrete. Spallation of concrete from reinforced concrete can occur especially if sufficient ingress of oxygen takes place for aerobic corrosion of the rebars.

The thermal impact on the damaged zone in poorly indurated (and indurated clays) has been investigated in the 6th framework programme TiMoDaz. There will be an increase in temperature in the host rock due to the conduction of the emitted heat by HLW for the HLW disposal cells. This 6th framework programme provided the evidence that the thermal-induced plasticity, swelling and creep of clay are likely beneficial for the sealing of fractures and recovery of the permeability of the EDZ to the original state of the clay host rock (Li et al., 2010).

2.3.3 Indurated clay

2.3.3.1 Construction

Road headers and tunnel boring machines are used to construct the excavation rooms in indurated clay. The lining does not need to be applied immediately. The virgin vertical hydraulic conductivity for indurated clay can be more than 10 times smaller than in poorly indurated clays, for example, 1×10^{-13} m/s for Callovo-Oxfordian clay and 10^{-14} m/s for Opalinus Clay (Levasseur et al., 2021). The excavation has a higher impact on the transport properties of indurated clay surrounding the lining than for poorly indurated clay. The fractures generated in clay host rocks are believed to have an atmospheric pressure immediately after excavation. The driving forces to close these cracks are compressive load or confining pressure and access to water. The smectite content of indurated clays can be less than 2 wt% (see Supplementary Material Section 3.1). The dominant process for closure of fractures is cementation, i.e., precipitation of minerals (self-sealing). This precipitated phase has a smaller tensile strength than the surrounding restored clay host rock. The closure of cracks can be measured as the increase in pore water pressure; equilibrium is achieved when the formation pressure is achieved (Alcolea et al., 2014). The EDZ is characterised in clay host rocks as a zone with a larger porosity and permeability than the virgin host rock. The values for hydraulic conductivity or permeability are largest near the interface between concrete and clay. These values asymptotically decrease as a function of the radial distance till the values measured for the virgin host rock after about 6 m from this interface.

2.3.3.2 Operation

The necessary ventilation in the operational phase may have an impact on the clay host rock at the start of the post-closure phase. The lining of a facility built in indurated clay decreases further drying by ventilation; the associated formation of drying shrinkage cracks of this clay host rock is limited but the porosity of the shotcrete is larger than that of clay, so further drying cannot be prevented. The formation pressure is therefore expected to be achieved in the post-closure phase and not in the operational phase. After recovery of the formation pressure, the modelled variation in hydraulic conductivity has decreased by less than 2 orders in magnitude (Alcolea et al., 2014).

After the concrete of the lining has hardened (in the case of a lining made with in-situ curing), the clay may be too dry for dissolved species in the clay pore water to enter the lining in the operational phase. Any chemical alteration of the lining before emplacement of the waste is expected to be mainly caused by ingress of carbon dioxide from the ventilation air.

3 Phenomenological description of processes at interfaces

The long-term safety of the geological disposal of radioactive wastes is based on a multi-barrier concept combining man-made engineered barriers (such as waste form, waste canister, backfill and sealing materials) with a suitable geological barrier (i.e., the host rock). The prediction of the evolution of the waste matrices, the waste canisters and overpacks, the engineered barriers (e.g., bentonite or cementitious backfill) with time in response to physical and chemical perturbations is an important aspect with respect to the performance and long-term safety of a repository. The introduction of "foreign materials" such as borosilicate glasses, metallic canisters, and cementitious materials will induce chemical gradients across the repository components, which can induce perturbations such as pH and redox changes, or changes in mineralogy and microstructure that may alter the performance of the barriers over time (e.g., NAGRA, 2002). Dissolution and precipitation processes occurring in this context can be associated with modification of porosity and pore architecture, thus affecting permeability and diffusivity of porous media and consequently transport of solutes or transfer of gases. Predicting the interactions between the different materials entails understanding and evaluating the pertinent coupled thermal, hydraulic, mechanical, and (radio and/or bio)geochemical processes. A number of studies on deep geological disposal of nuclear wastes showed that chemical and physical interactions are focused on interfaces between the different barrier materials, due to the prevailing chemical gradients (e.g., Claret et al., 2018; Bildstein et al., 2019). In this context, the nature and the extent of the alteration within the different materials, the progress of the perturbations with time and the evolution of the material properties are essential to evaluate the impact on the overall performance of the disposal system.

A valid starting point is using the knowledge available at the scale of interfaces between two materials in order to build models for assessing the chemical evolution at the disposal cell scale. This section describes the state-of-the-art on the phenomenological chemical processes occurring at the interface between two materials for the combinations relevant for European repository concepts (cf. section 2.1; see also Neeft et al. (2020)). For each interface, a short description of the phenomenology is given together with references to studies that give evidence for these processes. A comprehensive and structured overview of existing information and data on relevant processes occurring at the interfaces, including natural/archaeological analogues that may provide insight/data for long-term processes relevant to the chemical evolution of the disposal cells, as well as on conceptual and numerical models used to describe the processes at the interfaces has been compiled in Deissmann et al. (2021).

3.1 Interface "glass—Steel"

This interface is related in particular to the disposal of vitrified HLW and has been investigated in the context of the disposal concepts of countries where spent nuclear fuels have been or are reprocessed or form part of the waste inventory, as, e.g., in France, Belgium, Russia, Japan, Germany, the Netherlands, the UK or the United States of America (Gin et al., 2013). The glasses developed for this purpose (i.e., in particular borosilicate glasses) are contained in stainless steel canisters, which are placed usually in carbon steel overpacks prior to disposal (cf. section 2.1.1). However, it should be noted that in recent years some preliminary studies conducted, e.g., within the frame of the European collaborative project THERAMIN, investigated also vitrification of ILW (e.g., Clarke et al., 2020; Scourfield et al., 2020), where the treated product may also be packed in steel containers.

The main physico-chemical interactions at the glass-steel interface will start once the overpack and the canister are breached due to corrosion and/or lithostatic pressure and water can enter the canister. Thus, besides metallic iron/steel, corrosion products from the metal containers will also be present as surrounding materials close to the glass-steel interface. Corrosion products formed during anaerobic corrosion of low-alloy steel disposal containers are mainly composed of iron oxides such as magnetite (Fe_3O_4), or iron carbonates such as siderite ($FeCO_3$) or chukanovite ($Fe_2(OH)_2CO_3$) (e.g., Honda et al., 1991; Taniguchi et al., 2004). Localised variations in pH and in concentrations of carbonates may favour the formation of the one or other corrosion products (Michelin et al., 2015). In some cases, FeIII oxy-hydroxides were detected; they may have formed during the initial period of the corrosion test with remaining traces of oxygen (e.g., Kursten and Van Iseghem, 1999; Leon et al., 2017).

The glass-steel interface is only relevant at the later stages of the repository (i.e., after canister failure). A distinction needs to be made with respect to corrosion products formed in a first phase, in which the steel container or overpack corrodes in the groundwater until its failure, where the corrosion products formed are characteristic of corrosion in the host rock medium and some residual metallic iron remains in the system. In a subsequent phase, the disposal container continues to corrode in parallel to the alteration of the glass, i.e., the nature of the corrosion products forming may then be influenced by the solution chemistry at the glass/iron interface, including elements released by the glass.

The alteration and dissolution of nuclear waste glass in contact with water is controlled by several inter-related processes at the glass surface. Independent of the glass composition and the alteration conditions, the most important processes comprise (e.g., Ferrand et al., 2006; Gin et al., 2013; Marcial et al., 2024):

- Water diffusion into the glass,
- Ion exchange between hydrogenated species and alkalis (interdiffusion),
- Hydrolysis of covalent and iono-covalent bonds in the glass matrix,
- Formation and evolution of a surface alteration layer (gel layer),
- Silica saturation of the solution,
- Precipitation of secondary phases,
- Retention of radionuclides in the gel layer and secondary phases,
- Removal of silicon from the solution by sorption, chemical reaction or transport.

Based on extensive studies on the dissolution of nuclear waste glasses and in particular simulated HLW borosilicate glasses, a general picture on the typical dissolution behaviour of HLW borosilicate glasses under conditions representative for geological disposal environments has been established (Figure 6, cf. van Iseghem et al. (2006); Gin et al. (2013); Gin (2014)).

Understanding the glass/steel interactions and their consequences on the long-term behaviour of nuclear waste glasses requires knowledge regarding the main processes controlling the aqueous alteration of glass. According to Vienna et al. (2013) and Gin et al. (2015), glass alteration leads to the formation and dissolution of an alteration film layer, which is likely to incorporate chemical elements from the solution and acts as a diffusion barrier for reactive species. The effectivity of this barrier depends primarily on the concentration of silicon in solution in the vicinity of the glass, with glass dissolution rates increasing when the activity of Si decreases. Other parameters affecting the glass alteration and its rate are (local) solution pH and solution composition, since some elements may stabilise (e.g., calcium (Paul, 1977; Gin et al., 2012) or destabilise (e.g., magnesium (Aréna et al., 2016)) the hydrated glass layer. Glass alteration rates are lowest at circumneutral pH and increase both under acidic and alkaline conditions.

Generally, the presence of iron and iron corrosion products (from steel canisters and/or overpacks) has been found to increase glass alteration by maintaining high alteration rates over longer periods than in the same leaching solution without iron or corrosion products (Martin, 2021). However, this impact is only perceptible at local scale, and seems to be significantly attenuated as the distance between glass and the iron source increases. There are four possible mechanisms that are discussed in literature to explain the increase in glass alteration rates due to the presence of iron or iron corrosion products (Rebiscoul et al., 2015):

- silicon sorption at surface sites of corrosion products, or silica precipitation at the iron source;
- formation of iron silicates;
- retention of iron in the gel layer, which could modify its structure and its protective properties;
- increase in pH due to iron corrosion.

The first two mechanisms both lead to the consumption of cross-linking elements, in particular silicon, leading to either (i) a depletion of the concentration of silicon in solution, which increases glass dissolution rates, or (ii) the formation of a gel depleted in silicon which is, therefore, less protective (Lemmens, 2001). These effects both hinder the formation of a protective layer, delaying saturation of the aqueous solution needed for its formation. In the first case, the effect works by making the initial rate phase (r_0) last longer, and, in the second case, by slowing down the rate drop (cf. Figure 6).

3.1.1 Sorption of silicon on corrosion products

The sorption of species like silicon produced by glass alteration on steel corrosion products close to the glass/steel interface can delay the beginning of the rate drop. This effect has been demonstrated in the presence of steel corrosion products such as magnetite (Bart et al., 1987; Grambow, 1987; Grambow et al., 1987), goethite (Bart et al., 1987; Grambow, 1987; Grambow et al., 1987), and siderite (Michelin et al., 2013a). Since the number of surface sites on the corrosion products available for sorption is finite, the effect of silicon sorption on glass alteration lasts for a period that is proportional to the sorption capacity of the corrosion products. The higher the sorption capacity of the corrosion products, which is dependent on their amounts and their specific surface areas, the longer it takes to reach silicon saturation in solution, which in consequence delays the rate drop. However, the results from different glass alteration experiments carried out in the presence of corrosion products seems to indicate that the sorption of silicon to corrosion products does not prevent a slowing of the alteration rate over time. Studies on silicon sorption on steel corrosion products (magnetite, siderite, goethite) indicate (i) that the maximum sorption occurs at pH values between 6 and 9 and decreases, both under more acidic and alkaline conditions, and (ii) that silicon sorption by steel corrosion products will be maintained for a relative short period of time compared to the time scales relevant for geological disposal (Philippini et al., 2006; Philippini et al., 2007).

3.1.2 Precipitation of iron silicates

Sorption of silicon on corrosion products alone seems not to be sufficient to explain the quantities of altered glass in experimental tests since even after saturation of the sorption sites, glass alteration rates in the presence of steel and corrosion products remained higher than the residual rate (r_r) observed in the absence of steel and corrosion products over longer periods. Thus, other mechanisms such as the formation of silicates may prolong the consumption of silicon in the longer-term. Most studies performed in this context suggest the formation of various ferrosilicates (e.g., McVay and Buckwalter, 1983; Shade et al., 1983; Björner et al., 1987; Grambow, 1987; Grambow et al., 1987; Werme et al., 1990; Shanggeng et al., 1995; Kim et al., 1997; Michelin et al., 2013a; Godon et al., 2013; Dillmann et al., 2016), sometimes in nano-colloidal form. The precipitates formed may incorporate other elements in addition

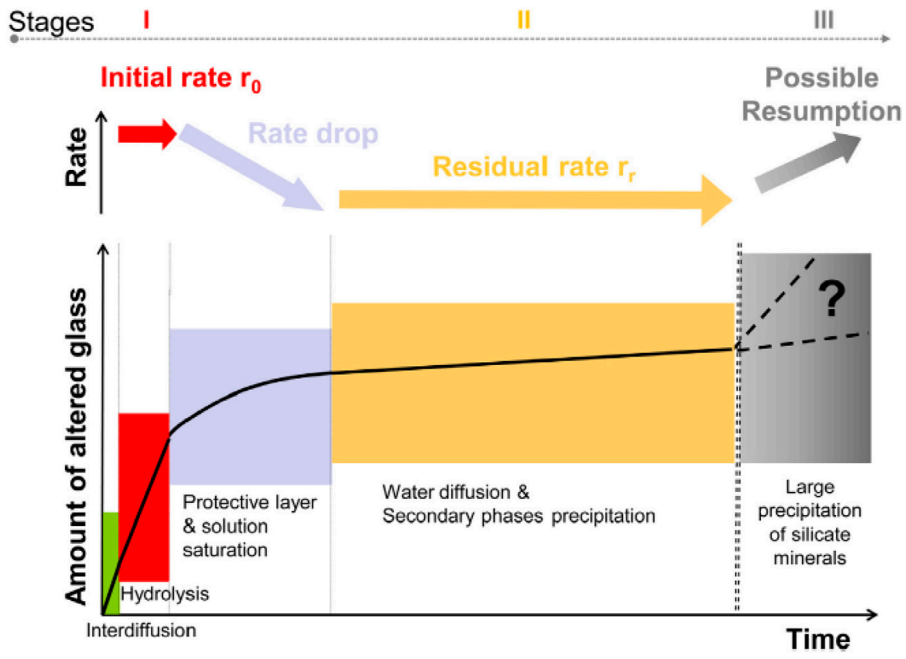

FIGURE 6
Stages of nuclear glass corrosion and related potential rate-limiting mechanisms (Gin et al., 2013).

to iron, such as magnesium, aluminium, sodium and calcium, depending on solution chemistry (e.g., Burger et al., 2013). The silicates formed in this context may include trioctahedral serpentines (e.g., greenalite, berthierine, cronstedite), trioctahedral smectites (e.g., hectorite, saponite) or dioctahedral smectites (e.g., nontronite). The (Fe + Mg)/Si ratio of the silicates formed can vary, especially depending on the distance from the iron source. Moreover, the nature of the precipitated silicates highly depends (i) on temperature (e.g., favouring the formation of serpentines at higher temperature), and (ii) on local pH, since iron/magnesium silicates can only be precipitated above a certain pH, which is a function of the silicon activity imposed by glass alteration.

Experimental observations indicate that the formation of ferrosilicates is limited in the presence of steel corrosion products alone (e.g., Björner et al., 1987) but significantly higher in the presence of metallic iron in which iron silicates may form from the start of alteration. Therefore, the formation of corrosion products *in situ* at the same time as glass alteration seems to modify the predominant mechanisms and causes more precipitation of secondary silicate phases. This may be explained by a more or less significant iron flux induced by iron corrosion or the solubility of the corrosion products (Dillmann et al., 2016). The formation of iron silicates correlates to more extensive glass alteration; these ferrosilicates thus have the same effect on glass alteration as other secondary phases, such as zeolites, which consume silicon and inhibit the effects of solution saturation, except that in this case their formation is conditioned by the flux of iron released by the corroding steel. Thus, the formation of ferrosilicates and their impact on glass alteration depends on the quantity of metallic iron remaining, its corrosion rate, and on the solubility of iron in solution.

3.1.3 The influence of iron on the morphology and structure of the gel layer

The interactions between silicon and steel corrosion products, playing the role of "silicon sink", could be detrimental to the protective properties of the gel layer on the glass surface. During glass alteration in the presence of corroding iron or iron corrosion products, a large quantity of iron is dissolved, from the first stage of hydrolysis at r_0 (Figure 6). In this case, the gel layer on the glass becomes depleted in silicon (relative to pristine glass) and enriched in iron (Reiser et al., 2005; Rebiscoul et al., 2015; De Echave et al., 2019), though, according to Reiser et al. (2017), this enrichment may only affect parts of the gel layer. de Combarieu et al. (2011) suggested that the increased alteration of glass in the presence of iron is due to a higher porosity of the (iron-enriched) gel layer, depleted in cross-linking elements (e.g., silicon, aluminium, etc.), thus reducing its protective nature. Dillmann et al. (2016) related the iron enrichment of the gel formed during glass alteration in the presence of iron or corrosion products to the presence of structural nano-crystals similar to greenalite ($Fe_{2-3}Si_2O_5(OH)_4$), possibly precipitated due to the highly porous structure of the amorphous gel layer (cf. Burger et al., 2013). The impact that these nano-crystalline phases may have on the properties of the gel has not yet been clearly assessed. The presence of iron changes the equilibrium between the glass and the solution and alters the stoichiometry of the gel. Furthermore, the iron precipitating in the form of ferrosilicates may influence the depolymerisation of the silicate network. Burger et al. (2013) suggest a possible clogging of porosity and, as a result, a decrease in the diffusion coefficient of the reactive species.

3.1.4 Impact of iron corrosion on pH

In addition to the consumption of silicon, iron corrosion also affects the pH of the solution. The corrosion of metallic iron and the

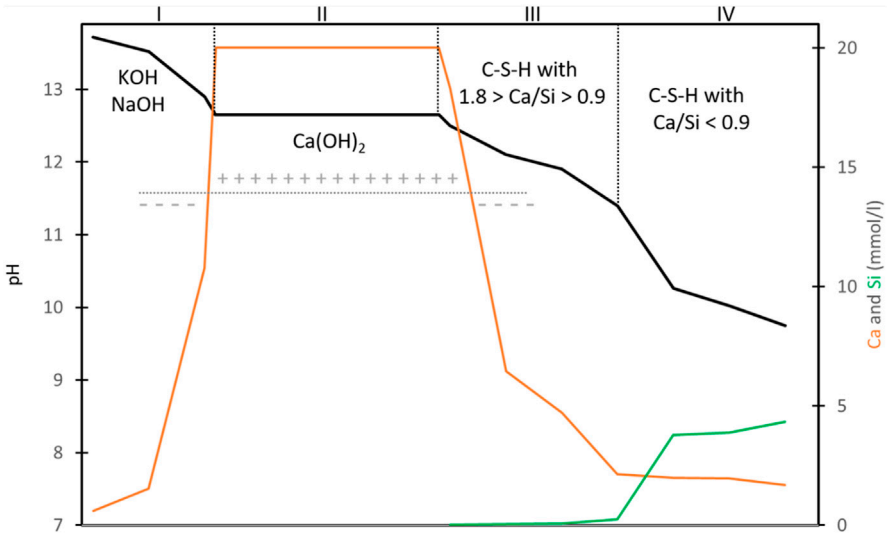

FIGURE 7
Concrete pore water in terms of pH (black line), dissolved calcium (orange line) and silicon (green line) at room temperature together with controlling cement phases. Kind of surface potential of C-S-H mineral is indicated. Stages in pH by Atkinson et al. (1985) with added calcium and silicon by Berner (1992) at a pH < 12.65, dissolved calcium at a pH > 12.65 from van Eijk and Brouwers (2000) and nature of the surface potential of C-S-H mineral from Pointeau et al. (2006).

formation of corrosion products occurring at the same time as glass alteration, tends to raise the pH (Bildstein et al., 2007), thereby favouring glass alteration (e.g., Utton et al., 2012; Corkhill et al., 2013; Utton et al., 2013) and the formation of magnesium silicates, which, concomitantly affects glass alteration due to consumption of silicon. The pH values during glass alteration in aqueous media in the absence of corroding iron (i.e., governed by the presence of the glass) are generally neutral to slightly alkaline (e.g., between 7.5 and 8.7 in clay water) and have been found to increase up to 9.7 in the presence of metallic iron (cf. Martin, 2021). This increase in the pH is due to the formation of hydroxyl ions (OH^-) during anoxic corrosion of iron in an aqueous medium according to Equation 1:

$$Fe + 2H_2O \rightarrow Fe^{2+} + 2OH^- + H_2 \quad (1)$$

which may be followed by precipitation of Fe(II)-hydroxide. Moreover, also in the presence of corrosion products like magnetite the solution pH during glass alteration was found to be higher than in leaching tests on glass alone (Rebiscoul et al., 2015). Here, the increase in pH is the result of a larger quantity of altered glass, i.e., of a higher quantity of alkaline species (e.g., Ca, Na) being released into solution.

3.1.5 Concluding perspective

The physico-chemical interactions at or close to the interface glass/steel lead generally to an increase in glass alteration rates compared to the absence of metallic iron and/or corrosion products. The main phenomenon related to this is the consumption of silicon delaying the formation of a passivating gel. This impact on glass alteration is conditioned by the geometry of the system and the transport and fluxes of dissolved iron and silicon in solution and seems to be significantly weaker when the glass is far from the iron source (e.g., corrosion products or metallic iron). Assessing the processes at the interface on glass alteration requires an understanding of the nature of the corrosion products, their position in relation to the glass, and the transport conditions within the system investigated, bearing in mind the influence of physical and chemical conditions (properties of the host rock, composition of the porewater, redox conditions, pH) and hydrodynamics on glass alteration processes. Glass/iron interactions occur as a result of very localised conditions which depend on the dissolution rates of iron and glass, and on the transport of different elements in solution. In spite of the importance of understanding the coupling of transport processes and geochemical reactions in the evaluation of interactions occurring at the glass/steel interface with respect to nuclear waste disposal, coupled reactive transport simulations addressing this glass/steel/(clay) interactions are scarce to date (cf. Bildstein et al., 2007; Bildstein et al., 2012; Claret et al., 2018; Bildstein et al., 2019).

3.2 Interface "steel—Concrete"

An interface between steel and cement-based materials is present in many disposal concepts for geological disposal of radioactive wastes in Europe (see section 2.1; Neeft et al. (2020)). The interface between steel and cementitious materials may occur at different locations and with different functions/roles. In some disposal systems, reinforced concrete is used with carbon steel, for example, for the container of ILW waste packages. In this case, the carbon steel/concrete interface is typically located at a few centimetres from the boundary of the concrete component. In some HLW disposal concepts, carbon steel is used as overpack of the vitrified waste package. In some countries like Belgium and the

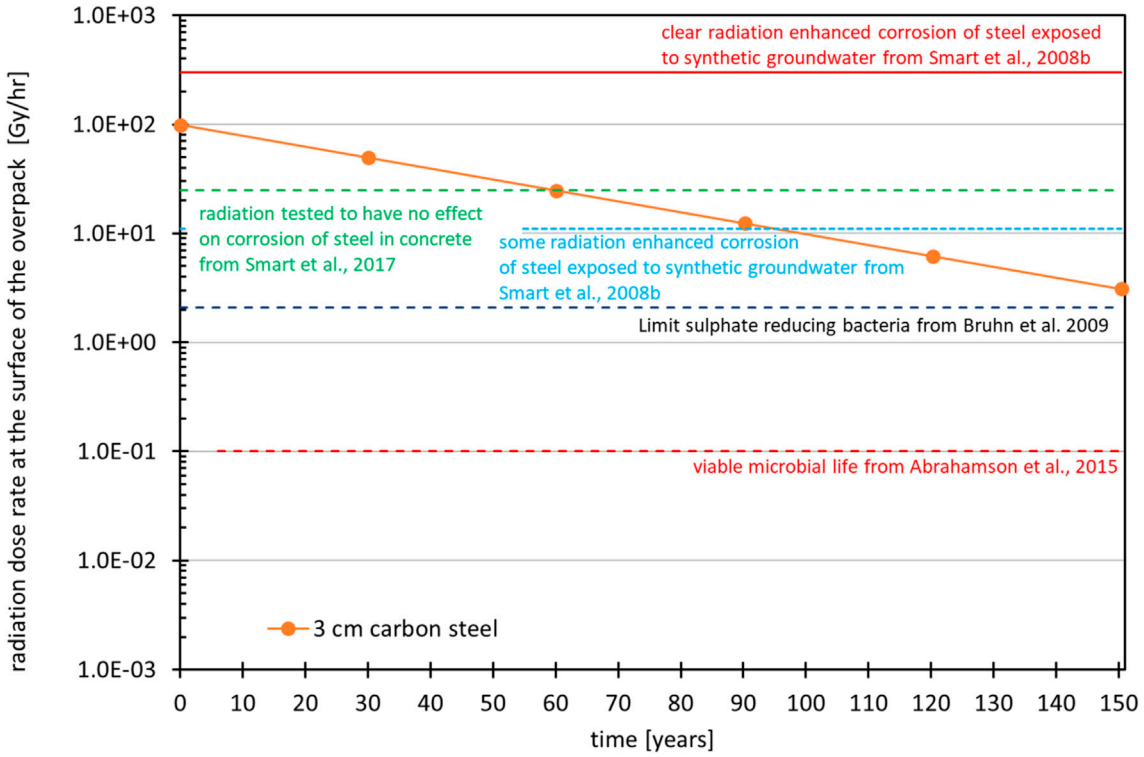

FIGURE 8
Radiation dose rate as a function of the time after CSD-V fabrication calculated with Microshield. Activity ^{137}Cs at 0 years is assumed to be 6,600 TBq.

Netherlands, a cement-based buffer is placed around the carbon steel overpack to ensure high pH conditions and thus lower corrosion rates for a long period of time (supercontainer concept, see Figure 4C). Here, the concrete cover is typically several decimetres thick. In the management of ILW, waste packages may contain also stainless steel or waste canisters are made of stainless steel (e.g., CSD-C canisters). The latter are often immobilized inside a concrete or steel container with cement-based materials such as mortar or grouts. In the following sections, the focus is on the interface between carbon steel and cementitious materials, since these interfaces are more relevant for the long-term performance and safety of the disposal cells. There exists a significant amount of literature of processes at the steel-concrete interface under aerobic conditions, which is relevant for many civil structures. However, most of the discussion here is limited to anoxic conditions, as the oxic period in a geological disposal facility, even if it lasts several hundreds of years, will most probably occur under conditions of high pH (buffered by the cementitious material) with low passive steel corrosion rates.

3.2.1 Steel corrosion in anoxic cementitious environments

In a deep geological repository in saturated conditions, oxygen is assumed to be depleted relatively quickly, so that anoxic conditions will be established soon after repository backfilling and closure. Oxic conditions then mainly prevail during the operational phase and when the disposal cell is not completely saturated. However, many different processes in an ILW or HLW disposal cell compete for oxygen (corrosion, oxidation of minerals, microbial respiration). In addition, the steel interface is embedded in mortar or concrete materials (reinforced concrete in HLW and ILW disposal cells, overpack in some HLW disposal cells, waste containers and waste in ILW disposal cells) which pose diffusion-limited oxygen availability at the interface and induce a passivating protective layer at the steel-concrete interface (e.g., Smart et al., 2019). In addition, also the cement used to produce the mortar or concrete can contribute to an anoxic environment. Concrete made from pure ordinary Portland cement (OPC) cement or OPC cement blended with micro silica are slightly oxidizing since they lack redox sensitive species. Blended cements can contain fly ash, which is a by-product from coal-firing power plants or blast furnace slag, which is a by-product from steel production, besides OPC. In the first case, the concrete also lacks redox sensitive species and is therefore slightly oxidising. However, the second case, the concrete contains pyrite and is therefore reducing after fabrication.

Several studies show that the formation of a passivating film on the steel occurs relatively fast (L'Hostis et al., 2011; Chomat et al., 2017). For a HLW disposal cell, a transition phase is sometimes thought to exist due radiolysis of water producing, *inter alia*, hydrogen, oxygen, hydrogen peroxide and reactive radicals, which might temporarily sustain relatively constant, mildly oxidising conditions (Kursten et al., 2011) although some experiments indicated a decrease in redox potential under gamma irradiation (Smart et al., 2019).

Oxic corrosion of iron is described by the following global reaction (Equation 2):

$$4Fe + 6H_2O + 3O_2 \rightarrow 4Fe^{3+} + 12\,OH^- \quad (2)$$

Corrosion products under oxic conditions are for example, goethite (alpha-FeOOH), ferrihydrite ($Fe(OH)_3$) and lepidocrocite (gamma-FeOOH) (L'Hostis et al., 2011). Anaerobic corrosion of iron is associated with the generation of hydrogen through the following global reaction:

$$Fe + 2\,H_2O \rightarrow Fe(OH)_2 + H_2 \quad (3)$$

or, if the Schikorr reaction occurs, by the reaction:

$$3\,Fe + 4\,H_2O \rightarrow Fe_3O_4 + 4\,H_2 \quad (4)$$

The rate of hydrogen generation can be monitored and is often used in experimental programmes to estimate corrosion rate assuming either iron (II)hydroxide (1 mol hydrogen generated per mol iron corroded, Equation 3) or magnetite (1.33 mol hydrogen per mol iron, Equation 4) as main corrosion product. Under anoxic conditions, corrosion products as magnetite (Fe_3O_4) and hematite (Fe_2O_3) are formed (L'Hostis et al., 2011).

Corrosion processes may be subdivided into a uniform passive corrosion mechanism and localised corrosion mechanisms (e.g., pitting corrosion, crevice corrosion, and stress corrosion cracking, see e.g., (Jacques et al., 2021b),). In a concrete-based geological disposal concept, the followed strategy is usually to demonstrate that localised corrosion phenomena cannot occur in highly alkaline disposal conditions. Therefore, the focus of the experimental studies with respect to this interface is on rate measurements of uniform passive corrosion through different methods and techniques (for details see Kursten et al. (2021)). Thus, for the interface between carbon steel and cementitious materials, mainly uniform corrosion processes and coupled processes are relevant, so that in geological disposal conditions, the main corrosion process would be passive corrosion of steel/iron in anoxic, alkaline conditions. Due to the formation of a passivating oxide film on the steel surface in these environments, the measured initial corrosion rates (up to some tens of μm yr^{-1}) decrease over time towards constant (steady state) and very low values. Long-term corrosion rates (exposure times >365 days) in the range of 0.1 μm yr^{-1} or lower have been reported for temperatures up to 80°C in chloride-free solutions with a pH between 11.8 and 13.5 (cf. compilation in Kursten et al. (2021)).

However, depending on the steel type and the evolution of the environment, the corrosion processes can be influenced by several factors such as temperature, degree of water saturation, radiation gradients, the composition of the near-field water with respect to pH and the content of potentially aggressive species (e.g., chloride, sulphate, thiosulphate), and the presence of microbial activity. The steel corrosion products may take a volume that is larger than the bare material, leading in turn to stress and (local) alteration of the pore structure at the interface and consequently to changes in transport properties. Spallation of concrete has so far only been observed for oxic corrosion of steel. The volume of bare material is reduced if the corrosion rate equals the iron dissolution rate from the corrosion product as measured for anoxic corrosion of (stainless) steel in the FP7 CAST project (Mibus et al., 2018). The thickness of the layer of corrosion products does not increase in such a case by which the induced stress in concrete is too limited to cause fractures. The corrosion process is bounded to equilibrium between diffusion of water through the oxide layer and dissolution at the solid-liquid interface.

3.2.2 Factors influencing corrosion rates

Temperature can play an important role in the corrosion of steel in concrete in many different ways because all processes and many parameters involved can be influenced by changes in temperature, such as:

- kinetic parameters of the corrosion reaction;
- rate of diffusion of O_2 and aggressive ions into the concrete;
- solubility of oxygen;
- pore solution chemistry of concrete.

The corrosion of steel reinforcement is an electrochemical reaction; its rate can be greatly affected by temperature. Generally, the (initial) corrosion rate increases significantly as temperature increases (e.g., Smart et al., 2004; Fujisawa et al., 1999; Fujisawa et al., 1996, for details see also Kursten et al., 2021). On the other hand, the solubility of oxygen in water is known to decrease with increasing temperature, which results in a significant decrease of the concentration of dissolved oxygen as reactant for the process of steel corrosion, thereby lowering the corrosion rate (Davis, 2000; Živica, 2002). However, this effect might be more relevant under oxic conditions, i.e., during the operational phase of a repository. Other physicochemical properties affected by temperature are the viscosity and the conductivity of the concrete pore solution. The viscosity will decrease with increasing temperature, which will aid oxygen diffusion. Ionic mobility will also increase with temperature, increasing the overall conductivity of the electrolyte. Moreover, the chloride binding capacity of cementitious materials can be reduced at elevated temperatures, leading to an increase in chloride concentrations of the pore water of the cementitious material (Hussain and Rasheeduzzafar, 1993; Maslehuddin, 1994; Hussain et al., 1996; Maslehuddin et al., 1996), which has been attributed to the decomposition of Friedel's salt (i.e., a chloride containing AFm phase) at elevated temperatures. However, data on long term (i.e., >365 days) corrosion rates for carbon steel in anoxic alkaline environments for different temperatures reported in the literature show that at the later stages of the corrosion process (i.e., when steady state conditions prevail), temperature no longer has an effect on the uniform corrosion rate (Kursten et al., 2021).

Corrosion of steel in concrete strongly depends on the moisture condition of the concrete. This is due to the fact that moisture affects both the resistivity of the concrete and the diffusion rate of oxygen. In dry concrete, which is characterized by a high resistivity, oxygen diffusion can take place unhindered. The resistivity in water saturated concrete is low but, on the other hand, the diffusion rate of oxygen is slow compared to the diffusion rate in dry concrete. This means that the corrosion rate is slow and that the corrosion is under diffusion control (Bertolini et al., 2004). According to Tuutti (1982) steel corrosion rates in concrete reach a maximum for a moisture content equivalent to the equilibrium with a relative atmospheric humidity of about 95%; moving away from these values of humidity in either direction, the corrosion rate decreases (Bertolini et al., 2004). On the other hand, ionic mobility will increase with increasing saturation degree, thereby

facilitating transport of aggressive species (e.g., chlorides) towards the overpack surface. However, Michelin et al. (2013a,b) showed that when steel in concrete is in a passive state, the corrosion rate is not affected by the moisture conditions of the concrete.

The pH of the pore solution in cementitious material has a distinct effect on the corrosion of steel at the interface, since the protective oxide film is believed to remain stable only as long as the pH stays higher than a threshold value (~9 < pH < ~11.5). If the pH should drop below this threshold value (e.g., due to leaching of alkalis and complete removal of portlandite from the cementitious material in the long-term, cf. Section 4.1), depassivation of the steel surface can take place and the protection is lost, leading in turn to an increase in the rates of uniform corrosion. Moreover, a decrease in pH can also increase the susceptibility to localized corrosion, though this effect is coupled to the exceedance of a threshold concentration of chloride ions in the pore water. Although this assumption has been generally accepted, there is little agreement concerning the quantitative function relating the two (cf. Kursten et al., 2021).

The corrosion rates of (carbon) steel can be distinctively enhanced due to the presence of aggressive species, in particular chloride ions, in the contacting solution. A huge amount of information is available in the literature on the effect of chloride on the corrosion rates of carbon steel in concrete under aerobic conditions (e.g., Goñi and Andrade, 1990; Deshpande et al., 2000; Zhang et al., 2009), where a general trend of increasing corrosion rates with increasing chloride concentration could be observed. Studies on the effect of the chloride concentration on carbon steel corrosion under anoxic and highly alkaline conditions have been performed in particular within the context of various national nuclear waste management programmes (e.g., L'Hostis et al., 2011; Smart et al., 2004; Smart, 2009; Ashikawa et al., 2001; Mihara et al., 2002). Corrosion rate data reported in the literature for mild steel in anoxic and alkaline solutions containing elevated chloride concentrations indicate that the measured (initial) corrosion rates decrease with increasing exposure time even in the presence of chloride ions. From comparison with data obtained in chloride-free solutions, it can be concluded that the presence of chloride (up to 20,000 mg L^{-1}) has no discernible effect on the long-term corrosion rate of carbon steel in anaerobic high pH media (Kursten et al., 2021). However, it is important to note that high chloride concentrations, combined with the potential risk of the passive film being destroyed locally, may result in a significant increased susceptibility to localized corrosion phenomena such as pitting corrosion, crevice corrosion, and/or stress corrosion cracking.

3.2.3 Consequences of steel corrosion on concrete properties

During the corrosion of steel embedded in a concrete structure, a layer of corrosion products is formed on the surface of the steel. The volume of these corrosion products can be much larger than that of the initial bare metal (e.g., Broomfield, 2007; Caré et al., 2008; McCafferty, 2010). The corrosion products will first fill the available pore space near the interface, which depends on the chemical state of the concrete and the process that initiated the faster corrosion. With the ingress of aggressive species, initiation of active corrosion may occur without significantly changing the microstructural properties of the concrete and thus the available pore space is close to the initial porosity of the concrete. However, when active corrosion occurs as a consequence of a pH decrease due to chemical degradation of concrete, the available pore space might be smaller or larger depending whether carbonation (resulting typically in a porosity decrease) or decalcification, i.e., dissolution of portlandite and incongruent dissolution of C-S-H (resulting typically in a porosity increase) is the dominant degradation process (e.g., Glasser et al. (2008) for a description of these processes). After filling of the available pore space, the corrosion products will gradually increase the mechanical stress in the concrete. Fracture formation is initiated when the mechanical stress exceeds the tensile strength (Höglund, 2014) but the time for the first appearance of fractures depends on different factors such as thickness of concrete cover, quality and strength of the concrete, and corrosion rate (Andrade et al., 2011). Note that creep of concrete can accommodate partly the effects caused by the corrosion products retarding to a given extent the initiation of fracture formation. Also, the anoxic corrosion rate can become equal to the iron dissolution rate from corrosion products. At that stage, there is no longer a volume increase.

The aerobic corrosion rate can be so fast that there is a volume increase. The fractures initiated by the corrosion products may influence the geochemical evolution of the concrete near the interface, especially when they are penetrating from the steel/concrete interface to the outside boundary of the concrete (e.g., an interface with host rock)). From these fractures, alteration fronts may develop within the concrete matrix and potentially creating larger regions of degraded concrete. Degradation fronts in fracture-matrix concrete systems can be described with approximated analytical models (e.g., (Höglund, 2014)), or with coupled reactive transport models (e.g., Perko et al., 2010; Perko et al., 2015).

Studies performed by L'Hostis et al. (2011) and Chomat et al. (2014, 2017) revealed the formation of an Fe-enriched layer in the cementitious material close to the interface. In this region Fe interacts with the cement hydration phases and may form Fe-containing hydration phases. In addition, the cementitious material may also alter the composition of the corrosion product layer with an enrichment of calcium closer to the interface of the corrosion product layer and the cement/concrete (cf. L'Hostis et al., 2011).

3.2.4 Concluding perspective

Under the anoxic conditions prevailing in a geological disposal facility in the long-term, the corrosion of steel in a highly alkaline, cementitious environment is governed by passive uniform corrosion due to the formation of a passivating oxide film, leading to very low corrosion rates. Thus, in a concrete-based geological disposal concept, one focus is on the demonstration that localised corrosion phenomena cannot occur in the highly alkaline disposal conditions. Corrosion products, that have a higher molar volume (per metal ion) than that of the metal, may reduce porosity, leading to clogging and gradually increase the mechanical stress in the concrete and may lead to fracture formation. However, the thickness of the corrosion layer is not increased over time when the corrosion rate is equal to the dissolution rate of iron from corrosion products. Furthermore, there are indications that a Fe-enriched

layer will form in the cementitious material close to the interface, leading eventually to the formation of Fe-containing cement hydration phases.

Existing thermodynamic modelling studies of the solution chemistry in the context of iron/steel corrosion (e.g., calculating saturation indices of ferrous and ferric minerals), focus so far mainly either on steel corrosion in alkaline conditions (with a substantial knowledge base on reinforcement corrosion in concrete structures) or on corrosion in anoxic environments. However, only few examples have been found for thermodynamic modelling related to iron/steel corrosion in both anoxic and alkaline conditions, i.e., relevant for the disposal environment (e.g., Ma et al., 2018; Furcas et al., 2022).

Although a number of experimental studies on iron corrosion in concrete have been performed in the context of nuclear waste disposal, no reactive transport modelling studies addressing the interface steel/concrete in the context of a deep geological repository are available so far (cf. Bildstein et al., 2019). However, similar tools as for other interfaces, in particular the steel/clay interface might be used. Since electrochemical models for corrosion (e.g., Bataillon et al., 2010; Macdonald et al., 2011) are a pivotal issue of this problematic, the coupling of such models to reactive transport models could result in significant advances in modelling the steel/concrete interface (cf. Bildstein et al., 2019).

3.3 Interface "steel—Clay"

Carbon steel canisters have been proposed for the storage and disposal of high-level radioactive wastes (HLRW) in deep geological repositories (DGR) in countries like Switzerland, France, Belgium, Germany, United Kingdom, Czech Republic, and Spain (cf. Neeft et al., 2020). The host rock and the design of the repository differ in each country but in many cases the canister will be in contact with compacted bentonite blocks or pellets. The main perturbations at the steel–clay/bentonite interface are canister failure due to corrosion and the interaction of corrosion products with the bentonite/clay, which could potentially result in the formation of new iron-rich minerals that alter some of its basic properties, such as hydraulic conductivity, diffusion coefficient and capacity to swell or retain radionuclides.

Canisters are estimated to provide containment for at least 1,000 years, although results from experiments, analogues and models indicate that failure is unlikely in less than 10,000 years. It depends, among others, of its thickness and chemical reliability. This section has to do with what it is known so far on the evolution of the DGR environment (thermal, hydraulic and/or chemical gradients - redox, pH and dissolved species - from the initial post-closure stage until the system reaches equilibrium) and its impact on the chemical evolution of the steel/iron-bentonite interface.

There are a number of papers about the corrosion of metals that provide results coming from laboratory experiments under a variety of conditions (e.g., Marsh et al. (1989); Marsh et al. 1986; Gdowski and Bullen, (1988); Blackwood et al. (2002); Azcárate et al. (2004); Kursten et al. (2004a; b); King (2008; 2014); Necib et al. (2016; 2017a; b)). Padovani et al. (2017) made an analysis of the expected corrosion behaviour of candidate container materials and future R&D work. Results of corrosion rates and products obtained from the study of archaeological objects can be found in Qin et al. (2004), Smart and Adams (2006), Neff et al. (2010), Neff et al. (2006), Yoshikawa et al. (2008) and Michelin et al. (2013b), amongst others.

The interaction of corrosion products with bentonite has been reviewed in Marcos (2003), Landolt et al. (2009), Bradbury et al. (2014), Wilson et al. (2015) and Wilson (2017), among others. There are also various papers and reports from European projects NF-PRO, PEBS, TBT, and activities in underground research laboratories (e.g., FEBEX experiments at Mt. Terri) presenting the results from both laboratory and *in situ* experiments in URLs designed to advance in the understanding of iron-bentonite (and clay rock) interaction (e.g., Guillaume et al., 2004; Charpentiera et al., 2006; Wilson et al., 2006b; Wilson et al., 2006a; Carlson et al., 2007; Hunter et al., 2007; Smart et al., 2008a; Milodowski et al., 2009; Fukushi et al., 2010; Osacký et al. (2010; 2013; Torres 2011; Lanson et al., 2012; Schlegel et al. (2014; 2016; Torres et al., 2014; Cuevas et al., 2016; Wersin and Kober, 2017; Hadi et al., 2019). Some authors focused on the study of natural analogues from which obtaining information about influence of iron on the transformation of bentonite to iron-rich clays (e.g., Smart and Adams, 2006; Pelayo et al., 2011).

The changing environmental conditions during the life of the repository influence the corrosion processes and products, the interaction of corrosion products with bentonite and finally, the integrity of both, the steel/iron and the bentonite. In the following, two phases are distinguished: i) a first phase with initially aerobic conditions at elevated temperatures (>90°C) before repository closure, including a transient phase with progressively anaerobic conditions, encompassing a time scale of in total about 100 years, and ii) a second (long-term) phase with anaerobic conditions at temperatures <90°C, which will decrease to ambient host rock temperatures with time.

At the initial stages (≈emplacement to 20 (50) years) water vapor and dissolved oxygen act as the oxidizing agents. Low steel corrosion rates and general corrosion occur and no changes are expected in the bentonite properties (cf. Turrero et al., 2021).

- Oxidizing conditions will prevail before closure of the repository or parts of it (e.g., during stepwise sealing of disposal drifts after waste emplacement) and in the early post-closure stage. Oxygen trapped in the buffer and backfill materials will be consumed in several ways: corrosion of metallic elements, oxidation of pyrite (both in certain bentonites (e.g., FEBEX) and in host rock (e.g., Opalinus Clay and Callovo-Oxfordian formation). The high initial thermal load imposed by the vitrified HLW will probably impede biofilm formation on the surface of the canisters.
- Following the emplacement, the canister surface will be subjected to temperatures >90°C and thermally-induced drying at the canister surface/bentonite interface occurs (dry-out stage). Water activity will be low and under those conditions, low corrosion rates and general corrosion processes occur, which do not endanger the performance of the metallic canister (Turrero et al., 2021).

- Aerobic corrosion under oxidizing/unsaturated conditions can produce multi-layered corrosion products, which in order of proximity to the metal surface can be magnetite/maghemite, hematite, goethite and lepidocrocite. Green rust may form as an intermediate product transforming later into hematite or magnetite (cf. Majzlan et al., 2003; Torres et al., 2009; Torres, 2011; Torres et al., 2014).
- At this phase, changes in the bentonite properties due to iron/clay interaction are not expected since there is no water to mobilize iron (Torres et al., 2014; Turrero et al., 2021), though some bentonite properties may intrinsically change due to the elevated temperatures.

During a transient phase to anaerobic conditions (≈20 (50) to 100 years), temperature and hydration gradients induce an increase in the corrosion rate and localized corrosion. The mineralogy of the bentonite can be altered to non-swelling Fe-rich phyllosilicates.

- In this stage corrosion will occur mainly under unsaturated condition, but as system hydrates relative humidity will increase and a moisture film will form on the metal surface. The temperature at the canister/bentonite interface will be around 90°C or higher, depending on the disposal concept, which have to be taken into account, as corrosion rate increase with that higher humidity and high temperature. The time leading from aerobic to anaerobic conditions will depend primarily on the (advective-)diffusive transport of oxygen, either in the gas or liquid phase, in the unsaturated compacted bentonite, and on the corrosion rate of iron and accessory minerals (e.g., pyrite) as well, as corrosion progressively consumes the oxygen of the system.
- The aqueous chemistry at the interface will depend on the interaction between the groundwater (fresh or saline) and the bentonite, which may lead to precipitation of salts (e.g., NaCl and $CaSO_4$). At this stage temperature is still high; the saturation of the system progresses and the bentonite at the interface remains unsaturated although relative humidity increases. Under these conditions, geochemical evolution of the bentonite barrier can result in the formation of saline fronts in the vicinity of the canister (e.g., Cuevas et al., 2002), which can affect the corrosion rate and promote localised corrosion (e.g., Druyts et al., 2001; Bradbury et al., 2014). The existence of hygroscopic salts can decrease the value of critical relative humidity (CRH) and significantly enhance corrosion processes at relative humidity quite lower than 100%. Hygroscopic salts sorb moisture and form concentrated brines that promote the electrochemical corrosion of steel and the nucleation of pits on the metal surface leading to localized corrosion. The nucleation time for pits depends on factors such as the oxidizing character of the environment, the concentration of aggressive ions such as chlorides, pH and the alloy composition of the metal. Sulphates could also be relevant in the presence of microorganisms because sulphate reducing bacteria are primarily responsible for microbial induced corrosion.
- As saturation advances, the chemical composition of bentonite porewater will homogenize along the clay barrier due to diffusion and the generated saline fronts will disappear. When the residual oxygen is consumed other mechanism could be responsible for localized corrosion, for example, the reductive dissolution of Fe(III) corrosion products coupled to Fe dissolution of the inner layers (electrochemical corrosion). Once oxygen has been depleted and anaerobic conditions are reached, corrosion will turn general and uniform. Green Rust (GR), a group of mixed Fe(II)/Fe(III) hydroxides will be the prevailing corrosion product in moderately reducing environments and circumneutral pH as those expected in this phase (e.g., Torres et al., 2007; Turrero et al., 2021).
- As canister corrosion progresses and relative humidity increases alteration in the bentonite mineralogy can occur, in terms of precipitation of iron corrosion products in the surroundings of the interface, destabilization of montmorillonite and replacement by Fe-rich smectites or by non-swelling Fe-rich phyllosilicates (e.g., chlorite, berthierite, cronstedite, serpentine) and cementation due to precipitation of iron corrosion products or of SiO_2 resulting from montmorillonite transformation (e.g., Guillaume et al. (2003; 2004); Wilson et al. (2006a); Charpentiera et al. (2006); Mosser-Ruck et al. (2010); Torres (2011); Jodin-Caumon et al. (2012)).

The radiation fields in the vicinity of the steel/bentonite interface may cause water to decompose into a range of redox-active species which can significantly influence corrosion kinetics. Then, an increase of the corrosion rate of the steel may occur (Kursten et al., 2004b; Padovani et al., 2017). Over a certain dose of γ-radiation (>10–20 Gy h^{-1}) the bentonite properties might be affected as well, mainly decreasing cation sorption capacity, what indeed affect the swelling potential of clay, and inducing changes in the redox reactivity of the material (through changes in the Fe(II)/Fe(III) ratio) (Allard et al., 2012; Holmboe et al., 2012; Lainé et al., 2017). During first stages of the repository life, radiation could also have an impact on the decreasing of microbial activity at the steel-bentonite interface.

After the transient stage (i.e., after about 100 years), conditions are expected to be anaerobic and with decreasing temperatures long-term conditions will be approached. At this stage the chemical environment at the interface between steel and bentonite/clay is anoxic and the pH is close to neutral. The saturation of the clay, decreasing of temperature and reducing conditions will favour uniform corrosion. Anaerobic corrosion of steel will lead to the generation of H_2 gas at this stage. Microbially-mediated corrosion might also occur. However, in compacted bentonite there may be too limited space for microbial activity.

- As time advances, average temperature in the steel surface will decrease to 50 or 60°C, enhancing saturation and swelling of the bentonite at the contact. As relative humidity increases, canister surface will become uniformly wetted. In this phase, it is foreseen that residual oxygen has totally been depleted and reducing conditions are achieved. Then, anaerobic corrosion of the steel canister will occur and corrosion will become uniform (Turrero et al., 2021).

- Anaerobic corrosion of steel consumes water and involves the generation of gas (H_2) (see section 3.2). Hydrogen produced could alter physical properties of the bentonite (e.g., formation of microfractures or preferential pathways). However, the expected corrosion rates will be extremely low. Therefore, gas generation is expected to be low as well. Hydrogen pressure is unlikely to exceed the breakthrough pressure of compacted bentonite (Levasseur et al., 2023; Mollaali et al., 2023). In the case of exceeding it, microfractures can be formed. However, bentonite is expected to be able to self-seal these fractures under saturated conditions.
- Microbial activity, in particular sulphate reducing bacteria may be important during this period by modulating redox conditions and transformation of iron phases (e.g., Smart et al., 2017c); However, temperature, low porosity and swelling pressure of saturated bentonite is expected to act as a protective film against microbially-influenced corrosion (MIC) (e.g., Stroes-Gascoyne et al. (2007, 2010)).
- Corrosion rates will be below 10 μm yr^{-1} and corrosion products will be largely tied to site-specific conditions (e.g., Kursten et al., 2004a; Smart et al., 2017b). Magnetite, siderite and iron sulphides will be mainly formed, depending on the clay and the chemistry of solution (e.g., carbonate, chloride and sulphide concentration), pH and redox potential (Wersin et al., 2003; Smart et al., 2004; Torres et al., 2007; Necib et al., 2019). Green rust may occur as a metastable intermediate phase. Iron corrosion products formed *in situ* in the presence of claystone are typically iron silicates and carbonates and, more rarely, iron sulphides (De Combarieu et al., 2007; Schlegel et al., 2014; 2016).
- Sorption sites on the clay can be filled by ferrous ions (e.g., Charlet and Tournassat, 2005; Gehin et al., 2007), which may compete with radionuclides or may act as a precursor of new Fe-Si phases. Also, reduction of structural Fe(III) can occur increasing the cation exchange capacity. Bentonite can be transformed into Fe-rich non-swelling silicates such as berthierine, cronstedtite or chlorite (e.g., Lantenois et al., 2005; Montes-H et al., 2005; Wilson et al., 2006a; Bildstein et al., 2006; Schlegel et al., 2008; Lanson et al., 2012). This could jeopardize the long-term performance of the clay barrier by decreasing the swelling capacity, enhancing the hydraulic conductivity and increasing brittle failure.
- The formation of secondary minerals at the interface steel-bentonite/clay can affect physical properties such as porosity and microstructure of the bentonite, which in turn would have an impact on the transport properties for solutes or gases at the interface.

3.3.1 Concluding perspective

The evolution of the repository environment (thermal, hydraulic and/or chemical gradients) from the initial post-closure stage until the system reaches long-term conditions will impact on the chemical evolution of the steel/iron-bentonite interface. Laboratory and *in situ* experiments, as well as investigations on analogues, evidence that many of the processes and mechanisms occurring at the steel canister/bentonite interface are reproducible under similar conditions and are well understood under a broad range of temperature and physico-chemical conditions. Results show that corrosion rates and products are well established and can be predicted by reactive transport models, if a number of variables such as humidity, pH, concentrations of dissolved salts, organic carbon and oxygen concentration are known in each stage of the repository evolution. However, to do that, it is necessary to establish clearly the evolution of the system from the dry-out stage up to system get equilibrium conditions, which is a difficult issue since is highly dependent not only on *in situ* conditions at each stage, but also on variables still not well known, such as the role of gamma-radiation in the corrosion rate during first stages of the repository and also the role of microbial activity along the lifetime of the repository. The results of laboratory and *in situ* experiments, as well as from archaeological or natural analogues (see Deissmann et al., 2024) highlight the ability of the clay to absorb or react with Fe(II) when anaerobic corrosion occurs. Swelling capacity of the smectite may decrease as a consequence of the formation of Fe-rich non-swelling clays (e.g., berthierine, cronstedtite and chlorite). Also, sorption sites on the clay can be filled by ferrous ions that can compete with radionuclides. The understanding of the interactions at the interface between steel and bentonite/clay is continuously increasing on the basis of laboratory experiments, field experiments in underground research laboratories and modelling studies. Extensive numerical reactive transport modelling studies of the interactions occurring at the steel-bentonite/clay interface under typical repository conditions and the effects of corrosion products on the bentonite have been performed in the last two decades (cf. Bildstein and Claret (2015); Claret et al. (2018); Bildstein et al. (2019) and references therein). Although the numerical studies often differ on the precise nature of the main secondary minerals, the extent of the perturbation is always predicted to be limited to a few centimetres (<20 cm) into the clay barrier in the long term. Further improvements of reactive transport simulations of steel-clay interfaces are expected by the coupling of electrochemical corrosion models that calculate the steel corrosion rates as function of geochemical conditions (e.g., Bataillon et al., 2010; King, 2014) to reactive transport modelling codes (Bildstein et al., 2019).

3.4 Interface "steel—Crystalline rocks"

In general, a direct interface between steel and crystalline host rocks does not exist in repository concepts since there is always cementitious backfill or bentonite between the steel containers and the crystalline bedrock (Neeft et al., 2020). For example, in Finland at the Olkiluoto site, parts of the low and intermediate level waste (containing both, carbon steel and stainless steels) are packed into carbon steel containers that are buried into concrete layered silos located 60–100 m under the sea level in crystalline bedrocks (Somervuori and Carpen, 2021). Thus, the main interaction between steel (e.g., in waste containers) and granite can occur via granitic ground water. In case of a cementitious backfill, the evolution at the surface of the steel would be similar to those described in section 3.2, until the cementitious material is nearly completely degraded, and the pH and composition of the pore water approaches the one of the bedrock groundwater.

In the following paragraphs, only the interactions of steel with bedrock groundwater in a crystalline repository environment are considered, since the host rock is deemed not to be affected by the presence or corrosion of steel (Somervuori and Carpen, 2021). In contact with (granitic) groundwater, corrosion of steel is affected by pH, temperature, oxygen content (redox), ground water

composition, radiation, and the presence of microbial activity. Generally, groundwaters in crystalline rocks can exhibit a wide range of hydrogeochemical characteristics, ranging from lowly mineralised waters (representing, e.g., also glacial meltwater) to higher saline brackish or marine waters, or basement brines, depending on repository site and depth.

The pH conditions in bedrock groundwater in crystalline rocks are usually close to neutral (about 8). In anoxic conditions, corrosion rates of carbon steels are very low unless the groundwater is highly acidic or microbial activity is high. In neutral anoxic and abiotic environments, corrosion rates of carbon steel were found to be about 1 μm yr^{-1} or below (e.g., Smart et al. (2001). Under these conditions, formation of a magnetite (Fe_3O_4) film on carbon steel retards the rate of corrosion in groundwater environments (Smart et al., 2001).

Temperature is an important factor in corrosion of steel because a higher temperature usually means accelerated corrosion rates. In the bedrock, the temperature depends on the depth from the surface and the geothermal gradient and therefore on repository site and concept. Moreover, disposal of high-level waste can lead to elevated temperatures in the repository near field for several hundreds of years, depending on the heat output of the waste and the repository lay-out. Smart et al. (2001) found a large increase in the initial corrosion rates of carbon steel (1–2 orders of magnitude compared to ambient conditions) at elevated temperatures (up to 85 °C) in anaerobic granitic groundwater. The initial corrosion rates were at the level of 10–30 μm yr^{-1} but dropped to less than 0.1 μm yr^{-1} after an oxide film had formed on the steel surface. This suggests that the diffusion of various (aggressive) species through the film becomes more determinative for the corrosion process and the corrosion becomes less sensitive to temperature over time (cf. section 3.2).

The redox environment is very important in metal corrosion since many corrosion reactions need oxygen. In oxygen containing aqueous environments, the corrosion rates of iron and carbon steel are typically in the range from 0.05 to 0.15 mm yr^{-1}, i.e., several orders of magnitude higher than under anoxic conditions (Tunturi, 1988). In oxygen free (anoxic) water, the corrosion of carbon steel is very low unless the water is acidic or there is microbiological activity on the surfaces (e.g., due to the presence of biofilms), due to the formation of a passivating magnetite film on carbon steel surface. In the anoxic abiotic Finnish bedrock groundwaters the average corrosion rate of carbon steel was between 1.1 μm yr^{-1} and 0.4 μm yr^{-1}, which was higher than the recorded values for corrosion rates of stainless steels (Carpén et al., 2018).

The groundwater composition in crystalline bedrocks can exhibit a wide range of compositions and salinities, depending, *inter alia*, on the source of the groundwaters (e.g., fossil seawater, glacial meltwaters, near-surface groundwater, basement brines), ground water age and the extent of water-rock interaction. From the viewpoint of steel corrosion, in particular the concentration of chlorides and sulphates are of interest, since they are known to increase the steel corrosion rates at elevated concentrations and promote pitting corrosion (cf. section 3.2).

The effect of the radiation fields in a nuclear waste repository on the corrosion of steel is not clear and experimental results have been found to be inconclusive. Whereas some authors found no significant effects of gamma irradiation on the uniform corrosion of low-carbon steel aside from some pitting corrosion and an increase in hydrogen generation (e.g., Ahn and Soo, 1995), Liu et al. (2017) reported an increase in the corrosion rate of a carbon steel intended as canister material for high-level waste by 33% due to gamma irradiation with a rate of 2.98 kGy per hour. This radiation rate is not expected for vitrified HLW disposal cells (see Figure 8).

The corrosion of carbon steel in anoxic groundwater is strongly affected by microbial biofilms and their metabolic activity, since microbiological activity on the steel surface accelerates the corrosion rate in oxygen free water (i.e., under anoxic conditions), e.g., due to decrease in the local pH (Small et al., 2008). Corrosion induced by microorganisms is mainly localized corrosion (Rajala, 2017). In the presence of carbon steel, the microbial community in anaerobic groundwater was found to be more diverse and abundant than in the same environment without carbon steel (Rajala et al., 2015). Černoušek et al. (2019) found that in natural granitic water in anaerobic conditions, the corrosion rate of carbon steel was accelerated due to biofilm formation. However, the formation of a biofilm, which was dominated by sulphate-reducing bacteria inhibited the corrosion rate at slightly elevated temperatures.

3.4.1 Concluding perspective

A direct interface between steel and crystalline bedrocks does not exist in geological repository concepts for nuclear wastes (except, e.g., for the use of rock bolts), since there is always cementitious backfill or bentonite between the steel containers and the crystalline bedrock (cf. sections 2.2.2 and 2.2.3). Thus, only an indirect interaction via groundwater occurs, which, however, is modified by the presence and nature of the backfill material. Corrosion of steel/iron in contact with ground water is affected by many factors including pH, redox and composition of water. High pH tends to decrease corrosion rates of steel whereas high chloride and sulphide contents in groundwater induce localized corrosion. During glaciation events, glacial meltwaters with low salinity and enriched in oxygen intruding on fractures may enhance the steel corrosion. However, Fe(II)-minerals in the host rocks may act as redox buffer and may counterbalance advective oxygen fluxes (e.g., Trinchero et al., 2017; 2018). The role of microbes on the corrosion of steel in anaerobic conditions is important and has to be taken into account in crystalline bedrock environments. The effect of radiation on the corrosion of steel is not resolved yet. The effect of steel corrosion on the crystalline bedrocks is deemed to be negligible.

3.5 Interface "concrete—Clay"

In many disposal concepts for radioactive wastes, significant use is made of cementitious materials, for example, as structural support material for access galleries and disposal drifts or cells (e.g., concrete/shotcrete), as well as grouts/mortars used as containment material for intermediate level wastes (cf. section 2; Neeft et al. (2020)). Thus, these cementitious materials can be in contact with both, the host rock clay formation and bentonite barriers (cf. NEA, 2012; Sellin and Leupin, 2013; Neeft et al., 2020). Due to the contrasting chemical and mineralogical properties of cementitious materials and clays, interactions will occur at the cement-clay interface as a result of the chemical gradients. For example, the pH of pore waters in either clay formations (e.g., Opalinus clay, Callovo Oxfordian clay, or Boom clay) and bentonite is typically in the range of pH 7 to 8.5. In contrast, the progressive degradation of cementitious materials after

resaturation of the repository leads to a pH in the cement pore fluids ranging over time from 13.5 (for systems based on Ordinary Portland Cement, OPC) to 10 (for details see section 2.2.6), slowly approaching the pH of the surrounding ground water in the long-term (Berner, 1992; Glasser, 2011; Beattie and Williams, 2012; Hoch et al., 2012; Drace and Ojovan, 2013). Even in so-called low-pH cementitious materials the initial pH of the young pore water can often be above pH 12 (e.g., Vehmas et al., 2020). The term low-pH cementitious material is used here for cementitious materials/concrete where significant amounts of OPC in the binder is replaced by siliceous supplementary cementing materials, in particular silica fume, ground granulated blast furnace slag, or fly ashes.

Within the context of deep geological disposal of nuclear waste disposal, cement/clay interactions have been investigated for more than three decades by means of laboratory and *in situ* experiments, studies on natural and industrial analogues, and reactive transport modelling. Comprehensive reviews on various aspects of cement/clay interactions have already been published in the past decades (e.g., Metcalfe and Walker 2004; Michau 2005; Gaucher and Blanc 2006; Savage et al. (2007; 2009; 2011; Sidborn et al., 2014; Bildstein and Claret, 2015; Dauzeres, 2016; Claret et al., 2018; Savage and Cloet, 2018; Bildstein et al., 2019).

Short term laboratory (e.g., Adler, 2001; Adler et al., 1999; Dauzères et al. (2010; 2014; Fernández et al., 2016; Balmer et al., 2017) and longer-term *in situ* experiments (up to about 20 years) at different underground research laboratories like HADES, Mol, Belgium (Read et al., 2001), Mont Terri, Switzerland (e.g., Jenni et al., 2014; Dauzeres et al., 2016; Lerouge et al., 2017; Mäder et al., 2017), Bure, Department Meuse/Haute Marne, France (e.g., Gaboreau et al. (2011; 2012); Dauzeres et al. (2016)), or at the Tournemire site in France (e.g., Tinseau et al. 2006; Techer et al. (2012a; b); Lalan et al. (2016); Bartier et al. (2013)), as well as the FEBEX experiment in the Grimsel test site in Switzerland (e.g., Alonso et al., 2017; Fernández et al., 2017; Turrero and Cloet, 2017) have demonstrated that at the cement/clay interface, alteration of both cement paste and clay material take place, leading to mineralogical changes that modify the microstructure of the altered region, which may influence transport relevant properties such as porosity and permeability, or the radionuclide retention behaviour of the materials.

3.5.1 Processes at the interface

Due to the contrasting chemical and mineralogical properties of cementitious materials and clay rocks or bentonite, reaction zones will develop, with diffusive transport of aqueous species across the material interface in response to chemical gradients. These gradients develop typically from the higher concentrations (activities) of species such as OH^-, K^+, and Ca^{2+} in the cementitious materials, thus tending to diffuse towards the clay materials[3]. In contrast, the concentrations of species such as Mg^{2+}, $SiO_2(aq)$ and HCO_3^-, are often higher in the pore water of the clay formation/bentonite, thus tending to diffuse into the cementitious materials. Based on the existing literature the following key processes have to be considered at cement/clay interfaces, as observed in laboratory and *in situ* experiments, and/or as inferred from natural analogue studies, performed in Maqarin (Jordan), Cyprus or the Philippines (e.g., Alexander et al. (1992; 2008); Alexander and Smellie (1998); Crossland (2006); Alexander and Milodowski (2011); Reijonen and Alexander (2015)), Milodowski et al. (2015,2016), Savage (1998)) and various modelling studies:

- Diffusion of hydroxyl anions from the cement into the clay will destabilize silicate/aluminosilicate minerals, leading to slow hydrolysis of montmorillonite and other aluminosilicate minerals present (e.g., Cuevas et al., 2006; Yamaguchi et al., 2007), consuming OH- ions and neutralising the high pH fluids, but leading to a decrease in swelling pressure of smectitic clays.
- Replacement of clay minerals by calcium silicate hydrates (C-S-H), sheet silicates, and/or zeolites, with the secondary minerals forming in a zonal fashion (e.g., Cuevas et al., 2006; Gaucher and Blanc, 2006; Savage and Benbow, 2007; Savage et al., 2007; Bamforth et al., 2012), potentially leading to an overall decrease in porosity (due to differences in molar volumes) and changes in the rheological properties of the clay (e.g., Jefferies et al., 1988).
- Decalcification due to dissolution of portlandite ($Ca(OH)_2$) and C-S-H, thus reducing its Ca/Si-ratio, in the cementitious material accompanied by rapid precipitation of Ca-carbonates, such as aragonite and calcite, directly at the interface, due to steep gradients in hydroxyl ion concentrations (higher on the cementitious material) and the partial pressure of carbon dioxide ($pCO_2(g)$, higher in the clay rock formation) across the cement/clay-interface; these reactions lead to an increase in porosity in the cementitious material and a porosity decrease in the clay in the longer term. In low-pH cementitious materials, where portlandite may be lacking, the decalcification of the C-(A)-S-H can proceed directly, leading to an earlier formation of amorphous silica as residue. However, low-pH cementitious formulations with slag and micro silica have a more refined pore structure leading to lower diffusivity and thus lower rates of mineral alteration.
- Formation of calcium aluminium silicate hydrates (C-A-S-H) and (amorphous) magnesium silicate hydrates (M-S-H) at the interface, affecting porosity and transport properties at the interface (e.g., Dauzeres et al., 2016), and replacement of portlandite, C-S-H gel and monosulphoaluminate by ettringite (e.g., Savage, 2014). Note that in low pH formulations, C-A-S-H can be present already as initial hydration phase.
- Redistribution of sulphate towards the unaltered cementitious matrix due to the decrease in pH close to the interface, destabilizing earlier formed Ca-Al-sulphates (ettringite, monosulphate (AFm)) that re-precipitate in the higher pH regions (e.g., (Mäder et al., 2017)).
- Fast exchange of cations in interlayer sites in montmorillonite, due to diffusion of K^+, Na^+ and Ca^{2+} from the cementitious material into the clay, leading to a decrease of swelling pressure.

3 In more saline clay host rocks, i.e., in France, Switzerland and the Netherlands, the dissolved Ca2+ concentration can be higher than this concentration in concrete pore water (see Supplementary Information).

- Fast protonation-deprotonation reactions at clay edge sites, retarding the diffusive migration of hydroxyl ions due to reversible sorption processes.
- Slow hydrolysis of montmorillonite and other minerals present, either as additives (e.g., quartz sand), or as accessory minerals reactions consuming hydroxyl ions, thus chemically neutralizing the advancing cementitious porewater, leading to an increase in porosity and a decrease in clay swelling properties.

The studies performed have shown that there is a strong coupling between fluid and solute transport, dissolution of solids and precipitation of secondary phases, ion exchange and edge site sorption on clays, and the consequential changes in physical properties of the materials (i.e., porosity, permeability, swelling pressure of clay) (cf. Savage and Cloet, 2018). Depending on the extent of porosity/permeability changes (e.g., pore clogging), changes in hydraulic conductivity, diffusivity, and gas permeability may occur. Moreover, the potential dissolution and replacement of clay minerals may alter the safety-relevant swelling properties and sorption capacity of the clay materials. However, the extent of alkaline disturbance in the clay host rocks is limited to a few meters in the long term. The processes occurring at the cement/clay interface as well as their kinetics will depend to a large extent on the initial properties of the materials, such as the nature of the cementitious binder (OPC or low pH binder), the mineralogy and pore water composition of the clay material, and their initial transport properties (e.g., porosity, diffusivity, incl. water saturation) and thus on repository concept and site. Thus, the extent and significance of these processes will need to be assessed on a site-specific basis (cf. NDA, 2016). Due to this complexity and diversity, it is difficult to establish a general sequence of secondary minerals forming in the cement domain due to the impact of the clay pore water. Details on experimental observations with respect to secondary phases formed at the interfaces between various cementitious materials and clays, clay rocks or bentonite have been compiled e.g., by Dauzeres (2016) and Deissmann and Ait Mouheb (2021).

The (long-term) interaction of cementitious materials with clays, clay rocks and bentonites have been subject to a large number of reactive transport modelling studies (cf. reviews in Bildstein and Claret (2015); Claret et al. (2018); Bildstein et al. (2019); Deissmann and Ait Mouheb (2021)). In these simulations, cement-clay interactions have been mainly modelled as coupled Thermal-Hydraulical-Mechanical-Chemical (THMC) processes in continuum scale reactive transport simulations, based on thermodynamic equilibria sometimes with the inclusion of kinetic data and diffusive transport, with various degrees of complexity. Most simulations addressed the interactions between cementitious materials and natural clay rocks, whereas relatively fewer studies investigated the interaction with bentonites. In the majority of the cases, OPC-based high-pH cementitious materials were addressed (CEM I); only recently, interface processes between low pH cementitious materials have been addressed in reactive transport modelling studies at different time and length scales (e.g., Berner et al., 2013; Dauzeres et al., 2016; Idiart et al., 2020). With respect to the simulation of laboratory and *in situ* experiments, it can generally be concluded that reactive transport modelling shows a great capability for reproducing the experiments, e.g., regarding mineralogical transformation pathways and net porosity evolution (cf. Bildstein et al., 2019). Despite the differences in the approaches of long-term simulations of cement-clay interactions, there are general similarities in terms of the predicted thickness of the altered zones in the clay and cement domain, the types of secondary solid products and changes in porosity. Simulations of the long-term evolution of the interface revealed a narrow zone (mainly in the order of cm to dm) of perturbed mineral and fluid chemistry located close to the interface, for timescales up to and beyond 100,000 years (cf. Savage and Cloet, 2018; Bildstein et al., 2019). Regarding the predicted mineral transformations there are recurring results, such as decalcification of cementitious materials (i.e., portlandite dissolution, decrease of the Ca/Si ratio in C-S-H), precipitation of ettringite in the presence of sulphates, and/or carbonation and smectite dissolution, dedolomitisation, as well as formation of C-(A)-S-H solids, clay minerals (illite, saponite), zeolites and carbonates in the clay domain. Critical parameters identified in the various studies comprise dissolution/precipitation kinetics and the description of evolving reactive surface areas that can play an important role in sequential minerals' appearance or disappearance, the localization of porosity reduction and increase, the kinetics and the laws controlling the porosity/permeability and porosity/diffusivity feedback, and the inclusion of certain secondary phases (e.g., zeolites) and their thermodynamic/kinetic parameters.

3.5.2 Concluding perspective

The evolution of the interface between cementitious materials and clays (incl. poorly indurated clays, clay rocks, or bentonites) within the context of nuclear waste disposal has received widespread attention in the last decades. Substantial progress has been made in the characterization of the mineralogical and microstructural changes over relatively long time periods in the frame of experimental studies and by investigation of natural analogues. Additionally, reactive transport modelling appears to predict well the chemical evolution occurring at the interface between cementitious and clay materials. The inclusion of new thermodynamic data on relevant phases (e.g., M-S-H, C-A-S-H, zeolites) that were made available recently (e.g., Roosz et al. 2018; Ma and Lothenbach (2020a, b, 2021); Lothenbach et al. 2019) will probably lead to a further improvement of long-term predictions and the understanding of the interactions of cementitious materials with clays in the context of the evaluation of repository safety.

3.6 Interface "concrete—Granite"

Cementitious materials are employed for various purposes also in waste repositories in crystalline (granitic) rocks (cf. Neeft et al., 2020). For example, the disposal tunnels are sealed with concrete end plugs to ensure mechanical and hydrological isolation of different compartments. In the Finnish final repository for HLW (i.e., spent nuclear fuel), several thousand tons of Ordinary Portland Cement (OPC)–based grouts, shotcrete and rock bolt mortars will be

present in structural applications and for sealing of fractures. Also, in the LLW repository in Finland, isolation is achieved by a combination of cementitious barriers and the granitic host rock (cf. Leivo, 2021). Processes occurring at the interface of cement/mortar/concrete and granite can change both the properties of the cementitious material and the granite properties at the interface.

3.6.1 Processes in concrete

In general, cement-based materials used in the groundwater environment are fundamentally unstable in a long-term perspective, due to thermodynamic disequilibrium with their environment. Thus, concretes and cementitious materials/barriers used in geological disposal facilities in crystalline rocks (or clay rocks) will inevitably change their mineralogical, chemical and physical properties in the long-term, both as a consequence of recrystallisation and chemical interactions with their environment. With respect to the long-term evolution of cementitious materials at the interface to granitic/crystalline rock, interactions are mainly related to the contact with the groundwater present in the bedrock. Generally, groundwaters in crystalline rocks can exhibit a wide range of chemical characteristics ranging from lowly mineralised waters (representing, e.g., also glacial meltwater) to higher saline brackish or marine waters, or basement brines, depending on repository site and depth. The processes occurring in the cementitious materials in a repository due to the contact with granitic groundwaters depend on the local environmental conditions (in particular the groundwater composition) and comprise the typical processes described in detail in the respective literature in the context of the performance and degradation of cementitious construction materials in the subsurface (e.g., Taylor, 1997; Hewlett, 1998). These processes include in particular.

- removal of alkalis and decalcification,
- carbonation,
- attack by aggressive species (e.g., magnesium, sulphate, chloride), and
- alkali-aggregate reactions.

Leaching of alkalis and decalcification causes changes of many physical and mechanical properties of cement-based materials such as porosity, elastic modulus, compressive strength, internal friction angle and creep. Leaching of concrete by percolating or flowing water can cause severe damage, e.g., in dams, pipes or conduits, and is potentially important for the long-term evolution of repository systems for nuclear wastes. These processes are expected to remove alkali hydroxides, dissolve portlandite ($Ca(OH)_2$) and decompose the hydrated silicate (i.e., calcium silicate hydrates, C-S-H) and aluminate phases (AFm/AFt), leading to a concomitant decrease of the pH of the pore solution in the cementitious materials. Initially, dissolution of KOH and NaOH within the cement will form a pore water with pH ~13. The pore water pH will then decrease to ~12.5 where it will be buffered by equilibration with portlandite. This pH will remain until all portlandite has dissolved, after which, pH will be controlled by equilibrium with the incongruent dissolution of the C-S-H gel and will decrease to ~10.5. The ultimate residue will consist essentially of hydrous forms of silica, alumina and iron oxide, while all CaO will be lost. By this stage, the cement paste will be disintegrated. The schematic evolution of pore solution pH during degradation of OPC based cementitious materials by pure, demineralised water is shown in Figure 7. Removal of alkalis and decalcification generally lead to an increase in porosity/permeability and diffusivity in cementitious materials.

Carbonation occurs when carbon dioxide dissolves in the pore solution of cement paste, producing CO_3^{2-}ions, which will react with Ca^{2+} and produce $CaCO_3$ (calcite) on the expense of portlandite. Later, when portlandite is consumed, C-S-H is first decalcified and later decomposed. The AFm and AFt phases react with the carbonate anions and can form special carbonate phases (e.g., thaumasite, $Ca_3Si(OH)_6SO_4CO_3{\cdot}12H_2O$ and has been observed for buried concrete (Tsivilis et al., 2007)). If pH is lowered further by addition of more carbon dioxide, these initially formed carbonate species will decompose. The residues from complete carbonation of cementitious materials are calcite, amorphous silica, hydrocarboaluminates and different Al- and Fe-hydroxides. The pH value of the carbonated cement paste first drops to around 10 when all portlandite is consumed and later to a pH around 8, when the other phases are decomposed. These carbonation reactions are mostly happening at a slow rate and are especially pronounced during the operational phase of the repository, when the cementitious materials are in contact with gaseous CO_2 from the ventilated tunnels, and, in later stages, due to CO_2 production from degrading organic wastes, or due to interaction with carbonate-rich groundwaters. Due to microstructural changes, carbonation is often accompanied by a reduction of permeability and diffusivity of cementitious materials.

Sulphate attack in concrete originates mainly from interaction with sulphate rich groundwaters. The damage to concrete structures resulting from external sulphate attack is related to the chemical reactions between sulphate ions and the solid cement hydration products, leading in particular to the formation of ettringite ($Ca_6(Al,Fe)_2(OH)_{12}(SO_4)_3{\cdot}26H_2O$) and gypsum ($CaSO_4{\cdot}2H_2O$), which occupy a larger volume than their educts. This can lead to the generation of stress in the interior of the concrete as a result of the formation of the expansive products, which in consequence results in a mechanical response of the bulk material, such as cracking. However, the potential effects of sulphate attack in cementitious repository materials can be minimized by the utilisation of sulphate resistant cements.

The attack by magnesium ions present in groundwaters can be particularly deteriorating for concrete structures, as it can cause a complete disintegration of the C-S-H phases in the long term. In contact with magnesium rich groundwaters, the magnesium replaces the calcium in the hydration phases leading to the formation of amorphous $Mg(OH)_2$, magnesium silicate hydrates (M-S-H) as well as Mg-containing SiO_2 gel, accompanied with a drop in pH to approx. 10.5 (e.g., Taylor, 1997; Eglinton, 1998).

Deterioration of materials properties due to chloride ingress is one of the main causes of concrete degradation worldwide. Concrete itself is generally not adversely affected by chloride ingress, though the formation of some new chloride-bearing phases such as Friedel's salt ($Ca_4(Al,Fe)_2(OH)_{12}C_{l2}{\cdot}nH_2O$) at the expense of other AFm/AFt phases is possible. However, the steel reinforcement and other steel materials inside concrete can be corroded at elevated chloride concentrations, which may lead to the formation of (expansive) corrosion products accompanied by crack formation due to

mechanical stress. However, this is deemed to be more relevant under oxic conditions that may occur in concrete-granite systems when an insufficient concrete cover has been used or in the presence of glacial meltwaters. The transport and distribution of chlorides in a concrete structure are very much a function of the environmental exposure, i.e., chloride concentration and duration of exposure to solutions in contact with the concrete surface.

Alkali-aggregate reactions (AAR), also termed alkali-silica-reactions (ASR), are chemical reactions occurring between minerals present in certain types of aggregate, and alkali (Na^+ and K^+) and hydroxyl (OH^-) ions present in the pore solution of the cement paste in concrete. These dissolution reactions occur due to the high solubility of certain amorphous, disordered or poorly crystalline forms of silica (SiO_2) in highly alkaline solutions leading to formation of a hygroscopic alkaline gel. In general, these reactions are expansive in nature, resulting in internal stresses in concrete and consequently cracking. It is often accompanied by the appearance of efflorescence and exudations on the surface of the concrete. They can significantly decrease the durability of concrete as a result of cracking favouring other processes of deterioration, particularly in the cases of carbonation or chloride penetration resulting in reinforcement corrosion. However, ASR can be prevented in cementitious materials in the repository environment by using either non-siliceous aggregates, e.g., carbonates or using cements with a low alkali content (e.g., blended low-pH cements). The absence of ASR with the use of quartz aggregates and low-alkali binders has such extensive demonstrated experience that this combination has turned into a best practice for civil engineering. Different time frames are active for geological disposal of waste and ASR can thermodynamically not be excluded. Kinetically, ASR can be minimised through the reaction rims (see Deissmann et al., 2024). The extent of this minimization determines whether ASR has an impact on the chemical evolution of disposal cells.

3.6.2 Processes in crystalline host rocks

The production of alkaline leachates (high-pH plume with evolving pH analogues) developing at the concrete/granite interfaces from alteration of concrete may cause degradation of silicate minerals (e.g., feldspars) in the crystalline bedrock around the repository and precipitation of secondary phases further along fractures, where more neutral pH conditions prevail (Baker et al., 2002). These interactions between the cement leachate and the rock are a potentially important factor for altering flow in the near-field rock, due to clogging of fractures by formation of secondary minerals (e.g., Mäder et al., 2006; Alexander, 2012). However, there are still a number of uncertainties associated with this sealing of fractures due to the formation of secondary minerals (Savage and Cloet, 2018). It has been stated that the beneficial effect of fracture sealing due to cement-host rock interaction cannot be taken into account in the safety case because they cannot be quantified (e.g., Pastina et al., 2012; Koskinen, 2014).

In the last two decades, a number of laboratory studies and experiments in underground research laboratories (e.g., at the Grimsel Test Site in Switzerland) have been performed addressing the interaction of cement leachates with crystalline granitic rocks (e.g., Bateman et al., 1999; Mäder et al., 2006; Pfingsten et al., 2006; Moyce et al., 2014; Lanyon, 2015; Watson et al., 2017), complemented by respective reactive transport simulations (e.g., Soler et al. (2006; 2011); Soler and Mäder (2010); Watson et al. (2017); Chaparro et al. (2017)). There is a general agreement that the dissolution of the primary silicate minerals in granitic rocks by cementitious leachates is followed by the precipitation of secondary phases such as C-S-H, Ca-Al-Si-hydrates (C-A-S-H), magnesium-silicate-hydrates (M-S-H), calcite, clays and zeolites, mainly on fractures. Subsequent transformation of C–S–H to feldspars and zeolites can occur in the longer-term. In general, these reactions are very slow and highly dependent on pH, temperature and groundwater composition.

Recently, Szabó-Krausz et al. (2021) evaluated the geochemical interactions occurring at the granite-concrete interface in the operating LLW/ILW repository at Bátaapáti, Hungary. The main secondary phases observed at the interface after 1–15 months of reaction were the Ca-carbonates calcite and vaterite. Calcite veins occurred along the granite-concrete contact while vaterite precipitated in the pores of the concrete near the interface. This carbonation was explained by Szabó-Krausz et al. (2021) by reaction of Ca released by the dissolution of the cementitious material and HCO_3^- from the local granitic pore water. The carbonation process was found to reduce the porosity and permeability in the contact zone, avoiding or slowing down further interaction of the materials. Moreover, a frequent occurrence of titanite along or near the granite-concrete interface, but always on the side of the granite was observed. It was concluded by Szabó-Krausz et al. (2021) that titanite formed where i) the Ca concentration was not high enough to form carbonates, and ii) sufficient dissolved SiO_2 was in the solution, with the granite serving as a source of TiO_2. The observation of neighbouring calcite and titanite precipitation was seen as indicator for distinctively changing geochemical conditions within short distance of the interface.

3.6.3 Concluding perspective

The physico-chemical processes occurring at the interface between cementitious materials and crystalline, granitic rocks in a deep geological repository can change the mineralogical, geochemical and solute transport properties of both materials. However, compared to the interface between cementitious materials and clays or clay rocks, the interface with granitic/crystalline rocks has received less attention so far. Changes on the concrete side are related to the contact with the groundwater present in the crystalline bedrock and comprise typical alteration phenomena observed in subsurface construction materials, which depend in particular on the composition and pH of the contacting water. The alkaline plume caused by the leaching of concrete due to interaction with the bedrock groundwater will have an influence on the granite by dissolving primary silicate minerals and the precipitation of secondary phases at the interface and on fractures, which may result in changes in the flow regime in the repository near field. In general, the chemical alteration processes at the concrete/granite interface in underground repositories are expected to be rather slow.

4 Narrative time-space evolution at disposal cell scale

An important step in the quantitative assessment of the chemical evolution at the disposal cell scale is the integration of individual studies

in an integrated phenomenological description of the time-space evolution at the disposal cell scale. This section presents narrative evolutions for disposal cells defined using the main characteristics of the HLW and ILW disposal cells in European programmes, based on the information from the individual interfaces (Deissmann et al., 2021) and from the current handling of chemical evolution in European programmes (Neeft et al., 2020). The handling of the chemical evolution can be a compromise between "what occurs", for example, what are the most relevant processes, and "what can be modelled". "What occurs" is an understanding of the processes taking place in the chemical evolution and those processes are included in this section. The 'what occurs' includes assumptions that need to be substantiated. In this section, the chemical evolution is described for evolutions that typically falls under the conditions of an expected or a normal evolution scenario that includes the most likely processes.

4.1 HLW disposal cells

This review contains no overview of experimentally investigated radiological and microbiological processes but it needs to be assessed whether their consequences need to be included in the chemical evolution. The carbon steel overpack (see Sections 2.1.2 and 2.1.3) is considered as an example in order to show how such an assessment can look like. Radiation enhanced corrosion depends on the radiation rate and access to water. Radiolysis of water can generate O_2 by which a more oxidising environment becomes present in the vicinity of the metal overpack. Aerobic steel corrosion rates are larger than anaerobic corrosion rates of steel. The radiation rate can be determined by the activity of the radionuclides in the vitrified waste form and the penetrating power of gamma rays that are released upon decay of these radionuclides. Figure 2 shows that the radiotoxicity of the waste is initially dominated by ^{90}Sr and ^{137}Cs but only ^{137}Cs and its daughter release upon decay a sufficient high gamma energy to contribute to the radiation dose rate at the surface of the carbon steel overpack. The vitrified waste form has guaranteed maxima in activity content of these two radionuclides of 6,600 TBq for ^{137}Cs and 4,625 TBq for ^{90}Sr (AREVA, 2007). The maxima are assumed to be the activity of these radionuclide at time 0 years in Figure 8. The vitrified waste form is not immediately emplaced in a disposal facility but is cooled for a couple of decades; for example, the French programme uses an age of 85 years and 70 years depending on the thermal power of the waste form, in their disposal concept (Cochepin et al., 2020). The half-lives of the radionuclides that initially dominate the radiotoxicity are 29 years for ^{90}Sr and 30 years for ^{137}Cs. Consequently, the radiation dose rate has been significantly reduced upon emplacement of vitrified HLW. The metal overpack has a high density of about 8,000 kg/m^3 and can therefore provide shielding that also limits the radiation dose rate at the outside of the metal overpack. Two examples of thickness of carbon steel overpack have been calculated in Figure 8:

- A thickness of 3 cm, which is characteristic for a disposal package with a concrete buffer as used in the concepts in the Belgian and Dutch disposal programmes (Neeft et al., 2020);
- A thickness of 14 cm, which is the thickness considered in the Swiss programme (Leupin et al., 2016; Levasseur et al., 2021).

Based on the research by Smart et al. (2017b), Figure 8 shows that the thinner carbon steel overpack of 3 cm has a high enough radiation dose rate for radiation enhanced corrosion for a disposal package with a concrete buffer for vitrified HLW with an age of 60 years. If specified, all programmes consider older waste packages (Neeft et al., 2020). Consequently, radiation enhanced corrosion does not need to be included in the chemical evolution in this HLW disposal cell.

Relevant literature about the impact of radiation on steel interfacing bentonite has not been found but the values found for steel exposed to groundwater (Smart et al., 2008b) are considered as a minimum, since the process is attributed to the radiolysis of water and accessible amount of water. Figure 8 shows that the radiation dose rates for a thicker carbon steel overpack interfacing bentonite is too low for radiation enhanced corrosion at any age of vitrified HLW. Also, the dose rates of 10–20 Gy per hour listed in section 3.3 to affect the properties of bentonite do not occur.

It can be deduced from the available literature that radiation enhanced corrosion and microbial induced corrosion can never occur at the same time, i.e., microbial activity is only possible at lower radiation doses rates than required for radiation induced corrosion. Radiation has been known to kill microbes and this information is also used for health reasons such as sterilization of food. The decrease in the number of viable (i.e., culturable on a chosen medium) bacteria as a function of increasing total dose is determined and expressed as the D_{10} value, the total dose required to reduce the viable population by one order of magnitude or 90% (Abrahamsen et al., 2015). D_{10} values are additive; for a reduction of three orders in magnitude, a total dose equal to 3 times the D_{10} value is required. The D_{10} values for relevant bacteria range between 0.5 and 1.57 kGy (Stroes-Gascoyne and West, 1997). Consequently, sterilization can be achieved for any considered age of vitrified HLW since these doses between 0.5 kGy and 1.57 Gy are received multiple times during storage. In research, usually sterilisation levels are achieved with high radiation dose rates, higher than representative for geological disposal. What lacks in the radiation sensitivity of microbes is the equilibrium between the reduction in viable population by radiation and increase in viable population by growth of this population by consumption of nutrients and electron acceptors and donors. Nevertheless, there are several other arguments by which microbial induced corrosion is highly unlikely, i.e., the high temperature load at the start of the post-closure phase, too small connecting pore throats that limit transport of food and energy sources, the drying of the buffers at the start of the post-closure phase by the heat emitted by the waste, and for the concrete buffer also the high pH of the concrete pore water. Microbial induced corrosion is therefore excluded in the narrative for HLW disposal cells, the only microbial activity considered possible is at the interface between bentonite and granitic rock and localised at the fractures in the rock. These microbial processes have negligible effects on the chemical evolution at disposal cell scale.

The chemical alterations of the engineered materials in HLW disposal cells in the post-closure phase are thus determined by:

1) the formation of an alteration layer between two interfacing materials. This alteration layer may have been formed already before or in the operational phase;
2) the diffusional exchange of species through this alteration layer and/or the thickness of the diffusional layer of dissolved species near the alteration layer. The maximum dissolved concentration in this diffusion layer is in equilibrium with the alteration layer. The thickness of this diffusion layer in the interfacing material depends on the speed of migration of the dissolved species in this material and sorption of dissolved species by minerals in this material.

4.1.1 From closure till about 1,000 years

The heat generated by decay of the radionuclides in the vitrified HLW has initially an important effect on the chemical evolution of the engineered barriers. The temperature increase results into a decrease in saturation degree in the buffers by which the access to water needed to continue chemical corrosion is minimized. This effect has been modelled in the Spanish programme for the bentonite buffer in which saturation of the bentonite buffer was achieved within 20 years for HLW disposal cells in granite (Neeft et al., 2020). The input for these modelling studies came from experiemental work performed in the previous century e.g., FEBEX experiment at Mt Terri (see section 3.3). This short period is specific for granitic host rocks since there is sufficient access of water to saturate the buffer. There is less water available to saturate the bentonite buffer in indurated clay. A period between 100 and 1,000 years is foreseen for saturation of HLW disposal cells with bentonite buffers in indurated clay (Leupin et al., 2016). The impact of this difference in access of water is visualized in Figure 9 (first row) with a smaller corroded part of the steel overpack for disposal cells in indurated clay compared to disposal cells in granitic rocks. Such modelling results for the saturation degree in the concrete buffers are available for poorly indurated clay (Poyet, 2006; Weetjens et al., 2006) and are foreseen to have a negligible effect on the chemical corrosion rate, since a temperature of 80°C is achieved within a few decades (Neeft et al., 2020) and the same corrosion rate was measured at 25°C and 80°C (Smart et al., 2017a). After about 1,000 years, a temperature below 50°C is achieved at the steel overpack, and in disposal concepts in which the overpack is enclosed in a bentonite or concrete buffer, the host rock is almost no more heated by the waste (Neeft et al., 2020). Figure 9 (first row) shows that the chemical evolution at disposal cell scale after about 1,000 years is envisaged to be small.

There can be aerobic and anaerobic corrosion processes in this period from closure till about 1,000 years. An alteration layer is formed during this corrosion process. There is thermodynamic data and software available to calculate the stability of alteration layers as a function of the pore water chemistry. Figure 10 shows the Pourbaix diagrams with the available phases of calcium, iron-oxides with and without calcium and bicarbonate in the pore solution. Please note that supersaturated iron solutions have been used in the calculated Pourbaix diagrams; for example, the actual range in pH of the thermodynamically stable magnetite is smaller. The minimum in solubility has been calculated to be 10^{-9} M at 100°C and 10^{-10} M at 25°C (Hermansson, 2004).

4.1.1.1 Aerobic corrosion

Bentonite and concrete buffers contain entrapped oxygen as a result of the fabrication process. This oxygen is consumed by corrosion of steel or by reaction with traces of pyrite; these traces can be present in bentonite and in concrete that has been made with cement that is blended with blast furnace slag (BFS). The alteration layer formed during aerobic corrosion would be hematite as shown in Figure 10. The period in time for aerobic corrosion of the carbon steel overpack by this entrapped oxygen is expected to be smaller than a few years, but section 3.3 considers a transient phase to anaerobic conditions lasting till 100 years. Nevertheless, the available oxygen can be quantified for aerobic corrosion and conservative estimates predict a corroded thickness of 0.7 mm (Alexander and McKinley, 1999).

A period with aerobic corrosion can also be absent for example, in the case of carbon steel interfacing a cementitious material that was a blend of Ordinary Portland Cement (OPC) and BFS (Naish et al., 1991) in which the rest potential is immediately achieved. Magnetite could only be measured on the carbon steel interfacing this cementitious material with BFS that was run for almost 2 years. This magnetite measurement using Raman spectroscopy and the electrochemical measurement provided the evidence that steel had become passivated. Other blends of OPC with fly ash and OPC showed no corrosion product on carbon steel, i.e., steels embedded in these cements still experienced active corrosion after 2 years. But like for clays, also for cementitious materials the available oxygen for aerobic corrosion can be quantified and a maximum in aerobic corroded thickness can be set. A maximum in air content in fabricated concrete is quality controlled through EN 12350–7 (CEN, 2019).

4.1.1.2 Anaerobic corrosion

The anaerobic corrosion of steel uses water as an oxidant and magnetite is predicted in Figure 10. Passive corrosion of steel is achieved when the corrosion rate has become equal to the dissolution rate of the passive film (Grauer, 1988); the magnetite layer constitutes a barrier against transport of water towards steel and of dissolved iron species into solution. This passivation is expected to extend beyond the thermal phase for concrete buffers due to its high pH. However, the presence of magnetite is also assumed and measured for steel exposed to pore water with a lower pH. Precipitation of magnetite as a corrosion product in bentonite has been modelled at 25°C in the Czech and Spanish disposal programmes due to an increase of pH till 10 by iron corrosion at the vicinity of the bentonite-iron interface (Neeft et al., 2020). This rise in pH near the steel surface, which makes precipitation of magnetite thermodynamically possible, can be caused by insufficient dissipation of the generated hydroxyl ions in bentonite. This insufficient dissipation is also present in bentonite pore water by which the formation of magnetite was measured due to a local increase in pH of 10 (Kreis, 1991). The presence of bicarbonate in the pore water has an effect on the formation of the chemistry of the alteration layer. The ingress of bicarbonate into the bentonite buffers may result into a change of the alteration layer from magnetite to siderite as predicted in Figure 10.

The thickness of the steel overpack is at least three times smaller for countries considering a concrete buffer compared to countries that have chosen a bentonite buffer. The found long term corrosion

rates, i.e., after an alteration layer has been formed, are also different by orders of magnitude. The long-term corrosion rates of carbon steel from section 3 are:

- below 10 μm per year, if this steel interfaces bentonite (see section 3.3);
- in the range of 0.1 μm per year or lower, if this steel interfaces concrete (see section 3.2);
- below 0.1 μm, if this steel interfaces granitic pore water (see section 3.6).

The higher corrosion rates for steel interfacing bentonite may be understood from the surface charge of minerals in the buffers. The zeta-potential of clay minerals in bentonite buffers is negative by which there is preferably sorption of cations. The speciation of dissolved iron is $Fe(OH)^+$ for pH < 11 and $Fe(OH)_3^-$ for pH > 11 as shown for the Pourbaix diagrams in Figure 10, as long as the bicarbonate content of the pore water is limited. The selective sorption of $Fe(OH)^+$ onto the clay minerals reduces the thickness in the diffusion double layer for the dissolved concentration of iron species. This reduction in thickness enhances the dissolution of the alteration layer and thereby corrosion. It is known that the tendency of the sorption of dissolved iron may increase the corrosion rate in clay (Johnson and King, 2008; Savage, 2014).

The zeta potential of cement minerals in concrete is positive at a pH > 11.8 (Pointeau et al., 2008)[4] (see Figure 7). There could also be sorption of dissolved iron species such as $Fe(OH)_3^-$.

Archaeological analogues (e.g., Dillmann et al., 2014) indicate that the chemical interaction between the buffers (clay and concrete) and steel remain in the vicinity of the interfaces. Cross section analysis from the metal or iron towards the porous materials - soils (e.g., argillaceous sediments) or cementitious materials - show similar patterns: steel, a Dense Product Layer (DPL) with corrosion products, a zone in which the porous medium (soil or concrete) has chemically altered (Transformed Medium, TM) and the porous medium (soil or concrete).

4.1.1.3 Dense Product Layer/inner layer

The porosity of DPL has been measured to be 10 vol% (Chitty et al., 2005). Archaeological analogues of steel with a porous medium (soil or concrete) are obtained at lower temperatures than envisaged at the steel overpack. The chemical interaction at the clay-iron interface at 90°C shows however a similar result, except that the DPL is further subdivided in an internal and external DPL (Figure 5-2[5] in Deissmann et al. (2021)). Other definitions of DPL and TM are a fairly dense Inner layer and an Outer layer (Atkins et al., 1991). The DPL is more or less the alteration layer magnetite or siderite as calculated in Figure 10. I.e., these minerals are expected to be formed in the vicinity of steel interfacing bentonite or concrete. The impact of calcium on the formation of the alteration layer has not been included in the corrosion process in section 3.2 but dissolved calcium in clay and concrete seems to have a crucial role in the formation rate of the spinel-type passivation film (Kreis, 1991). At both the clay-steel interface (Neff et al., 2004) and the concrete-steel interfaces (Chitty et al., 2005), the formed spinel corrosion product magnetite contains traces of calcium. Magnetite (Fe_3O_4) and $CaFe_2O_4$ are both spinels that cannot be distinguished by Raman spectroscopy; this technique is used to provide evidence that the steel has become passivated (e.g., Naish et al., 1991). Thermodynamically, it is possible to have a calcium-iron containing passivating film as calculated in Figure 10, especially at a pH > 12.5, but so far it has not been identified as a passivating film[6]. The impact of calcium may therefore be important for understanding the corrosion process of the overpack enclosed in the concrete buffer. The chemical analysis of the surface films and difference in corroded thickness measured by weight loss and hydrogen generation monitoring also showed that another corrosion product than magnetite (Fe_3O_4) would have been formed on the surface of steel (Kaneko et al., 2004).

4.1.1.4 Transformed medium/outer layer/alteration zone

The transformed medium is a result of an interaction between the dissolved species from iron corrosion and clay or cement minerals. The quartz grains in concrete and sediment (soil) seem to remain unaffected in analogues of steel interfacing concrete or soil.

4.1.1.4.1 Zone in bentonite. The transformed medium can be the alteration zone of bentonite with a reduced porosity due to cementation of clay by precipitation of magnetite. The diffusion values in this zone may be smaller than in unaffected bentonite due to this decrease in porosity. There can however also be an increase of diffusion values in this zone due to the reaction between dissolved iron and the swelling clay mineral montmorillonite into a non-swelling sheet silicate. The chemical characteristics of the transformed medium is quite well known for bentonite which is Fe-rich non-swelling silicates (see section 3.3). The work done by Savage (2014) includes some quantification of the processes at

4 The surface charge as a function of the Ca/Si ratio of CSH-gel has been explored in Cebama (Grivé and Olmeda, 2015) since this Ca/Si ratio depends on pH (Berner, 1992). Indeed, CSH gels with a Ca/Si ratio of 1.4 show anionic exchange that has been proven with the $MoO_4$2- uptake and CSH-gels with a Ca/Si ratio of 1.2 and 0.8 have lost this uptake (Grambow et al., 2020).

5 Hematite instead of magnetite can be measured using Raman spectroscopy if the laser power heated the specimen beyond 400°C (Neff et al., 2004). Only magnetite would be measured in deaerated soils (Dillmann et al., 2014).

6 However, some experimental results support the hypothesis of a calcium-iron containing passivating film. Removal of dissolved calcium has been confirmed from batch sorption experiments with a fine powder of iron and cementitious pore water with a pH of 13.5. On the reacted iron particles - despite the calcium concentration being undersaturated - precipitation of $Ca(OH)_2$ had taken place as deduced from pair distribution function analysis. Interspersed $Ca(OH)_2$ within the iron-oxide layer is formed during the corrosion process, but co-precipitation into a solid solution between calcium and iron might also occur (Ma et al., 2018).

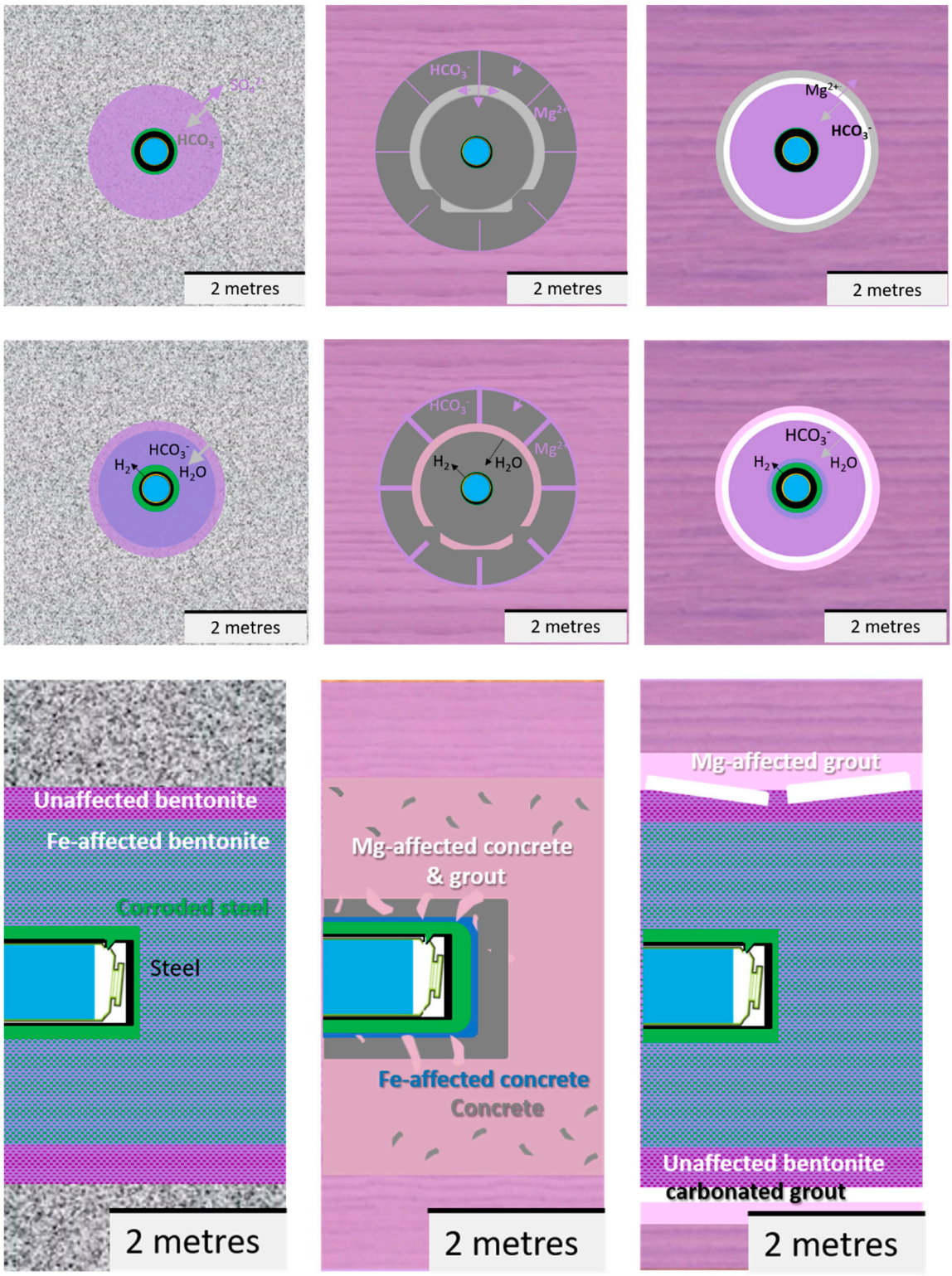

FIGURE 9
(First row) Chemically evolved disposal cells after about 1,000 years containing vitrified HLW for the host rocks: granite, poorly indurated clay and indurated clay. Blue = vitrified HLW, black = left metallic substrate of steel overpack, green = corroded part of steel overpack, bentonite (purple), carbonated concrete (white), unaffected concrete (grey), grout (light grey). Ingress of ions are indicated, e.g., Mg^{2+} and HCO_3^- from granitic/clay host rock into bentonite buffer/concrete segment (Second row for section 4.1.2). Chemically evolved disposal cells after about 10,000 s years till 100,000 s of years containing vitrified HLW for the host rocks: granite, poorly indurated clay and indurated clay. Blue = vitrified HLW, black = left metallic substrate of steel overpack, green = corroded part of steel overpack, unaffected bentonite (purple), affected bentonite (blueish purple), carbonated concrete (white), unaffected concrete (grey), affected grout (lila) (Third row for section 4.1.3). Chemically evolved disposal cells after about 10,000 s years
(*Continued*)

FIGURE 9 (Continued)
till 100,000 s of years or more containing vitrified HLW for the host rocks: granite, poorly indurated clay and indurated clay. Blue = vitrified HLW, black = left metallic substrate of steel overpack, green = corroded part of steel overpack, unaffected bentonite (purple), Fe-affected bentonite (blueish purple), carbonated grout (white), Fe-affected concrete (blue), unaffected concrete (grey), Mg-affected concrete and grout (pink).

disposal cell scale by which the dominating processes can be elucidated.

As earlier explained, although the pH of the bentonite pore water is too low for magnetite, magnetite is formed by insufficient dissipation of hydroxyl ions. This local increase in pH due to steel corrosion determines the clay dissolution. This dissolution promotes the transformation of montmorillonite into non-swelling silicates e.g., berthierine and chlorite. The slow dissolution rate of montmorillonite is considered the rate limiting step for the transformation of bentonite. The maximum in calculated thickness of the alteration zone in bentonite in simulations with the clay dissolution as the rate-limiting step was 0.1 m after 5,000 years (Savage, 2014).

4.1.1.4.2 Zone in concrete. The transformed medium between DPL and binders also contains precipitated iron-hydroxides with a III + valence that have resulted in a reduction in porosity of concrete near the DPL (Atkins et al., 1991; Chitty et al., 2005). For non-carbonated concrete with a concrete-steel interface lasting for 23 years, portlandite crystallites are also present in the outer layer. These crystallites had a distinctly different morphology than portlandite in the cementitious matrix and the transformed medium contained loosely bound material (Atkins et al., 1991). The observed loosely bound may indicate that the strength locally has diminished and that the hydraulic conductivity has increased.

Negatively charged dissolved iron species are expected at the pH of the concrete pore water. Sorption of these species by positively charged cement minerals is envisaged. An iron-enriched layer has been measured (L'Hostis et al., 2011; Chomat et al., 2017) and it is assumed that iron (dissolved species) may form iron-containing cement hydration phases (see section 3.2.3). Recent work started the coupling of processes of reactions between steel and uptake of iron by cement minerals leading to other mineral phases (Wittebroodt et al., 2023; 2024) Modelling the fate of dissolved iron species in the cementitious phase would help to provide some quantification of the expected thickness of the alteration zones as a function of time, as has been performed for the interface clay-steel.

4.1.1.5 Engineered barriers and materials interfacing host rocks

Chemical interaction that leads to an alteration zone in the bentonite buffer is not expected for bentonite buffer interfacing granitic rock. No alteration layers and zones have therefore been drawn in Figure 9 (first row). The exchange of dissolved species between the bentonite buffer and the pore water within fractures in granitic rocks depends on the trace amounts of soluble salts that were present in bentonite and the pore water chemistry of the granitic pore water. Czech and Spanish granitic pore waters are not as saline as Swedish and Finnish granitic pore waters at suitable disposal depth, and the amounts of soluble salts present in bentonite buffers can be chosen for particular site characteristics. For example, the bentonite buffer in the Czech programme also contains sodium bicarbonate as a soluble salt while this salt is not present in the Swedish bentonite.

Alteration zones are expected in both the bentonite buffer and the clay host rocks interfacing concrete support materials. The coupling of processes to determine the alteration of clay by concrete is reasonably well understood. The overall impact of the transformation of swelling clay minerals into non swelling sheet silicates is a decrease in porosity, hydraulic conductivity and swelling pressure (Savage, 2014). Consequently, the primary safety function of clay to limit transport of radionuclides by the physical properties of clay may not have changed by this alteration. However, the mechanism for the closure of fractures changed from seal-healing of fractures into self-sealing of fractures. If fractures would have been induced, more time for their closure and the associated reduction in hydraulic conductivity would be required. Also, most of the formed secondary non-swelling minerals, e.g., CSH phases, illite and zeolites, also have sorption properties but their sorption capacities can be smaller than that of montmorillonite. The knowledge on the interaction of bentonite with cementitious pore fluids is sufficient to quantify the thickness of the alteration zone in clay. In many simulations, the overall reduction in porosity can achieve a porosity of 0% (Savage, 2014), by which the alteration is stopped. These calculations are performed with a uniform porosity and the distribution in size of pores may be needed in order to be able to predict natural systems as well as the multibarrier system used to dispose of waste. But the calculations with a uniform porosity are good enough to make design choices such as the thickness and cement content of a barrier made with concrete. This thickness of the alteration zone has been predicted to be 0.02 m after 100,000 years. There will however always be some continuation since the distribution in size of pores in the sedimentary clay rock and bentonite buffer allows existing diffusional pathways. A ten times large thickness is calculated after this period, i.e. 0.2 m, if no porosity reduction is assumed (Savage, 2014). Smaller alteration thickness is expected for clay interfacing concrete since:

- the egress of ions from concrete pore water takes place by limited diffusion due to the pore structure of concrete, and
- the transport of hydroxyl ions from concrete into clay is further decreased by the reduction in pH in concrete due to ingress of dissolved bicarbonate from the clay pore water.

Concrete may also have been gas carbonated in the operational phase by which no further alteration of the clay in the post-closure phase is expected, since the difference in pH between the pore waters of carbonated concrete and clay is negligible.

The initial porosity of bentonite and poorly indurated clay is about 40% (see Supplementary Material Section 3.1) which is larger than the so-called engineered impermeable concrete segments with an initial porosity between 10% and 15% (see section 2.3.2). The ingress of dissolved species from the clay host rock into these concrete segments is rather along the joints than within the concrete, as drawn in Figure 9. The shotcrete interfacing

10.3389/fnuen.2024.1433247

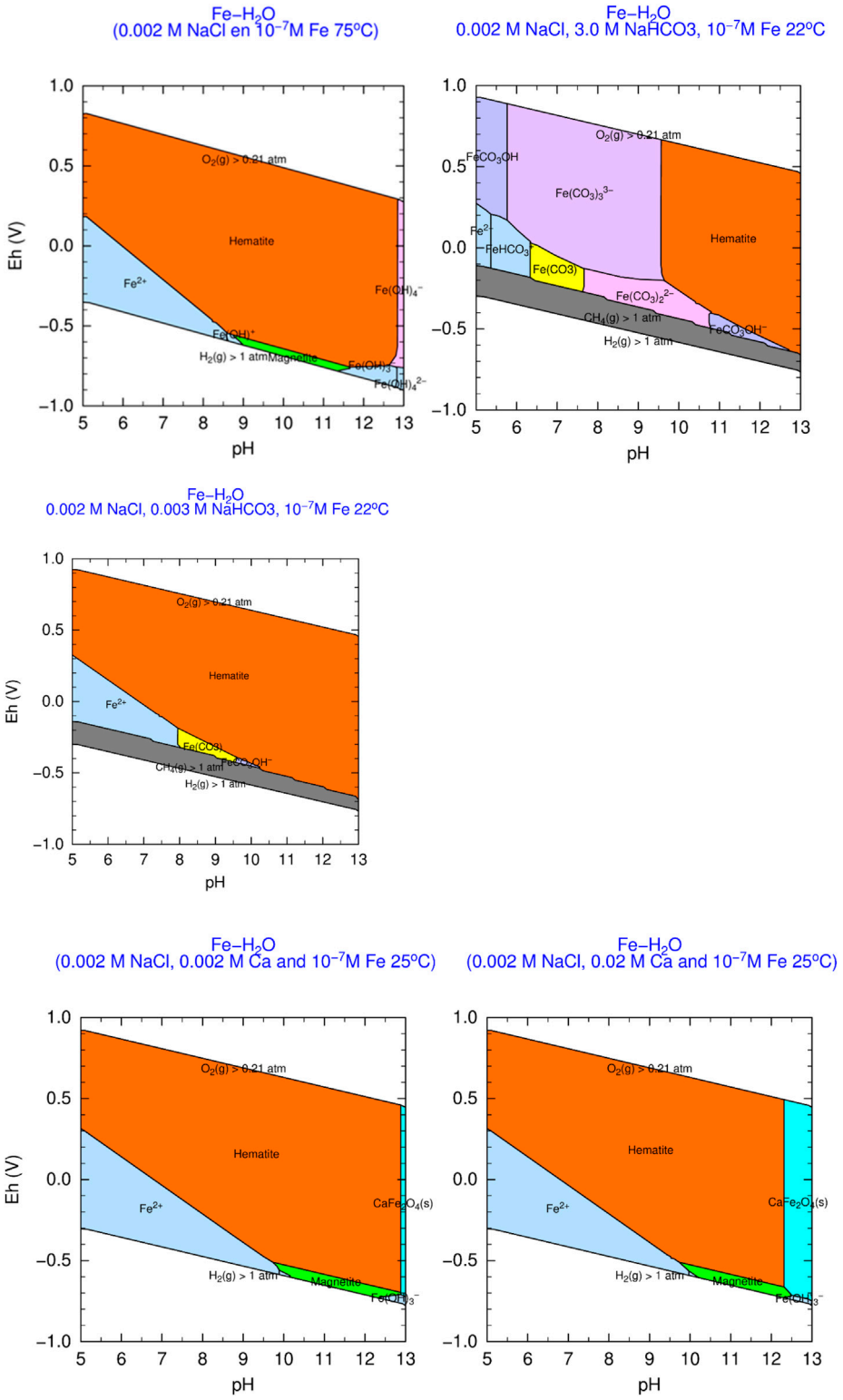

FIGURE 10
Pourbaix diagrams for the system Fe-H_2O with an activity of dissolved species of 10^{-7} M; 0.002 M Ca is a reasonable concentration for tap water and 0.02 M Ca is the maximum dissolved calcium concentration without alkalis (Berner, 1992; Vehmas and Itälä, 2019) and 3 × 10^{-3} M HCO_3^- is the concentration found in Spanish and Czech granitic rocks and French indurated clay (see Supplementary Material Section 2.1) Magnetite (green) is Fe_3O_4(s) and Hematite (orange) is Fe_2O_3(s) and Siderite (yellow) $FeCO_3$ (s) (made with PhreePlot (Kinniburgh and Cooper, 2009) using ThermoChimie v7b).

indurated clay may have been carbonated in the operational phase as explained in section 2.3.3. Consequently, the chemical and mineralogical alteration in the post-closure phase may be negligible for the carbonated shotcrete. The shotcrete is therefore envisaged to act as a permeable medium for the transfer of dissolved species from the clay host rock into the bentonite buffer.

4.1.2 From about 1,000 years until fracture of the carbon steel overpack

The decay of radionuclides in vitrified waste has occurred till such an extent that temperature in all disposal cells has achieved the virgin temperature of the host rock.

4.1.2.1 Alteration layers and zones in bentonite

Anaerobic corrosion of the carbon steel overpack has continued and although the thickness of the DPL (alteration layer) may have slightly increased, the extent of corroded steel can be estimated from the affected bentonite, i.e., the alteration zone with non-swelling sheet silicates. The consumption of bicarbonate to form siderite results into an influx of bicarbonate from the granitic pore water into the bentonite. This influx of bicarbonate and water is smaller from disposal cells constructed in indurated clay due to the smaller diffusion value of bicarbonate in indurated clay compared to granitic host rocks. The envisaged alteration zone in bentonite is therefore drawn smaller in disposal cells in indurated clay compared to granitic host rocks in Figure 9 (second row). The size of the alteration zone is bounded by the thickness of carbon steel overpack and stainless steel container (Savage, 2014). With the geometry used in Figure 4, a thickness of iron-unaffected bentonite of at least 10 cm can be calculated by mass balance calculations.

In NF-PRO, a project in the 6th Framework programme, experimental work has been performed to investigate the interaction between bentonite and carbon steel canisters (NF-PRO, 2008). Pieces of bentonite in contact with iron were no longer plastic but became brittle, only crumbled pieces of bentonite could be removed (Carlson et al., 2008). For the narrative, it is therefore assumed that the buffer has become more brittle with much less possibilities for creep and more vulnerable to form cracks, due to the compressive load of granitic rock. The alteration zones in bentonite have a higher hydraulic conductivity than virgin bentonite, which may enhance the dissipation of hydrogen further into the bentonite buffer. The radial dissipation quadratically reduces the hydrogen concentration in the bentonite buffer, which reduces the probability for gas perturbation. Anaerobic corrosion of the steel overpack also occurs in the disposal cell with the concrete buffer. An alteration zone in concrete may not be yet visible, due to the smaller corrosion rates in concrete compared to bentonite. First alteration zones within concrete by ingress of dissolved species from clay pore water are envisaged to be visible at disposal cell scale.

4.1.2.2 Alteration zones in concrete

Figure 7 in section 3.6.1 shows the schematic evolution of pH of concrete pore water during the four different stages of cement leaching (pH controlled by dissolved alkalis, portlandite and two C-S-H phases), since the stability of cement minerals is pH-dependent. The reduction in pH by leaching is however not expected for all stages since the calcium concentration in the host rock pore water is larger than the calcium concentration in concrete pore water in equilibrium with these cement minerals except for Boom Clay in Mol (Belgium) but rather by the reactions with ingress of gaseous CO_2 in the operational phase from the ventilation air and bicarbonate ions from the clay pore water. The concrete buffer and concrete segments have a high mechanical strength, which prevents the lithostatic load of the underground host rock being transferred to the waste package. Ingress of bicarbonate reduces the pH of the concrete pore water but the calcite precipitation in this alteration zone may result into an increase in strength of the concrete buffer and segments. The carbon steel overpack cannot be cracked as long as the concrete buffer has not reduced in mechanical strength. The ingress of dissolved magnesium and the transformation from calcium containing cement phases into magnesium containing minerals are considered to decrease the strength of concrete (Atkinson et al., 1985). There is almost always magnesium enrichment in concrete since all clay pore waters have a larger magnesium concentration than the concrete pore water, except for the Belgian clay pore water (see Supplementary Material Section 2.1). It is assumed that the progressive increase of a magnesium front accelerates the degradation. Apart from changes in pH, also other processes take place (Atkinson et al., 1985; Atkins et al., 1991; Berner, 1992; Pointeau et al., 2008; Grivé and Olmeda, 2015; Dauzeres, 2016). The progression front of brucite (can be formed in Al and Si poor locations) has been calculated to be less than 20 cm after 100,000 years for concrete interfacing indurated Callovo-Oxfordian clay (Idiart et al., 2020). A quantification of reacted zones is essential for disposal of waste since vitrified HLW has become less radiotoxic than uranium ore after 100.000 years (see Figure 2). Ultimately, there will be contact between pore water and the vitrified waste form by fracture of the carbon steel overpack but the health related risks may have become negligible.

4.1.3 Fracture of the carbon steel overpack

The bentonite buffers for HLW disposal cells in granitic and indurated clay host rocks are continuously compressed by the lithostatic pressure. An ice age can increase the load on these buffers as a function of the thickness of an ice sheet above the geological disposal facility. Further deformation of the bentonite buffers is restricted by the mechanical strength of the carbon steel overpack. This strength decreases by reduction in thickness of non-corroded carbon steel by chemical corrosion. The left carbon steel preferentially cracks in areas where there is empty volume. The 5 mm thickness of the stainless steel canister is too small to accommodate the lithostatic load and will fracture just below the mushroom that was used to lift the canister (see Figure 9, third row). Finally at fracture, bentonite in Figure 9 (third row) has one type of alteration size, i.e., the zone affected by iron corrosion.

Shotcrete interfacing indurated clay slowly lost its strength by ingress of magnesium from the clay host rock. Gaseous carbonation can increase the strength of concrete, but the carbonated thickness of shotcrete in the operational phase is considered here to be too thin to prevent fracturing in the post-closure phase. The concrete buffer has two alteration zones: an iron corrosion affected zone, and a zone that has lost its strength by the ingress of magnesium from the clay pore water. Like the bentonite buffer, also the concrete buffer is continuously compressed by the lithostatic pressure of the host rock, but this buffer has its own mechanical strength to prevent deformation. The outer parts of the concrete buffer have lost their strength due to the ingress of dissolved species from the clay pore water. The inner parts of the concrete buffer may still have a high pH, but the iron affected part is assumed to have lost its strength.

Only the chemically unaffected concrete part has strength but may be too thin to accommodate the lithostatic load. Consequently, fracture of the carbon steel overpack will be a combination of the reduction in thickness of the carbon steel overpack by chemical corrosion as well as reduction in thickness of the concrete buffer that still has compressive strength. Also, similarly as the carbon steel overpack that was encapsulated in the bentonite buffer, fracture is envisaged at the empty volume between the mushroom and vitrified waste form.

4.1.3.1 Corrosion and fracturing stainless steel overpack stainless steel

Corrosion of the stainless steel (see Section 2.1.1) only starts after fracturing of the carbon steel overpack. Stainless steel is a high alloy steel that can form different corrosion products than low alloy steel, e.g., carbon steel. Contact between pore water and the stainless steel canister is thermodynamically predicted to generate another spinel corrosion product than magnetite, i.e., chromite ($FeCr_2O_4$). At a similarly low concentration of dissolved iron species as in Figure 10, the pH stability region of chromite is larger than that of magnetite, i.e., this spinel phase is thermodynamically stable at neutral pH and the environment needs to be less reducing conditions (Figure 11). Of course, solid solutions between magnetite and chromite are probably present as corrosion products but thermodynamic data were not available in the used database.

Chlorine is present in clay and granitic pore water[7] (Supplementary Material Section 2.2). Chlorine is frequently associated with an increase in the corrosion rate. Chromium-chlorine complexes are already formed at very small dissolved chlorine concentrations but the concentrations for iron need to be much larger than chlorine concentrations for tap water in order to be visible in the Pourbaix diagrams. These chlorine complexes may however not influence the chemical evolution since their presence is in the more acidic regime, even in environments as saline as seawater. Consequently, the small corrosion rates for stainless steel measured in CAST with a maximum of 0.01 μm per year (Mibus et al., 2018) are also assumed at fracture.

4.1.3.2 Vitrified waste form

The general picture of the formation on an alteration layer induced by the interaction between glass and water is described in section 3.1. Silicon is used in the formation of clay minerals and zeolites and also contains the precipitated products for the elements that form insoluble hydroxides, e.g., iron, aluminium, zinc, titanium or magnesium. A diffusion and gel layer is present between virgin glass and these minerals and acts as diffusing, passivating barrier. Other elements initially contained in vitrified waste such as boron and with some reservations lithium, sodium and molybdenum are highly soluble and most of these elements will be dissipated towards the evolved pore water in the buffer.

Section 2.1.1 explained the presence of cracks in the bulk of the glass after fabrication of the vitrified waste form due to the stress induced by the cooling rate. Closure of these fractures takes place by precipitation of phases. Also, the formed clay minerals further diminish the ingress of reactive species into the diffusion and gel layers.

There is also a lot of dissolved iron present from the corroding stainless steel canister. The dissolved iron species is positively charged (see Figure 10) and can be preferentially sorbed on negatively charged clay minerals, similarly as explained in previous paragraphs for the chemical interaction between bentonite and carbon steel. Figure 11 shows that dissolved chromium is present as a negatively charged dissolved complex and is therefore expected to have a less detrimental effect on the alteration layer than dissolved iron complexes, if this alteration layer is mainly made from smectite. Also, the potential high alteration rate is only relevant for the vitrified waste form in the vicinity of steel and not for the bulk.

The dominant Si bearing species in a solution is usually H_2SiO_3 but changes at a pH higher than 10 into $HSiO_3^-$ (Conradt et al., 1986), and the solubility of SiO_2 is then increased. The 4th framework programme indicated that this silicic acid dissociation starts at a pH > 9 (Vernaz et al., 1996). In the 5th framework programme, it has been elucidated that the dissolved silica concentration at saturation exponentially increases from a pH beyond 9, but that the measured dissolved silica concentrations at saturation are smaller than the calculated ones (Ribet et al., 2007). In section 4.1.1, it was explained that the iron corrosion process of carbon steel can locally increase the pH up to 10, due to insufficient dissipation of the formed hydroxyl-ions. The vitrified waste form is interfacing stainless steel. The long-term corrosion rate of stainless steel can be ten times smaller than the corrosion rate of carbon steel and is therefore envisaged to induce a smaller increase in the local pH.

There may also be contact between pore water with a pH higher than 10 and the vitrified waste form for the disposal cells containing initially cementitious materials, provided that the chemically evolved concrete has sufficiently lost its mechanical strength. An alteration layer that limits further dissolution of the vitrified waste form is always generated whatever pH the vitrified waste form is exposed to. However, these layers are more effective at neutral pH than at high pH. Chemisorption of iron occurs by the generated clay minerals in the vicinity of corrosion products[8].

7 Dissolved chlorine does not react with portlandite and C-S-H-phases but the phases containing aluminium such as hydrogarnet. These cement minerals are replaced by Friedel's salt. Friedel salt precipitation is accompanied by a reduction in porosity (Höglund, 2014). This reaction process is not considered harmful for concrete and therefore not discussed in section 3.7.2.

8 Recently, a Nature paper has been published in which a self-accelerating corrosion process of stainless steel canister with vitrified waste is described (Guo, et al., 2020). The oxidizing conditions and 90°C are not considered representative for the geological disposal conditions considered in Europe in which reducing conditions in host rocks are frequently used as a siting criterion in order to have a small solubility of released radionuclides and the waste has cooled down till the disposal depth temperatures upon fracture of the stainless steel canister. Mechanical fracture in section 3.7.3 instead of pitting corrosion in this Nature paper is therefore considered as a mechanism for fracture of the stainless steel canister with which contact between pore water and vitrified waste form has been established. For ACED, the potential entrapped oxygen between the stainless steel canister and carbon steel overpack due to the fabrication of these containments is assumed to have a negligible role on the chemical evolution.

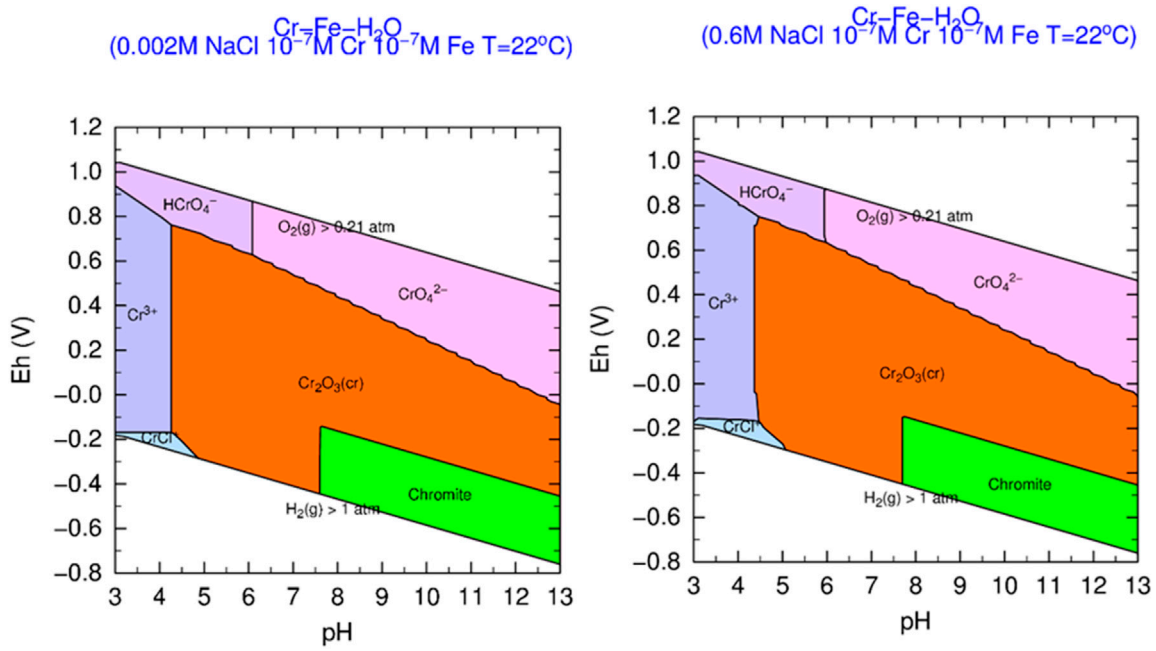

FIGURE 11
Pourbaix diagrams for the system Cr-Fe-H_2O with an activity of dissolved species of 10^{-7} M; 0.002 M NaCl is a reasonable concentration for tap water, 0.6 M NaCl is suitable chlorine concentration for seawater. Chromite (green) is $FeCr_2O_4$(s) (made with PhreePlot (Kinniburgh and Cooper, 2009) using ThermoChimie v7b).

Ion exchange reactions are proposed as the rate controlling processes. The presence of solid clay in the leachant is therefore known to enhance the dissolution rate since the sorption of the less soluble elements aluminium, iron and zirconium takes place. Corrosion products have the same influence (Van Iseghem et al., 1992; Vernaz et al., 1996). Corrosion products such as chromite (Souza et al., 2012) and magnetite (Kim et al., 2001 in Eisele et al., 2005) are also negatively charged at pH conditions representative for disposal and therefore also preferentially sorb these less soluble elements.

The glass alteration process requires water; the influx of water into the fractured stainless steel is restricted by diffusion for the disposal cells in clay host rocks. The influx of water in these canisters for disposal cells in granitic host rocks depends on the properties of the altered bentonite buffer; e.g., cracks are expected to be present due to chemical interaction with dissolved iron.

4.1.3.2.1 Impact of alteration of glass on the mechanism for radionuclide release. The radionuclide release from the vitrified waste form was not reviewed in this paper, but some basic rules can be suggested. For the radionuclides that are still left, the altered glass contains clays and zeolites that can also sorb dissolved cationic complexes. These cationic complexes are expected to be sorbed and very limitedly leave the fractured corroding evolving stainless steel canister. The glass alteration has therefore a very small impact on the potential radionuclide release, if the radionuclides are dissolved as cationic complexes. The released amount of plutonium, americium and radioactive caesium in solutions is only a fraction of the initially contained amount as has been measured in the 3rd framework programme (Van Iseghem et al., 1992).

Dissolved anionic complexes are not expected to be contained by the reaction layer. An example of a radionuclide that can be present in the vitrified waste form and becomes present as a dissolved anionic complex is ^{79}Se. The amount of ^{79}Se left at fracture of the stainless steel canister may also be limited due to the required period for fracture and a half-life of 327,000 years. The pore water in the bentonite buffer as well as the evolved concrete buffer are saturated with silica. Alteration rates of basaltic glass, the natural analogue for a borosilicate waste form, have estimated to be 0.1 μm per 1,000 years in these saturated environments (Lutze et al., 1987). Consequently, most of the left ^{79}Se is expected to decay within the vitrified waste form and not released to the surroundings.

4.2 ILW disposal cells

The radiological content in ILW packages is orders in magnitude smaller than in HLW packages. For example, the radionuclides contributing most to the radioactivity for CSD-C are, like CSD-V, also ^{137}Cs and ^{90}Sr. The guaranteed maxima are 65 TBq for ^{137}Cs and 115 for ^{90}Sr (COGEMA, 2001), i.e., about two orders in magnitude smaller than CSD-V that had 6,600 TBq for ^{137}Cs (see section 4.1). For vitrified HLW, radiation enhanced corrosion in water can be excluded after a cooling period of 90 years, i.e., an ^{137}Cs activity of about 800 TBq. Consequently, radiation enhanced corrosion of metallic ILW is excluded to have an impact on the chemical evolution of an ILW disposal cell since the required radiation dose rate for radiation enhanced corrosion are lowest for steel exposed to water. The radiological content of organic ILW such as spent ion exchange resins is smaller than CSD-C, for example, two

orders in magnitude (Verhoef et al., 2016). The most common form of resins, polystyrene divinylbenzene, is radiation resistant. Radiation enhanced degradation of these resins is therefore also excluded to have an impact on the chemical evolution of disposal cells.

Cementitious processing of metallic and organic ILW reduces the likelihood of microbial activity due to its high pH as explained in section 2. Limiting microbial activity by space restriction within the cementitious matrices depends initially on the fabricated porosity. The waste package mortar can be manufactured with a similar cement content, additives and similar grading in aggregates as the concrete buffer. In those cases, microbial activity is also limited in waste package mortar. The fabricated porosity is larger in cementitious materials without aggregates or a lower content of aggregates with more limited grading in aggregates. The connecting pore throats in these cementitious materials may be too large to limit microbial activity. This activity can also be positive for example, for the precipitation of biogenic calcite, which can make concrete stronger. For now, it is assumed that ingress of bicarbonate and magnesium into the liner made of shotcrete in granitic rocks (see Figures 4D,E), which started in the operational phase, continues in the post-closure phase. The liner is expected to fracture after the start of the post-closure phase, due to continued replacement of calcium-binding phases by magnesium phases, by which the zones in which the strength of concrete is lost have progressively grown as explained in section 4.1.2.

The EDZ generated in granitic rock in the construction phase had generated sufficient fractured material to eliminate the initial gap between shotcrete and crushed rock by creep. The crushed rock is soon saturated with granitic pore water through fractures in granitic rock and shotcrete. The advective water flow of granitic pore water within crushed rock generates a continued refreshing of granitic pore water at the caissons. This preferential flow path of granitic pore water also makes that cement leachates are removed from the disposal facility. These leachates can react with the siliceous phases and secondary mineral precipitation in the fractures of the rock takes place that might even lead to clogging within fractures (see section 3.6). Figure 12 shows the chemically evolved disposal cells.

For the reinforcement in caissons, it depends on the depth of the disposal facility how much oxygen is present in the granitic pore water. In case of anaerobic granitic pore water, anaerobic corrosion of the reinforcement bars is assumed. The initial pathway of granitic pore water within the caissons is assumed to be at the lid. The ingress of magnesium and bicarbonate in the caisson replaces the cementitious minerals by calcite, brucite and M-S-H phases. This continued replacement of calcium-binding phases by magnesium phases by which the zones in which the strength of concrete is lost has progressively grown as explained in Section 2.3.1.2. The loss in strength is accompanied by a permeability increase that also favour the ingress of dissolved species from host rock pore water into concrete.

Chemical corrosion of the metallic materials in metallic ILW results into an alteration layer of corrosion products. The thickness of this layer hardly changes in case of anaerobic corrosion, since the corrosion process is controlled by the dissolution of the alteration layer. The dissolved metallic compounds are sorbed by cement minerals, by which an alteration zone within the grout is formed. Similarly, as explained earlier for HLW disposal cells, this Fe-affected zone is assumed to have a smaller strength than fabricated concrete.

The left image in Figure 12 shows the evolved ILW disposal cell containing spent ion exchange resins. Diffusional flow of water into the waste containers is envisaged along interfaces. The oxygen trapped during fabrication is consumed by chemical corrosion of the stirrer or traces of pyrite present in the cementitious matrix; microbial activity is limited due to the high pH. The porosity of the cementitious matrix is considered to be too high to obtain a local reduction of oxygen at the corroding stirrer. After oxygen consumption, anaerobic corrosion may have started in the operational phase since the saturation degree of water in the cementitious matrix after processing of 90% is sufficiently high for corrosion of steel. The corrosion process can stop during the operational phase, if the consumption of water by the corrosion of the stirrer is not sufficiently supplemented by inflow of water into the container. Anaerobic corrosion of the steel container and sacrificial stirrer for the spent ion exchange resins processed with a cementitious matrix continues in the post-closure phase. The cementitious matrix is considered to be sufficiently porous in order to have the evolved hydrogen gas to be dissipated by diffusion. The same processes as described in Sections 3.2 and 2.3.1.1 for the concrete-steel interface will take place.

4.2.1 Organic ILW

Organic materials in organic waste can act as food for the growth of microbes. These organic materials are altered into another form when used as food. This alteration can have an impact on the potential radionuclide release. The MIND project classified the organic waste into two groups (Abrahamsen et al., 2015):

1) addition polymers that are resistant to biodegradation for example, polystyrene, polyethylene and polyvinylchloride;
2) condensation polymers that are susceptible to biodegradation for example, cellulose.

Resins are polystyrene polymers as explained in section 2.2.1. There is no energy for microbes to be obtained upon their degradation of these resins (Abrahamsen et al., 2015). Consequently, microbial degradation of resins is excluded. Organic ILW was mainly specified as spent ion exchange resins. (Neeft et al., 2020).

Cemented resins have been investigated in CAST (Norris and Capouet, 2018) and were to be studied in the EURAD WP Cement Organic Radionuclide Interaction (CORI) (Altmaier et al., 2021). Chemical degradation of polymers is initiated by a nucleophilic attack of OH^- ions on a carbon atom with a positive partial charge. Such carbon atoms are generally not present in addition polymers (Van Loon and Hummel, 1995). The chemical resistance of resins is high. A degradation rate of resins representative for the disposal conditions is therefore not yet available. Chemical degradation of resins can therefore be excluded as a factor for release of radionuclides such as carbon-14 (Capouet et al., 2018). Resins are like clays exchangers and any radionuclide release is expected to require sufficient ingress of anions and cations that have a stronger affinity than the sorbed anionic or cationic radionuclides (Neeft, 2018). For example, sulphate has a very strong affinity

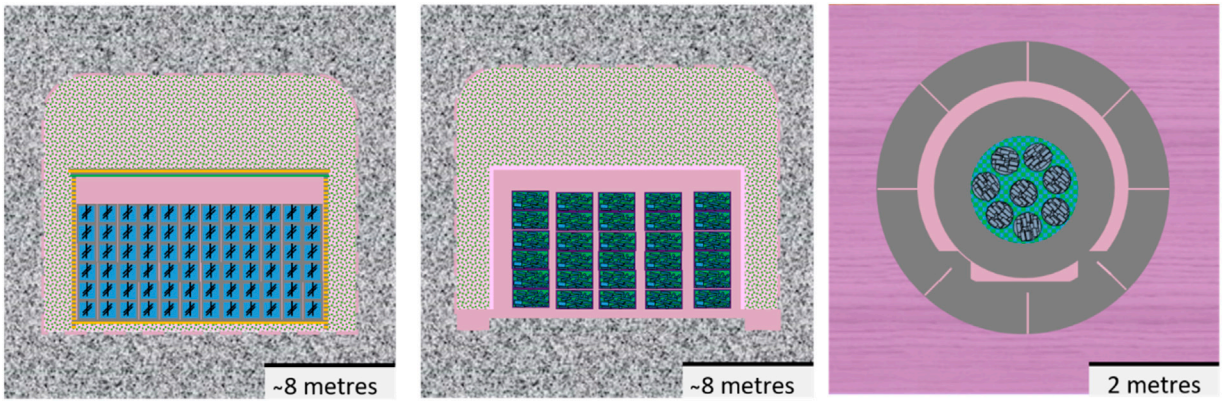

FIGURE 12
Chemically evolved disposal cells after about 10 s of years till 1,000 s of years containing cemented ILW considered in Europe for the host rocks: crystalline rock (left and middle) and poorly indurated clay (right). Blue = ILW or cemented ILW, black = steel, green and pink = crushed rock with granitic pore water, pink = Mg-affected grout, green = Fe-affected grout and corrosion products, unaffected concrete (grey).

(IAEA, 2002) and sufficient ingress of sulphate at these resins will cause an exchange of sorbed anionic radionuclides.

4.2.2 Metallic ILW

4.2.2.1 Steel

The middle image in Figure 12 shows the stacking of containers with metallic waste made of steel. The entrapped oxygen is expected to be consumed at a very fast rate. There is insufficient inflow of water into the container for anaerobic corrosion of all steel surfaces in the operational phase, and therefore microbial as well as chemical corrosion is expected to be stopped. In the post-closure phase, there can be sufficient inflow of water in ILW disposal cells in granitic host rocks for anaerobic corrosion of this waste. The interaction between neutron irradiated Zircaloy and neutron irradiated steel and cementitious pore water have been investigated in the CAST project from the FP7 programme (Williams and Scourse, 2015; Norris and Capouet, 2018). The speciation of radionuclides released from these waste forms can be studied in cementitious pore water while it is more complicated to study this speciation for metallic material interfacing concrete. Special care has been taken to simulate cementitious pore water, i.e., calcium saturated solutions have been used (e.g., (Cvetković et al., 2018; Necib et al., 2018)). The calcium-iron spinel type was thermodynamically more stable than magnetite in pore solutions containing calcium as shown in Figure 10 with which it is assumed that the dissolved calcium is crucial for the corrosion process of carbon steel. The spinel-type chromite calculated in Figure 11 is, however, also in calcium-saturated solutions of 0.02 M Ca^{2+} thermodynamically more stable than $CaFe_2O_4$. It is therefore expected that, unlike carbon steel, the dissolved amount of calcium in the pore solution has a negligible influence on the corrosion process of stainless steel. Another benefit of the performance of corrosion experiments with cementitious pore water is that the measurement of the hydrogen release from steel can be used to determine the anaerobic corrosion rate. In CAST, these corrosion rates measured in cementitious pore water had a maximum of 0.01 μm per year (Mibus et al., 2018). The hydrogen generation rate depends on the surface area of metallic waste that can be in direct contact with the pore water and corrosion rate. However, the long-term hydrogen generation rate cannot be larger than the consumption rate of water. Transport of water in the ILW disposal cells is therefore essential to determine long-term hydrogen generation rates.

4.2.2.1.1 Impact of alteration of steel on the mechanism for radionuclide release. There can be radionuclides present in steel waste as a result of contamination as well as neutron activated radionuclides. Most short-lived radionuclides have disappeared due to decay. The remaining radionuclides as a result of contamination diffuse through the concrete from the moment corrosion has started. The remaining neutron activated radionuclides have a similar release pattern as described for the vitrified waste form (see section 4.1.3.1); the radionuclides that become present in a cationic dissolved form in the corrosion process will be sorbed by corrosion products in the altered or reaction layer. The radionuclides that become present in anionic dissolved form in the corrosion process can be sorbed by cement minerals, if the pH of the concrete pore water is higher than 11.8, since the zeta potential is positive at these pH values (see section 4.1.2). These dissolved anionic complexes, however, compete with sorption of the metallic-dissolved complexes in equilibrium with the corrosion products.

4.2.2.2 Zircaloy

For the disposal cell in poorly indurated clay, e.g., the right image in Figure 12, the preferential flow of clay pore water into the cell is through the joints between concrete segments. The ingress of magnesium and bicarbonate into the cementitious materials in the disposal cell is expected to take place at a very small speed, but initially faster than in the HLW disposal cells, since there is no heat source desaturating these materials. The consumption of entrapped oxygen by chemical corrosion of the canister or traces of pyrite present in the mortar may have been completed in the operational phase and the porosity of the mortar may be too large to generate a local reduction of oxygen at the corroding canister surfaces. If the mortar has a too large porosity to render microbial activity through space restriction, microbial activity within the mortar is still limited

due to the high pH. Anaerobic corrosion may have started in the operational phase if the saturation degree of water in the mortar after processing is sufficiently high for the corrosion of any metal. The corrosion process can stop during the operational phase, if the consumption of water by metal corrosion is not sufficiently supplemented by inflow of water into the container. This anaerobic metal corrosion continues in the post-closure phase due to diffusional flow of water from the grout backfill into the concrete container. The preferential pathway is at the top of container, e.g., at interfaces with a lid. There are two possibilities to have contact with pore water and the metallic waste inside the stainless steel canister:

- Uniform corrosion of the canister walls has been completed i,e. all stainless steel has reacted into metal-oxides and metal-hydroxides. Mechanical support against lithostatic load is provided by a sufficient thickness of the concrete container that has ample strength;
- Non-completed uniform corrosion combined with mechanical failure of the stainless steel canisters since the thickness of concrete with sufficient strength became too small to provide sufficient mechanical support against the lithostatic load.

With a maximum of 0.01 μm per year as measured in CAST (Mibus et al., 2018), it would take thousands of years for a complete uniform corrosion of the 5 mm stainless steel wall. The second possibility requires a zonal progression of reaction fronts and the knowledge about the mechanical strength of concrete in each zone. The Cebama modelling results showed a progression front of brucite of less than 20 cm after 100,000 years for concrete interfacing indurated Callovo-Oxfordian clay (Idiart et al., 2020). Assuming loss in strength of concrete with this progression front, the second possibility is more likely, i.e., non-complete uniform corrosion combined with mechanical failure of stainless steel for clay pore waters with a high magnesium content such as in France, Switzerland and Netherlands (see Supplementary Material Section 2). The reference clay water composition in the Belgium programme has however, a far smaller magnesium content; then the first possibility would be more probable, i.e., complete uniform corrosion of the canister walls.

Contact between pore water and compacted hulls will cause anaerobic corrosion of Zircaloy. The surface charge of the resulting corrosion product is unknown and therefore a credit to sorption of the radionuclides contained by Zircaloy cannot be provided. The corrosion rates are however very small, i.e., below 1 nm per year (Necib et al., 2018). These very small corrosion rates can also be understood from thermodynamic data. Figure 13 shows that the solution is supersaturated already at Zr concentrations as low as 10^{-7} M. At these concentrations of 10^{-7} M, a pH dependent stability field for magnetite for carbon steel (see Figure 10) or chromite for stainless steel (see Figure 11) could be seen. The dissolved Zr complexes are not visible despite a larger range in pH from 1 to 13 for the Zr speciation instead of 3–13 used for the Fe and Cr speciation. Calculation of a pH dependent stability field for the alteration layer of Zircaloy requires far smaller concentration than carbon steel and stainless steel i.e., the solubility if Zr-corrosion products are much smaller than the corrosion products with steel leading to even smaller corrosion rates for Zircaloy than steel corrosion rates in water.

The ingress of bicarbonate from the clay pore water has an impact on the stability of the alteration layer and active corrosion can be present but only at very low Zr concentrations of 10^{-10} M at a pH < 10 (see Figure 13, right image). The predominant dissolved carbonate species changes from HCO_3^- to CO_2 at a pH of about 6.4. Dissolved zirconium-carbonate complexes cannot be made with CO_2. Consequently, the impact of bicarbonate on the zircaloy corrosion rate becomes negligible at a pH < 6.4 at the calculated concentrations.

Like steel as calculated in Figure 10, calcium has also been noted to have an effect. However, in this case it is a negative effect since the presence of dissolved calcium reduces the stability of the passivation layer of zircaloy (Gras, 2014), by which the corrosion rate increases. The required calcium concentrations of at least 0.05 M to have an effect on this stability may, however, not occur. Cementitious pore waters usually have a smaller calcium concentration than host rock pore water and the host rock pore waters do not exceed this required concentration of 0.05 M (see Supplementary Material Section 2).

4.2.2.2.1 Impact of alteration of Zircaloy on the mechanism for radionuclide release. The small corrosion rates below 1 nm per year as found in CAST for cementitious pore water (Necib et al., 2018) would make that most radionuclides generated by neutron activation will decay within the cladding and are not released to the surroundings. These corrosion rates would initially be representative for disposal in a clay host rock with a minor concentration of magnesium such as the Belgian case, since the concrete surrounding the canister can limit the ingress of bicarbonate from the clay pore water towards Zircaloy claddings. Higher corrosion rates are to be expected when the bicarbonate concentration at the Zircaloy claddings become larger. The radionuclides, however, may also be absent at that time.

Unlike steel, the generated hydrogen has no impact on the radionuclide release since most of the generated hydrogen is not released but picked-up. The Japanese studies (reported in Sakuragi (2017)) measured a hydrogen pick-up of at least 90% at 30 °C, when Zircaloy is exposed to alkaline water as well as pure water. The hydrogen pick-up decreases with increasing temperature (Sakuragi, 2017). Unlike steel, a hydrogen measurement from an experiment of Zircaloy in (cementitious) pore water will underestimate the corrosion rate since uptake of hydrogen takes place. The possibility of hydride formation in any type of metal has been known for many decades (Lacher, 1937). For iron, hydride formation is not expected. It has been found that tritium diffuses through stainless steel in a reactor environment at a high rate, the rate being significantly higher than tritium diffusion through zirconium alloys (IAEA, 2004). High diffusion rates can be attributed to an insignificant hydride formation.

5 Concluding remarks

Deep geological disposal is the foreseen end point in the long-term management of intermediate and high level radioactive waste in many (European) national programs. Given the time-scales over which safety and performance assessments have to be done (several tens-of-thousands to hundreds-of-thousands of years), geochemical alterations will occur at the interface between two materials but

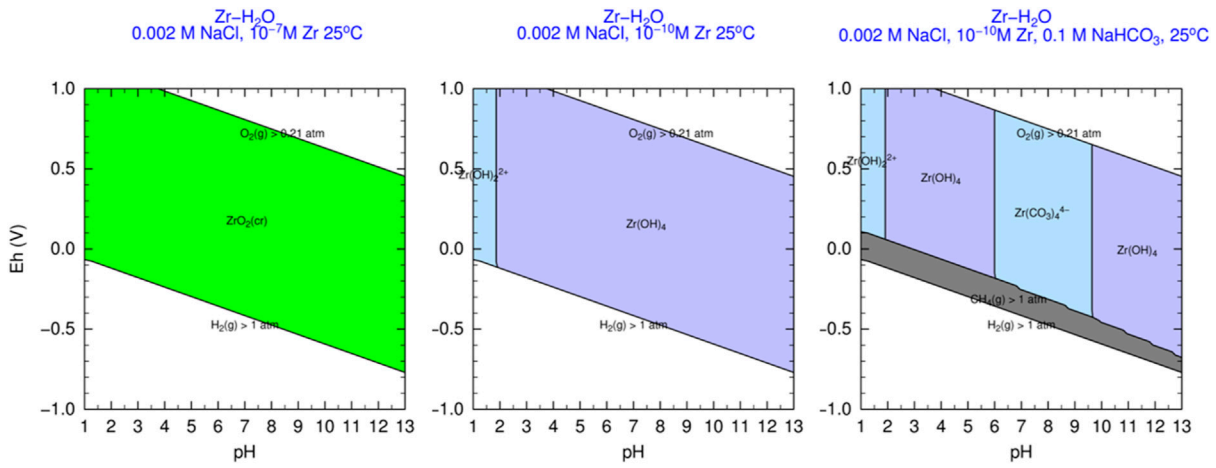

FIGURE 13
Pourbaix diagrams for the system Zr-H_2O with an activity of dissolved species of 10^{-7} M; 10^{-10} M, 0.002 M NaCl is a reasonable concentration for tap water and 0.1 M $NaHCO_3$ is an assumption for clay pore water (see Supplementary Appendix). $Zr(OH)_4$ (light purple) is $ZrO_2{\cdot}H_2O$ in Gras (2014) (made with PhreePlot (Kinniburgh and Cooper, 2009) using ThermoChimie v7b).

also at larger distances. These geochemical changes are induced by the strong and abrupt geochemical gradients that typically exist between the materials in the engineered barriers but also with the host formation.

This overview discussed following aspects (i) a comprehensive overview of the existing scientific knowledge base on geochemical processes at interfaces and (ii) a description of the characteristics of ILW and HLW disposal cells representative for Europe. Finally, this information has led to a narrative description of the geochemical evolution at the disposal cell scale.

There is a lot of literature available about the alteration processes of engineered barriers and host rocks when interfacing solutions and porous media with or without γ-radiation and microbial activity. Quantification of the radiological, chemical and physical properties of the engineered barriers and host rocks is necessary in order to deduce whether the described factors for the alteration processes are relevant for geological disposal of radioactive waste. From the quantification of the properties of the waste and engineered barriers, radiation enhanced alteration of engineered materials can be excluded to have an impact on the chemical evolution of HLW disposal cells. Radiation enhanced corrosion of metals in ILW disposal cells is also negligible compared to chemical corrosion. Natural and archaeological analogues can therefore be used to identify the relevant processes. Natural and archaeological analogues are discussed in detail in Part II of this overview (Deissmann et al., 2024) and led to the conclusion that this identification of processes has been performed for the following interfaces: steel-concrete, steel-clay, concrete-clay and concrete-granite.

The sorbed iron species can alter the clay mineralogy in bentonite and the incorporated iron species are assumed to alter the cementitious minerals in concrete. The Fe-affected zone in bentonite and the Fe-affected zone in concrete are alteration zones. These zones can also be called ‘transformed media’ in literature. The available information for the Fe-affected zone in bentonite and its impact is abundant i.e., transformation from swelling clay minerals into non-swelling minerals. Its low permeability may be maintained in this transformation. For concrete, this information on the Fe-affected zone is limited to some chemical characterizations and a published observation of more than 30 years ago of concrete in the vicinity of steel being identified as ‘loosely bound material’. In ACED, a start has been made in studying the fate of iron in concrete (Jacques et al., 2024).

The engineered materials in the HLW disposal cells are the waste form glass, steel, concrete and/or bentonite. Microbial induced corrosion is prevented on the short term by the thermal load and can also be excluded on the long term by design and quality assurance. In any disposal concept for vitrified HLW, a carbon steel overpack is used to prevent contact between the vitrified waste form and pore water until the heat emission of the waste has sufficiently been diminished. The period in time for a sufficient decay in heat depends on the disposal concept and can be 500 years or more than 1,000 years.

The carbon steel overpack can be covered by a buffer made from bentonite or concrete. The long-term corrosion (alteration) rate of steel interfacing bentonite is about 100 times larger than this rate of steel interfacing concrete, i.e., below 10 μm per year and 0.1 μm per year, respectively. By design, the carbon steel overpack is therefore thicker in bentonite buffers than concrete buffers.

Mineralogical changes due to bentonite interfacing the host rocks are not envisaged i.e., the beneficial properties of bentonite remain on the long-term. The vitrified waste form comes into contact with pore water when the carbon steel thickness interfacing the bentonite buffer has become too small to support the mechanical load of the host rock. This is different for concrete since concrete has its own strength.

The pore water chemistry of the host rock pore water determines the chemical evolution of concrete. In well-engineered concrete, sulphate attack can be prevented and the ingress of magnesium from the host rock results into Mg-affected concrete with limited mechanical strength compared to fabricated concrete strength. The vitrified waste form comes into contact with pore water

when the carbon steel thickness has become too small and the Fe-affected zones and Mg-affected zones in the concrete buffer have become too large. The mechanical load of the host rock is transferred to the carbon steel overpack by the bentonite but the concrete buffer has its own fabricated strength. In this paper, it is assumed that the strength of the Fe-affected zone in concrete is negligible compared to its fabricated strength.

The bentonite, concrete and clay host rocks are materials with a low permeability. The chemical evolution of the disposal cells is determined by the exchange in dissolved species. The rate in exchange of dissolved species is small due to the low permeability. The excavation and drying of the indurated clay host rock further minimizes this rate in exchange. Quantification in transport properties and saturation degree in these low permeable materials are crucial in the determination when the carbon steel overpack has become too thin and the thickness of affected zones in concrete has become too large. The calculated periods to have material sufficiently altered in order to have contact between pore water and vitrified waste form can supersede the period in which vitrified HLW is more radiotoxic than uranium ore.

The vitrified waste form for HLW is well understood and characterised. Metallic ILW has been identified from the contributions provided by the information available from national programmes. The metals in cemented metallic ILW are steel (carbon steel and stainless steel) and Zircaloy. Like for carbon steel, also for stainless steel and Zircaloy, an alteration layer is formed with a mineral in equilibrium with a dissolved metal-complex concentration. The stability of these alteration layers depends on the pH and the concentration of dissolved species. The stability is largest at high pH for carbon steel (low alloy steel) and stainless steel (high alloy steel). Thermodynamic modelling and experimental studies show that dissolved calcium at representative disposal concentrations enhances the formation of this alteration layer for carbon steel. This calcium effect has not yet been included in the modelling of the chemical evolution at the interface between concrete and steel. Dissolved calcium can hinder the formation of the alteration layer for Zircaloy, but the required dissolved calcium concentrations are too high to be representative for disposal. Also for stainless steel, no effect is envisaged with the dissolved calcium concentrations in the engineered materials or host rocks.

Stainless steel and Zircaloy are used in nuclear power reactors due to their high corrosion resistance. The envisaged radionuclide release mechanism is the alteration/corrosion rate. The envisaged corrosion rates are so small that many radionuclides decay within these neutron irradiated metals. The transport of water through the cementitious material from the host rocks can also limit the corrosion process since the envisaged anaerobic corrosion process consumes water.

Organic ILW has also been identified from the contributions provided by the information available from national programmes. Organic waste can be considered as a potential food source for microbes if the useable energy to breakdown the organic molecules provide sufficient energy. Microbial degradation of organic waste can therefore be a primary process for the potential release of radionuclides. Spent ion exchange resins are ILW that are processed with cementitious materials. These resins do not provide sufficient energy to be broken down and microbial enhanced degradation can therefore be neglected. These resins are used to clean nuclear reactor contaminated waters due to their high radiation and chemical resistance. The mechanism for radionuclide release may not be relevant with an alteration of the resins. Resins are like clays, exchangers. Any radionuclide release can therefore also be envisaged to require sufficient ingress of anions and cations that have a stronger affinity than the sorbed anionic or cationic radionuclide. Cellulosic waste such as paper and clothing are in exceptional cases also characterised as ILW. Microbial degradation of this waste can be a primary process for the potential release of radionuclides, provided that the high pH of cementitious materials does not minimize this activity. The chemical degradation can be stimulated by the high pH and reduced by the lack of fluid flow and anaerobic conditions in geologically disposed of cemented waste packages. The dominant processes for the chemical evolution of disposal cells with cellulosic waste are to be identified.

In part II (Deissmann et al., 2024), we further describe how information on the geochemical evolution can be obtained–experimental, analogues and through modelling–and what the consequences are for performance of materials in view of physical (transport and mechanical) and chemical properties.

Author contributions

EN: Writing–review and editing, Writing–original draft, Conceptualization. GD: Conceptualization, Writing–review and editing, Writing–original draft. DJ: Writing–review and editing, Writing–original draft, Conceptualization.

Funding

The author(s) declare that financial support was received for the research, authorship, and/or publication of this article. The manuscript was prepared within the framework of the work package ACED within EURAD (European Joint Programme on Radioactive Waste Management); Grant Agreement No 847593.

Acknowledgments

This work is based on additional deliverables from the work package ACED of EURAD (mentioned in reference list) and on discussions during the work package meetings. The authors acknowledge all partners from the work package ACED for their fruitful discussions and input and contribution to the work package ACED.

Conflict of interest

The authors declare that the research was conducted in the absence of any commercial or financial relationships that could be construed as a potential conflict of interest.

The reviewer AL declared a past co-authorship with the author GD to the handling editor.

Publisher's note

All claims expressed in this article are solely those of the authors and do not necessarily represent those of their affiliated organizations, or those of the publisher, the editors and the reviewers. Any product that may be evaluated in this article, or claim that may be made by its manufacturer, is not guaranteed or endorsed by the publisher.

Supplementary material

The Supplementary Material for this article can be found online at: https://www.frontiersin.org/articles/10.3389/fnuen.2024.1433247/full#supplementary-material

References

Abdel Rahman, R. O., Elmesawy, M., Ashour, I., and Hung, Y.-T. (2014). Remediation of NORM and TENORM contaminated sites—review article. *Environ. Prog. and Sustain. Energy* 33, 588–596. doi:10.1002/ep.11829

Abrahamsen, L., Arnold, T., Brinkmann, H., Leys, N., Merroun, M., Mijnendonckx, K., et al. (2015). *A review of anthropogenic organic wastes and their degradation behaviour - deliverable 1.1 MIND. EURATOM Grant Agreement no. 661880*.

Adler, M. (2001). *Interaction of claystone and hyperalkaline solutions at 30°C: a combined experimental and modelling study*. Switzerland: University of Bern. PhD-Thesis.

Adler, M., Mäder, U. K., and Waber, H. N. (1999). High-pH alteration of argillaceous rocks: an experimental study. *Schweiz. Mineral. Petrogr. Mittl.* 79, 445–454.

Ahn, T. M., and Soo, P. (1995). Corrosion of low-carbon cast steel in concentrated synthetic groundwater at 80 to 150°C. *Waste Manag.* 15, 471–476. doi:10.1016/0956-053x(96)00001-3

Alcolea, A., Kuhlmann, U., Lanyon, G. W., and Marschall, P. (2014). *Hydraulic conductance of the EDZ around underground structures of a geological repository for radioactive waste – a sensitivity study for the candidate host rocks in the proposed siting regions in Northern Switzerland*. Switzerland: NAGRA, NAB, 13–94.

Alexander, W. R., Arcilla, C. A., Mckinley, I. G., Kawamura, H., Takahashi, Y., Aoki, K., et al. (2008). A new natural analogue study of the interaction of low-alkali cement leachates and the bentonite buffer of a radioactive waste repository. *MRS Proc.* 1107, 493. doi:10.1557/proc-1107-493

Alexander, W. R., Dayal, R., Eagleson, K., Eikenberg, J., Hamilton, E., Linklater, C. M., et al. (1992). A natural analogue of high pH cement pore waters from the Maqarin area of northern Jordan. II: results of predictive geochemical calculations. *J. Geochem. Explor.* 46, 133–146. doi:10.1016/0375-6742(92)90104-g

Alexander, W. R., and Mckinley, I. G. (1999). The chemical basis of near-field containment in the Swiss high-level radioactive waste disposal concept. *Geol. Soc. Spec. Publ.* 157, 47–69. doi:10.1144/GSL.SP.1999.157.01.05

Alexander, W. R., and Milodowski, A. E. (2011). *Cyprus natural analogue project (CNAP) phase II final report*. Posiva: Finland. Working Report 2011-08.

Alexander, W. R., and Smellie, J. A. T. (1998) "Maqarin natural analogue project," in *ANDRA, CEA, NAGRA, nirex and SKB synthesis report on phases I, II and III. Nagra project report NPB 98-08*. Switzerland: Nagra.

Alexander, R. 2012. The impact of a (hyper)alkaline plume on (fractured) crystalline. *In:* (ed.) *Cementitious materials in safety cases for geological repositories for radioactive waste: role, evolution and interactions*. NEA/RWM/R (2012) 3 REV.

Allard, T., Balan, E., Calas, G., Fourdrin, C., Morichon, E., and Sorieul, S. (2012). Radiation-induced defects in clay minerals: a review. *Nucl. Instrum. Methods Phys. Res. Sect. B Beam Interact. Mater. Atoms* 277, 112–120. doi:10.1016/j.nimb.2011.12.044

Alonso, M. C., García Calvo, J. L., Cuevas, J., Turrero, M. J., Fernández, R., Torres, E., et al. (2017). Interaction processes at the concrete-bentonite interface after 13 years of FEBEX-Plug operation. Part I: concrete alteration. *Phys. Chem. Earth, Parts A/B/C* 99, 38–48. doi:10.1016/j.pce.2017.03.008

Altmaier, M., Blin, V., Garcia, D., Henocq, P., Missana, T., Ricard, D., et al. (2021). *SOTA on cement-organic-radionuclide interactions*. Final version as 19.05.2021 Deliv. D3.1 HORIZON 2020 Proj. EURAD. EC Grant Agreem. no, 847593.

Altmaier, M., Ricard, D., Vandenborre, J., Garcia, D., Henocq, P., Macé, N., et al. (2024). *Final report o results generated in CORI. Final version of deliverables D3.6, D3.7 and D.8 of the HORIZON 2020 project EURAD*. EC Grant agreement.847593

Andrade, C., Tavares, F., Toro, L., and Fullea, J. (2011). "Observation on the morphology of oxide formation due to reinforcement corrosion," in *Proceedings of the joint fib-RILEM workshop*. Editors C. ANDRADE and G. MANCINI (Madrid, Spain).

Aréna, H., Godon, N., Rébiscoul, D., Podor, R., Garcès, E., Cabie, M., et al. (2016). Impact of Zn, Mg, Ni and Co elements on glass alteration: additive effects. *J. Nucl. Mater.* 470, 55–67. doi:10.1016/j.jnucmat.2015.11.050

AREVA (2007). Specification for standard vitrified waste residue (CSD-v) with high actinide content produced at la Hague AREVA. *AREVA*.

Argo, J. (1981). A qualitative test for iron corrosion products. *Stud. Conservation* 26, 140–142. doi:10.2307/1505882

Ashikawa, N., Tajima, T., Saito, H., and Fujiwara, A. (2001) "Sorption behavior of radionuclides on calcium-leached mortar," in *Material research society symposium proceedings*.

Atabek, R., Beziat, A., Coulon, H., Dardaine, M., Debrabant, P., Eglem, A., et al. (1991). Nearfield behaviour of clay barriers and their interaction with concrete - task 3 Characterization of radioactive waste forms A series of final reports (1985-1989). *Nucl. Sci. Technol.* 26, 13877.

Atkins, M., Beckley, N., Carson, S., Cowie, J., Glasser, F. P., Kindness, A., et al. (1991). Medium-active waste form characterization: the performance of cementbased systems Task 3 Characterization of radioactive waste forms A series of final reports (1985-1989). *Nucl. Sci. Technol.* 1, 13452.

Atkinson, A., Goult, D. J., and Hearne, J. A. (1985). An assessment of the long-term durability of concrete in radioactive waste repositories. *MRS Online Proc. Libr.* 50, 239–246. doi:10.1557/proc-50-239

Azcárate, I., Insausti, M., and Madina, V. (2004) "Estudio de los productos de CORROsión de la cápsula y su interacción con la barrera arcillosa de BENtonita CORROBEN," in *Publicacion tecnica 02/2004*. Spain: ENRESA.

Baehr, W. (1989). Industrial vitrification processes for high-level liquid waste solutions. *IAEA Bull.* 4, 43–46.

Baker, A. J., Bateman, K., Hyslop, E. K., Ilett, D. J., Linklater, C. M., Milodowski, A. E., et al. (2002). *Research on the alkaline disturbed zone resulting from cement-water-rock reactions around a cementitious repository*. Harwell, Didcot, United Kingdom: UK Nirex Limited Report N/054, UK Nirex Ltd.

Balmer, S., Kaufhold, S., and Dohrmann, R. (2017). Cement-bentonite-iron interactions on small scale tests for testing performance of bentonites as a barrier in high-level radioactive waste repository concepts. *Appl. Clay Sci.* 135, 427–436. doi:10.1016/j.clay.2016.10.028

Bamforth, P. B., Baston, G. M. N., Berry, J. A., Glaser, F. P., Heath, T. G., Jackson, C. P., et al. (2012) "Cement materials for use as backfill, sealing and structural materials in geological disposal concepts. A review of current status,". Serco, Harwell, Didcot, United Kingdom. Serco Report SERCO/005125/001 Issue 3.

Bart, G., Zwicky, H. U., Aerne, E. T., Graber, T. H., Z'Berg, D., and Tokiwai, M. (1987). Borosilicate glass corrosion in the presence of steel corrosion products. *Mater. Res. Soc. Symposium Proc.* 84, 459–470. doi:10.1557/proc-84-459

Bartier, D., Techer, I., Dauzères, A., Boulvais, P., Blanc-Valleron, M.-M., and Cabrera, J. (2013). *In situ* investigations and reactive transport modelling of cement paste/argillite interactions in a saturated context and outside an excavated disturbed zone. *Appl. Geochem.* 31, 94–108. doi:10.1016/j.apgeochem.2012.12.009

Bataillon, C., Bouchon, F., Chainais-Hillairet, C., Desgranges, C., Hoarau, E., Martin, F., et al. (2010). Corrosion modelling of iron based alloy in nuclear waste repository. *Electrochimica Acta* 55, 4451–4467. doi:10.1016/j.electacta.2010.02.087

Bateman, K., Coombs, P., Noy, D. J., Pearce, J. M., Wetton, P., Haworth, A., et al. (1999). Experimental simulation of the alkaline disturbed zone around a cementitious radioactive waste repository: numerical modelling and column experiments. *Geol. Soc. Spec. Publ.* 157, 183–194. doi:10.1144/GSL.SP.1999.157.01.14

Baxter, S., Appleyard, P., Hartley, L., Hoek, J., and Williams, T. (2018). "Exploring conditioned simulations of discrete fracture networks in support of hydraulic acceptance of deposition holes," in *Application to the ONKALO demonstration area* (Posiva, Finland: Posiva SKB Report 07).

Beattie, T. M., and Williams, S. J. (2012). An overview of near-field evolution research in support of the UK geological disposal programme. *Mineral. Mag.* 76, 2995–3001. doi:10.1180/minmag.2012.076.8.15

Bel, J. P., Wickham, S. M., and Gens, R. M. F. (2006). Development of the supercontainer design for deep geological disposal of high-level heat emitting

radioactive waste in Belgium. *Mater. Res. Soc. Symposium Proc.* 932, 1221. doi:10.1557/proc-932-122.1

Berner, U. R. (1992). Evolution of pore water chemistry during degradation of cement in a radioactive waste repository environment. *Waste Manag.* 12, 201–219. doi:10.1016/0956-053x(92)90049-o

Berner, U., Kulik, D. A., and Kosakowski, G. (2013). Geochemical impact of a low-pH cement liner on the near field of a repository for spent fuel and high-level radioactive waste. *Phys. Chem. Earth, Parts A/B/C* 64, 46–56. doi:10.1016/j.pce.2013.03.007

Bernier, F., Li, X. L., Bastiaens, W., Ortiz, L., Van Geet, M., Wouters, L., et al. 2007. Fractures and self-healing within the excavation disturbed zone in clays (SELFRAC). EURATOM framework programme contract No: FI4CT96-0028, nuclear science and Technology European commission, EUR 22585

Bertolini, L., Elsener, B., Pedeferri, P., and Polder, R. (2004). *Corrosion of steel in concrete: prevention, diagnosis, repair*. Wiley-VCH Verlag.

Bildstein, O., and Claret, F. (2015). "Chapter 5 - stability of clay barriers under chemical perturbations," in *Developments in clay science*. Editors C. TOURNASSAT, C. I. STEEFEL, I. C. BOURG, and F. BERGAYA (Elsevier).

Bildstein, O., Claret, F., and Frugier, P. (2019). RTM for waste repositories. *Rev. Mineralogy Geochem.* 85, 419–457. doi:10.2138/rmg.2019.85.14

Bildstein, O., Lartigue, J., Pointeau, I., Cochepin, B., Munier, I., and Michau, N. (2012). "Chemical evolution in the near field of HLW cells: interactions between glass, steel and clay-stone in deep geological conditions," in 5th ANDRA International Meeting, Montpellier, France, October 22–October 25.

Bildstein, O., Trotignon, L., Perronnet, M., and Jullien, M. (2006). Modelling iron-clay interactions in deep geological disposal conditions. *Phys. Chem. Earth* 31, 618–625. doi:10.1016/j.pce.2006.04.014

Bildstein, O., Trotignon, L., Pozo, C., and Jullien, M. (2007). Modelling glass alteration in an altered argillaceous environment. *J. Nucl. Mater.* 362, 493–501. doi:10.1016/j.jnucmat.2007.01.225

Björner, I. K., Christensen, H., Hermansson, H. P., Tsukamo, M., and Werme, L. (1987). Corrosion of radioactive, crushed waste glass. *Mater. Res. Soc. Symposium Proc.* 127, 113–120. doi:10.1557/proc-127-113

Blackwood, D. J., Gould, L. J., Naish, C. C., Porter, F. M., Rance, A. P., Sharland, S. M., et al. (2002). *The localised corrosion of carbon steel and stainless steel in simulated repository environments*. Harwell, United Kingdom: AEA Technology. Report AEAT/ERRA-0318.

Blanc, P., Debure, M., Govaerts, J., Gu, Y., Jacques, D., Kosakowski, G., et al. (2002). *Description of ILW modelling results and recommendations for future experiments and numerical work: Deliverable 2.15 of the HORIZON 2020 project EURAD*. EC Grant agreement no: 847593.

Bradbury, M. H., Berner, U., Curti, E., Hummel, W., Kosakowski, G., and Thoenen, T. (2014) "The long term geochemical evolution of the nearfield of the HLW repository," in *NAGRA technical report NTB 12-01*. Switzerland: Nagra.

Broomfield, J. P. (2007). *Corrosion of steel in concrete: understanding, investigation and repair*. 2nd edition. Florida, United States: CRC Press.

Brown, A. R. (2013). *The impact of ionizing radiation on microbial cells pertinent to storage, disposal and remediation of radioactive waste*. United Kingdom: University of Manchester. PhD thesis.

Bruhn, D. F., Frank, S. M., Roberto, F. F., Pinhero, P. J., and Johnson, S. G. (2009). Microbial biofilm growth on irradiated, spent nuclear fuel cladding. *J. Nucl. Mater.* 384, 140–145. doi:10.1016/j.jnucmat.2008.11.008

Burger, E., Rebiscoul, D., Bruguier, F., Jublot, M., Lartigue, J. E., and Gin, S. (2013). Impact of iron on nuclear glass alteration in geological repository conditions: a multiscale approach. *Appl. Geochem.* 31, 159–170. doi:10.1016/j.apgeochem.2012.12.016

Capouet, M., Necib, S., Schumacher, S., Mibus, J., Neeft, E. A. C., Norris, S., et al. (2018). *CAST outcomes in the context of the safety case: WP6 Synthesis report D 6.4 of the EURATOM seventh framework project CAST grant agreement no. 604779*.

Caré, S., Nguyen, Q. T., L'Hostis, V., and Berthaud, Y. (2008). Mechanical properties of the rust layer induced by impressed current method in reinforced mortar. *Cem. Concr. Res.* 38, 1079–1091. doi:10.1016/j.cemconres.2008.03.016

Carlson, L., Karnland, O., Oversby, V. M., Rance, A. P., Smart, N. R., Snellman, M., et al. (2007). Experimental studies of the interactions between anaerobically corroding iron and bentonite. *Phys. Chem. Earth, Parts A/B/C* 32, 334–345. doi:10.1016/j.pce.2005.12.009

Carlson, L., Karnland, O., Rance, A., and Smart, N. (2008) *Experimental studies on the interactions between anaerobically corroding iron and bentonite*. Sweden: SKB R-08-28, SKB.

Carlsson, A., and Christiansson, R. (2007). *Construction experiences from underground works at Forsmark*. Sweden: SKB. SKB Rapport R-07-10.

Carpén, L., Rajala, P., and Kinnunen, T. (2018). "Real-time corrosion monitoring system under *in situ* conditions of crystalline groundwater," in *European corrosion congress* (Krakow, Poland). EUROCORR 2018.

CEA (2009). in *Nuclear waste conditioning*. Editor E. E. VERNAZ CEA.

CEN (2019). *Testing fresh concrete - Part 7: air content - pressure methods*. NEN-EN 12350-7:2019.

Černoušek, T., Kokinda, J., Vizelková, K., and Shrestha and Ševců, A. (2019). *Anaerobic microbial corrosion of canister material - deliverable 2.13 MIND. EURATOM Grant Agreement no. 661880*.

Chamssedine, F., Sauvage, T., Peuget, S., Fares, T., and Martin, G. (2010). Helium diffusion coefficient measurements in R7T7 nuclear glass by 3He(d,α)1H nuclear reaction analysis. *J. Nucl. Mater.* 400, 175–181. doi:10.1016/j.jnucmat.2010.02.023

Chaparro, M. C., Saaltink, M. W., and Soler, J. M. (2017). Reactive transport modelling of cement-groundwater-rock interaction at the Grimsel Test Site. *Phys. Chem. Earth, Parts A/B/C* 99, 64–76. doi:10.1016/j.pce.2017.05.006

Chapman, N. A., and Hooper, A. (2012). The disposal of radioactive wastes underground. *Proc. Geologists' Assoc.* 123, 46–63. doi:10.1016/j.pgeola.2011.10.001

Charlet, L., and Tournassat, C. (2005). Fe(II)-Na(I)-Ca(II) cation exchange on montmorillonite in chloride medium: evidence for preferential clay adsorption of chloride – metal ion pairs in seawater. *Aquat. Geochem.* 11, 115–137. doi:10.1007/s10498-004-1166-5

Charpentiera, D., Devineau, K., Mosser-Ruck, R., Cathelineau, M., and Villiéras, F. (2006). Bentonite–iron interactions under alkaline condition: an experimental approach. *Appl. Clay Sci.* 32, 1–13. doi:10.1016/j.clay.2006.01.006

Chitty, W.-J., Dillmann, P., L'Hostis, V., and Lombard, C. (2005). Long-term corrosion resistance of metallic reinforcements in concrete—a study of corrosion mechanisms based on archaeological artefacts. *Corros. Sci.* 47, 1555–1581. doi:10.1016/j.corsci.2004.07.032

Chomat, L., Amblard, E., Varlet, J., Blanc, C., and Bourbon, X. (2017). Passive corrosion of steel reinforcement in blended cement-based material in the context of nuclear waste disposal. *Corros. Eng. Sci. Technol.* 52, 148–154. doi:10.1080/1478422x.2017.1300378

Chomat, L., L'Hostis, V., Amblard, E., and Bellot-Gurlet, L. (2014). Long term study of passive corrosion of steel rebars in Portland mortar in context of nuclear waste disposal. *Corros. Eng. Sci. Technol.* 49, 467–472. doi:10.1179/1743278214y.0000000201

Claret, F., Marty, N., and Tournassat, C. (2018). "Modeling the long-term stability of multi-barrier systems for nuclear waste disposal in geological clay formations," in *Reactive transport modeling: applications in subsurface energy and environmental problems*. Editors X. YITIAN, W. FIONA, X. TIANFU, and C. STEEFEL (John Wiley and Sons Ltd).

Clarke, A. S., Scales, C., Patel, N., Roe, J., and Banford, A. W. (2020). Active demonstration of the thermal treatment of surrogate sludge and surrogate drums using the GeoMelt™ in Container Vitrification (ICV) melter installed in NNL Central Laboratory. *IOP Conf. Ser. Mater. Sci. Eng.* 818, 012004. doi:10.1088/1757-899x/818/1/012004

Cochepin, B., Martin, C., and Munier, I. (2020). "Chapter 10 France," in *Treatment of chemical evolution in National Programmes, D 2.4 of the HORIZON 2020 project EURAD*. Editors E. NEEFT, E. WEETJENS, A. VOKAL, M. LEIVO, B. COCHEPIN, C. MARTIN, et al. (EC Grant agreement), 847593.

COGEMA 2001. Specification for compacted waste standard residue from light water reactor fuel. COGEMA Technical document 300 AQ 055-03 (Confidential document not published openly).

Conradt, R., Roggendorf, H., and Ostertag, R. (1986) *The basic corrosion mechanisms of HLW glasses*, 10680. EUR: Commission of the European Communities - Nuclear Science and Technology.

Corkhill, C. L., Cassingham, N. J., Heath, P. G., and Hyatt, N. C. (2013). Dissolution of UK high-level waste glass under simulated hyperalkaline conditions of a colocated geological disposal facility. *Int. J. Appl. Glass Sci.* 4, 341–356. doi:10.1111/ijag.12042

Crossland, I. C. (2006). "Long-term properties of cement – evidence from nature and archaeology," in The 10th International Conference on Environmental Remediation and Radioactive Waste Management, Glasgow (Scotland) (United Kingdom: ASME). ICEM05-1272.

Cuevas, J., Ruiz, A. I., Fernández, R., Torres, E., Escribano, A., Regadío, M., et al. (2016). Lime mortar-compacted bentonite–magnetite interfaces: an experimental study focused on the understanding of the EBS long-term performance for high-level nuclear waste isolation DGR concept. *Appl. Clay Sci.* 124-125, 79–93. doi:10.1016/j.clay.2016.01.043

Cuevas, J., Vigil DE LA Villa, R., Ramirez, S., Sanchez, L., Fernández, R., and Leguey, S. (2006). The alkaline reaction of FEBEX bentonite: a contribution to the study of the performance of bentonite/concrete engineered barrier systems. *J. Iber. Geol.* 32, 151–174.

Cuevas, J., Villar, M. V., Cobeña, J. C., and Leguey, S. (2002). Thermo-hydraulic gradients on bentonite: distribution of soluble salts, microstructure and modification of the hydraulic and mechanical behaviour. *Appl. Clay Sci.* 22, 25–38. doi:10.1016/s0169-1317(02)00109-6

Cvetković, B. Z., Salazar, G., Kunz, D., Tits, J., Szidat, S., and Wieland, E. (2018). Quantification of dissolved organic 14C-containing compounds by accelerator mass

spectrometry in a corrosion experiment with irradiated steel. *Radiocarbon* 60, 1711–1727. doi:10.1017/rdc.2018.90

Dauzères, A. (2016). "Geochemical and physical evolution of cementitious materials in an aggressive environment," in *CEBAMA Deliverable D 1.03 - WP1 Experimental studies – state of the art literature review*. Editors T. VEHMAS and E HOLT

Dauzères, A., Achiedo, G., Nied, D., Bernard, E., Alahrache, S., and Lothenbach, B. (2016). Magnesium perturbation in low-pH concretes placed in clayey environment-solid characterizations and modeling. *Cem. Concr. Res.* 79, 137–150. doi:10.1016/j.cemconres.2015.09.002

Dauzères, A., Le Bescop, P., Cau-Dit-Coumes, C., Brunet, F., Bourbon, X., Timonen, J., et al. (2014). On the physico-chemical evolution of low-pH and CEM I cement pastes interacting with Callovo-Oxfordian pore water under its *in situ* CO2 partial pressure. *Cem. Concr. Res.* 58, 76–88. doi:10.1016/j.cemconres.2014.01.010

Dauzères, A., Le Bescop, P., Sardini, P., and Coumes, C. C. D. (2010). Physico-chemical investigation of clayey/cement-based materials interaction in the context of geological waste disposal: experimental approach and results. *Cem. Concr. Res.* 40, 1327–1340. doi:10.1016/j.cemconres.2010.03.015

Davis, J. R. (2000). *Corrosion: understanding the basics*. Materials Park, Ohio, USA: ASM International.

De Combarieu, G., Barboux, P., and Minet, Y. (2007). Iron corrosion in Callovo–Oxfordian argilite: from experiments to thermodynamic/kinetic modelling. *Phys. Chem. Earth* 32, 346–358. doi:10.1016/j.pce.2006.04.019

De Combarieu, G., Schlegel, M. L., Neff, D., Foy, E., Vantelon, D., Barboux, P., et al. (2011). Glass-iron-clay interactions in a radioactive waste geological disposal: an integrated laboratory-scale experiment. *Appl. Geochem.* 26, 65–79. doi:10.1016/j.apgeochem.2010.11.004

De Echave, T., Tribet, M., Gin, S., and Jégou, C. (2019). Influence of iron on the alteration of the SON68 nuclear glass in the Callovo-Oxfordian groundwater. *Appl. Geochem.* 100, 268–278. doi:10.1016/j.apgeochem.2018.12.007

Deissmann, G., and Ait Mouheb, N. (2021). "Interface "cement/concrete – clay"," in *Experiments and numerical model studies on interfaces*. Editors G. DEISSMANN, N. AIT MOUHEB, C. MARTIN, M. J. TURRERO, E. TORRES, B. KURSTEN, et al. *Final version as of 12.05.2021 of deliverable D2.5 of the HORIZON 2020 project EURAD. EC Grant agreement no: 847593*.

Deissmann, G., Mouheb, N. A., Martin, C., Turrero, M. J., Torres, E., Kursten, B., et al. (2021). *Experiments and numerical model studies on interfaces. Final version as of 12.05.2021 of deliverable D2.5 of the HORIZON 2020 project EURAD. EC Grant agreement no: 847593*.

Deissmann, G., Neeft, E., and Jacques, D. (2024). Assessment of the chemical evolution at the disposal cell scale – Part II – gaining insight in the geochemical evolution. *Front. Nucl. Eng.* this issue.

De Putter, T., Grainger, P., Lombardi, S., Manfroy, P., and Valentini, G. (1997). "Preservation of unaltered wood in clay formations: a natural analogue of clay barriers against RN migration," in *European Commission: Directorate-General for Environment, Directorate-General for Human Resources and Security and McMenamin, T., Fourth European conference on management and disposal of radioactive waste*. Editor T. McMenamin (EUR).

Deshpande, P. G., Seddelmeyer, J. D., Wheat, H. G., Fowler, D. W., and Jirsa, J. O. (2000). *Corrosion performance of polymer-coated, metal-clad and other rebars as reinforcement in concrete. Report FHWA/TX-03/4904-2*. Austin, TX, USA: Texas Department of Transportation.

Dillmann, P., Gin, S., Neff, D., Gentaz, L., and Rebiscoul, D. (2016). Effect of natural and synthetic iron corrosion products on silicate glass alteration processes. *Geochimica Cosmochimica Acta* 172, 287–305. doi:10.1016/j.gca.2015.09.033

Dillmann, P., Neff, D., and Féron, D. (2014). Archaeological analogues and corrosion prediction: from past to future. A review. *Corros. Eng. Sci. Technol.* 49, 567–576. doi:10.1179/1743278214y.0000000214

Dizier, A., Chen, G., Li, X. L., and Rypens, J. (2017). *The PRACLAY Heater test after two years of the stationary phase*. Belgium: EURIDICE. EURIDICE Report, EUR PH 17 043.

Drace, Z., and Ojovan, M. I. (2013). "A summary of IAEA coordinated research project on cementitious materials for radioactive waste management," in *Cement-based materials for nuclear waste storage*. Editors F. BART, C. CAU-DI-COUMES, F. FRIZON, and S. LORENTE (New York, NY: Springer New York).

Drake, H., Sandström, B., and Tullborg, E.-L. (2006). *Mineralogy and geochemistry of rocks and fracture fillings from Forsmark and Oskarshamn: compilation of data for SR-Can*. Sweden: SKB. SKB Report R-06-109.

Druyts, F., Kursten, B., and Van Iseghem, P. (2001). *Corrosion evaluation of metallic materials for long-lived HLW/Spent Fuel disposal containers. Final report to EDF for the period 1996-1998. SCK●CEN R-3533*. Belgium: SCK CEN.

Eglinton, M. (1998). "Resistance of concrete to destructive agencies," in *Lea's chemistry of cement and concrete*. Editor P. C. HEWLETT (London: Arnold).

Eisele, T. C., Kawatra, S. K., and Ripke, S. J. (2005). Water chemistry effects in iron ore concentrate agglomeration feed. *Mineral Process. Extr. Metallurgy Rev.* 26, 295–305. doi:10.1080/08827500590944063

Fernández, R., Ruiz, A. I., and Cuevas, J. (2016). Formation of C-A-S-H phases from the interaction between concrete or cement and bentonite. *Clay Miner.* 51, 223–235. doi:10.1180/claymin.2016.051.2.09

Fernández, R., Torres, E., Ruiz, A. I., Cuevas, J., Alonso, M. C., García Calvo, J. L., et al. (2017). Interaction processes at the concrete-bentonite interface after 13 years of FEBEX-Plug operation. Part II: bentonite contact. *Phys. Chem. Earth, Parts A/B/C* 99, 49–63. doi:10.1016/j.pce.2017.01.009

Ferrand, K., Abdelouas, A., and Grambow, B. (2006). Water diffusion in the simulated French nuclear waste glass SON 68 contacting silica rich solutions: experimental and modeling. *J. Nucl. Mater.* 355, 54–67. doi:10.1016/j.jnucmat.2006.04.005

Fujisawa, R., Cho, T., Sugahara, K., Takizawa, Y., Horikawa, Y., Shiomi, T., et al. (1996). The corrosion behavior of iron and aluminum under waste disposal conditions. *MRS Online Proc. Libr.* 465, 675–682. doi:10.1557/proc-465-675

Fujisawa, R., Kurashige, T., Inagaki, Y., and Senoo, M. (1999). Gas generation behavior of transuranic waste under disposal conditions. *MRS Online Proc. Libr.* 556, 1199. doi:10.1557/proc-556-1199

Fukushi, K., Sugiura, T., Morishita, T., Takahashi, Y., Hasebe, N., and Ito, H. (2010). Iron–bentonite interactions in the Kawasaki bentonite deposit, Zao area, Japan. *Appl. Geochem.* 25, 1120–1132. doi:10.1016/j.apgeochem.2010.04.016

Furcas, F. E., Lothenbach, B., Isgor, O. B., Mundra, S., Zhang, Z., and Angst, U. M. (2022). Solubility and speciation of iron in cementitious systems. *Cem. Concr. Res.* 151, 106620. doi:10.1016/j.cemconres.2021.106620

Gaboreau, S., Lerouge, C., Dewonck, S., Linard, Y., Bourbon, X., Fialips, C. I., et al. (2012). *In-Situ* interaction of cement paste and shotcrete with claystones in a deep disposal context. *Am. J. Sci.* 312, 314–356. doi:10.2475/03.2012.03

Gaboreau, S., Pret, D., Tinseau, E., Claret, F., Pellegrini, D., and Stammose, D. (2011). 15 years of *in situ* cement-argillite interaction from Tournemire URL: characterisation of the multi-scale spatial heterogeneities of pore space evolution. *Appl. Geochem.* 26, 2159–2171. doi:10.1016/j.apgeochem.2011.07.013

Gaucher, E. C., and Blanc, P. (2006). Cement/clay interactions – a review: experiments, natural analogues, and modeling. *Waste Manag.* 26, 776–788. doi:10.1016/j.wasman.2006.01.027

Gdowski, G. E., and Bullen, D. B. (1988) "Survey of degradation modes of candidate materials for high-level radioactive waste disposal containers. Oxidation and corrosion," in *LLNL report UCID-21362*, 2. Livermore, CA, USA: Lawrence Livermore National Laboratory.

Gehin, A., Greneche, J. M., Tournassat, C., Brendle, J., Rancourt, D. G., and Charlet, L. (2007). Reversible surface-sorption-induced electron-transfer oxidation of Fe(II) at reactive sites on a synthetic clay mineral. *Geochimica Cosmochimica Acta* 71, 863–876. doi:10.1016/j.gca.2006.10.019

Gin, S. (2014). Open scientific questions about nuclear glass corrosion. *Procedia Mater. Sci.* 7, 163–171. doi:10.1016/j.mspro.2014.10.022

Gin, S., Abdelouas, A., Criscenti, L. J., Ebert, W. L., Ferrand, K., Geisler, T., et al. (2013). An international initiative on long-term behavior of high-level nuclear waste glass. *Mater. Today* 16, 243–248. doi:10.1016/j.mattod.2013.06.008

Gin, S., Beaudoux, X., Angéli, F., Jégou, C., and Godon, N. (2012). Effect of composition on the short-term and long-term dissolution rates of ten borosilicate glasses of increasing complexity from 3 to 30 oxides. *J. Non-Crystalline Solids* 358, 2559–2570. doi:10.1016/j.jnoncrysol.2012.05.024

Gin, S., Jollivet, P., Fournier, M., Angeli, F., Frugier, P., and Charpentier, T. (2015). Origin and consequences of silicate glass passivation by surface layers. *Nat. Commun.* 6, 6360. doi:10.1038/ncomms7360

Glasser, F. P., Marchand, J., and Samson, E. (2008). Durability of concrete - degradation phenomena involving detrimental chemical reactions. *Cem. Concr. Res.* 38, 226–246. doi:10.1016/j.cemconres.2007.09.015

Glasser, F. (2011). "Application of inorganic cements to the conditioning and immobilisation of radioactive wastes," in *Handbook of advanced radioactive waste conditioning Technologies*. Editor M. OJOVAN (United Kingdom: Woodhead Publishing).

Godon, N., Gin, S., Rebiscoul, D., and Frugier, P. (2013). SON68 glass alteration enhanced by magnetite. *Proc. Fourteenth Int. Symposium Water-Rock Interact. Wri* 14 (7), 300–303. doi:10.1016/j.proeps.2013.03.039

Goñi, S., and Andrade, C. (1990). Synthetic concrete pore solution chemistry and rebar corrosion rate in the presence of chlorides. *Cem. Concr. Res.* 20, 525–539. doi:10.1016/0008-8846(90)90097-h

Grambow, B. (1987). Nuclear waste glass dissolution: mechanism, model and application. *Rep. JSS Proj. Phase IV*. Report No. JSS-87-02, Sweden.

Grambow, B., López-García, M., Olmeda, J., Grivé, M., Marty, N. C. M., Grangeon, S., et al. (2020). Retention and diffusion of radioactive and toxic species on cementitious systems: main outcome of the CEBAMA project. *Appl. Geochem.* 112, 104480. doi:10.1016/j.apgeochem.2019.104480

Grambow, B., Zwicky, H. U., Bart, G., Björner, I. K., and Werme, L. O. (1987). Modeling of the effect of iron corrosion products on nuclear waste glass performance. *Mater. Res. Soc. Symposium Proc.* 84, 471–481. doi:10.1557/proc-84-471

Gras, J.-M. (2014). *State of the art of 14C in Zircaloy and Zr alloys - 14C release from zirconium alloy hulls D 3.1 of the EURATOM seventh framework project CAST grant agreement no. 604779*.

Grauer, R. (1988). *The corrosion behaviour of carbon steel in portland cement*. Switzerland: Nagra. NAGRA Technical report 88-02 E.

Grivé, M., and Olmeda, J. (2015). *Molybdenum behaviour in cementitious materials*. Cebama project deliverable 2.03 WP2: State of the art report. *(initial)*.

Guillaume, D., Neaman, A., Cathelineau, M., Mosser-Ruck, R., Peiffert, C., Abdelmoula, M., et al. (2003). Experimental synthesis of chlorite from smectite at 300°C in the presence of metallic Fe. *Clay Miner.* 38, 281–302. doi:10.1180/0009855033830096

Guillaume, D., Neaman, A., Cathelineau, M., Mosser-Ruck, R., Peiffert, C., Abdelmoula, M., et al. (2004). Experimental study of the transformation of smectite at 80 and 300°C in the presence of Fe oxides. *Clay Miner.* 39, 17–34. doi:10.1180/000985543910117

Guo, X., Gin, S., Lei, P., Yao, T., Liu, H., Schreiber, D. K., et al. (2020). Self-accelerated corrosion of nuclear waste forms at material interfaces. *Nat. Mater.* 19, 310–316. doi:10.1038/s41563-019-0579-x

Hadi, J., Wersin, P., Serneels, V., and Greneche, J. M. (2019). Eighteen years of steel-bentonite interaction in the FEBEX "*in situ*" test at the Grimsel Test Site in Switzerland. *Clays and Clay Minerals* 67, 111–131. doi:10.1007/s42860-019-00012-5

Hedin, A., Andersson, J., Skagius, K., Spahiu, K., Zetterström Lilja, C., Sellin, P., et al. (2011). *Long-term safety for the final repository for spent nuclear fuel at Forsmark Main report of the SR-Site project Volume I*. Sweden: SKB. SKB Report TR-11-01.

Hermansson, H.-P. (2004) "The stability of magnetite and its significance as a passivating film in the repository environment," in *SKI report 2004:07*. Stockholm, Sweden: Swedish Nuclear Power Inspectorate.

Hewlett, P. C. (1998). *Lea's chemistry of cement and concrete*. London: Arnold.

Hoch, A. R., Baston, G. M. N., Glasser, F. P., Hunter, F. M. I., and Smith, V. (2012). Modelling evolution in the near field of a cementitious repository. *Mineral. Mag.* 76, 3055–3069. doi:10.1180/minmag.2012.076.8.21

Höglund, L. O. (2014). *The impact of concrete degradation on the BMA barrier functions*. Sweden: SKB. SKB Report R-13-40.

Holmboe, M., Jonsson, M., and Wold, S. (2012). Influence of γ-radiation on the reactivity of montmorillonite towards H2O2. *Radiat. Phys. Chem.* 81, 190–194. doi:10.1016/j.radphyschem.2011.10.009

Honda, A., Teshima, T., Tsurudome, K., Ishikawa, H., Yusa, Y., and Sasaki, N. (1991). Effect of compacted bentonite on the corrosion behavior of carbon-steel as geological isolation overpack material. *Sci. Basis Nucl. Waste Manag. Xiv* 212, 287–294. doi:10.1557/proc-212-287

Hunter, F., Bate, F., and Heath, T. (2007). *Geochemical investigation of iron transport into bentonite as steel corrodes*. Sweden: SKB. SKB Technical Report TR-07-09.

Hussain, S. E., and Rasheeduzzafar (1993). Effect of temperature on pore solution composition in plain cements. *Cem. Concr. Res.* 23, 1357–1368. doi:10.1016/0008-8846(93)90073-i

Hussain, S. E., Algahtani, A. S., and RASHEEDUZZAFAR (1996). Chloride threshold for corrosion of reinforcement in concrete. *Aci Mater. J.* 93, 534–538.

IAEA (2002). *Application of ion exchange processes for the treatment of radioactive waste and management of spent ion exchangers*. Vienna: IAEA.

IAEA (2004). *Management of waste containing tritium and carbon-14*. Vienna: IAEA.

IAEA (2013). *The behaviours of cementitious materials in long term storage and disposal of radioactive waste*. Vienna: IAEA.

Idiart, A., Lavina, M., Kosakowski, G., Cochepin, B., Meeussen, J. C. L., Samper, J., et al. (2020). Reactive transport modelling of a low-pH concrete/clay interface. *Appl. Geochem.* 115, 104562. doi:10.1016/j.apgeochem.2020.104562

Jacques, D., Neeft, E., and Deissmann, G. (2024). *Updated State of the Art on the assessment of the chemical evolution of ILW and HLW disposal cells. Final version as of 15.05.2024 of deliverable D2.2 of the HORIZON 2020 project EURAD*. EC Grant agreement no.847593

Jacques, D., Phung, Q. T., Perko, J., Seetharam, S. C., Maes, N., Liu, S., et al. (2021a). Towards a scientific-based assessment of long-term durability and performance of cementitious materials for radioactive waste conditioning and disposal. *J. Nucl. Mater.* 557, 153201. doi:10.1016/j.jnucmat.2021.153201

Jacques, D., Yu, L., Ferreira, M., and Oey, T. (2021b). Overview of state-of-the-art knowledge for the quantitative assessment of the ageing/deterioration of concrete in nuclear power plant systems, structures, and components. *Deliv. 1.1 ACES Proj*. Available at: https://aces-h2020.eu/deliverables/.

Jefferies, N. L., Tweed, C. J., and Wisbey, S. J. (1988). The effects of changes in pH within a clay surrounding a cementitious repository. *Material Res. Soc. Symposium Proc.* 112, 43–52. doi:10.1557/proc-112-43

Jenni, A., Mäder, U., Lerouge, C., Gaboreau, S., and Schwyn, B. (2014). *In situ* interaction between different concretes and Opalinus Clay. *Phys. Chem. Earth, Parts A/B/C* 70–71, 71–83. doi:10.1016/j.pce.2013.11.004

Jodin-Caumon, M.-C., Mosser-Ruck, R., Randi, A., Pierron, O., Cathelineau, M., and Michau, N. (2012). Mineralogical evolution of a claystone after reaction with iron under thermal gradient. *Clays Clay Minerals* 60, 443–455. doi:10.1346/ccmn.2012.0600501

Johannesson, L.-E., Hermansson, F., Kronberg, M., and Bladström, T. (2020). *Manufacturing of large scale buffer blocks Uniaxial compaction of block – test made with three different bentonites*. Sweden: SKB. SKB Report R-19-28.

Johnson, L., and King, F. (2008). The effect of the evolution of environmental conditions on the corrosion evolutionary path in a repository for spent fuel and high-level waste in Opalinus Clay. *J. Nucl. Mater.* 379, 9–15. doi:10.1016/j.jnucmat.2008.06.003

Kaneko, M., Miura, N., Fujiwara, A., and Yamamoto, M. (2004). Evaluation of gas generation rate by metal corrosion in the reducing environment. *RWMC Eng. Rep. RWMC-TRE-03003, U. K.*

Kim, D. K., Voit, W., Zapka, W., Bjelke, B., Muhammed, M., and Rao, K. V. (2001). Biomedical application of ferrofluids containing magnetite nanoparticles. *MRS Online Proc. Libr.* 676, 832. doi:10.1557/proc-676-y8.32

Kim, S. S., Lee, J. G., Choi, I. K., Lee, G. H., and Chun, K. S. (1997). Effects of metals, metal oxides and metal hydroxide on the leaching of simulated nuclear waste glass. *Radiochim. Acta* 79, 199–206. doi:10.1524/ract.1997.79.3.199

King, F. (2008) "Corrosion of carbon steel under anaerobic conditions in a repository for SF and HLW in Opalinus Clay," in *Nagra technical report NTB 08-12*. Switzerland: Nagra.

King, F. (2014). Durability of high level waste and spent fuel disposal containers – an overview of the combined effect of chemical and mechanical degradation mechanisms. *Quintessa Rep. QRS-1589A-R1_AppB2, Quintessa, Henley-on-Thames, U. K.*

Kinniburgh, D. G., and Cooper, D. M. (2009). PhreePlot: creating graphical output with PHREEQC. Available at: www.phreeplot.org.

Koskinen, K. (2014). *Effects of cementitious leachates on the EBS. Posiva Report 2013-04*. Posiva, Finland.

Kreis, P. (1991). *Hydrogen evolution from corrosion of iron and steel in low/intermediate level waste repositories*. Switzerland: Nagra. NAGRA Technical Report 91-21.

Kursten, B., Druyts, F., Macdonald, D. D., Smart, N. R., Gens, R., Wang, L., et al. (2011). Review of corrosion studies of metallic barrier in geological disposal conditions with respect to Belgian Supercontainer concept. *Corros. Eng. Sci. Technol.* 46, 91–97. doi:10.1179/1743278210y.0000000022

Kursten, B., Smailos, E., Azkarate, I., Werme, L., Smart, N. R., Marx, G., et al. (2004b) "Corrosion evaluation of metallic materials for long-lived HLW/Spent Fuel disposal containers: review of 15-20 years of research," in *Euradwaste04, 6th EC conference on the management and disposal of radioactive waste*. 29 March – 1 April 2004, Luxembourg.

Kursten, B., Smailos, E., Azkarate, I., Werme, L., and Smart, N. R. G. S. (2004a). COBECOMA, State-of-the-art document on the COrrosion BEhaviour of COntainer MAterials. *Eur. Comm. Contract N° FIKW-CT-20014-20138 Final Rep*.

Kursten, B., and Van Iseghem, P. (1998) "Geological disposal of conditioned high-level and long lived radioactive waste," in In situ *experiments. SCK●CEN R-3247, SCK CEN*. Mol, Belgium.

Kursten, B., Weetjens, E., and Jacques, D. (2021). "Interface steel/iron – concrete," in *Experiments and numerical model studies on interfaces*. Editors G. DEISSMANN, N. AIT MOUHEB, C. MARTIN, M. J. TURRERO, E. TORRES, B. KURSTEN, et al. Final version as of 12.05.2021 of deliverable D2.5 of the HORIZON 2020 project EURAD. EC Grant agreement no: 847593.

Lacher, J. R. (1937). A theoretical formula for the solubility of hydrogen in palladium. *Proc. R. Soc. Lond. A* 161, 525–545.

Lainé, M., Balan, E., Allard, T., Paineau, E., Jeunesse, P., Mostafavi, M., et al. (2017). Reaction mechanisms in swelling clays under ionizing radiation: influence of the water amount and of the nature of the clay mineral. *RSC Adv.* 7, 526–534. doi:10.1039/c6ra24861f

Lalan, P., Dauzères, A., DE Windt, L., Bartier, D., Sammaljärvi, J., Barnichon, J.-D., et al. (2016). Impact of a 70 °C temperature on an ordinary Portland cement paste/claystone interface: an *in situ* experiment. *Cem. Concr. Res.* 83, 164–178. doi:10.1016/j.cemconres.2016.02.001

Landolt, D., Davenport, A., Payer, J., and Shoesmith, D. (2009) "A review of materials and corrosion issues regarding canisters for disposal of spent fuel and high-level waste in Opalinus Clay," in *Nagra technical report NTB 09-02*. Wettingen, Switzerland: Nagra.

Lanson, B., Lantenois, S., Aken, P. A. V., Bauer, A., and Plançon, A. (2012). Experimental investigation of smectite interaction with metal iron at 80 C: structural characterization of newly formed Fe-rich phyllosilicates. *Am. Mineralogist* 97, 864–871. doi:10.2138/am.2012.4062

Lantenois, S., Lanson, B., Muller, F., Bauer, A., Jullien, M., and Plancon, A. (2005). Experimental study of smectite interaction with metal Fe at low temperature: 1. Smectite destabilization. *Clays Clay Minerals* 53, 597–612. doi:10.1346/ccmn.2005.0530606

Lanyon, G. W. 2015. Modellers summary of LCS experiment 2 (F16) tracer testing. *Nagra aktennotiz an 15-025-rev 1*.Nagra, Wettingen, Switzerland.

Leivo, M. (2021). "Interface "cement/mortar – granite"," in *Experiments and numerical model studies on interfaces*. Editors G. DEISSMANN, N. AIT MOUHEB, C. MARTIN, M. J. TURRERO, E. TORRES, B. KURSTEN, et al. *Final version as of 12.05.2021 of deliverable D2.5 of the HORIZON 2020 project EURAD. EC Grant agreement no: 847593*.

Lemmens, K. (2001). The effect of clay on the dissolution of nuclear waste glass. *J. Nucl. Mater.* 298, 11–18. doi:10.1016/s0022-3115(01)00590-6

Leon, Y., Dillmann, P., Neff, D., Schlegel, M., Foy, E., and Dynes, J. J. (2017). Interfacial layers at a nanometre scale on iron corroded in carbonated anoxic environments. *RSC Adv.* 7, 20101–20115. doi:10.1039/c7ra01600j

Lerouge, C., Gaboreau, S., Grangeon, S., Claret, F., Warmont, F., Jenni, A., et al. (2017). *In situ* interactions between Opalinus clay and low alkali concrete. *Phys. Chem. Earth, Parts A/B/C* 99, 3–21. doi:10.1016/j.pce.2017.01.005

Leupin, O. X., Smith, P., Marschall, P., Johnson, L., Savage, D., Cloet, V., et al. (2016). *High-level waste repository-induced effects*. Switzerland: Nagra. NAGRA Technical Report 14-13.

Levasseur, S., Collin, F., Daniels, K., Dymitrowska, M., Harrington, J., Jacops, E., et al. (2021). Initial state of the art on gas transport in clayey materials. Deliverable D6.1 of the HORIZON 2020 project EURAD. *Work Package Gas*.

Levasseur, S., Collin, F., Dymitrowska, M., Harrington, J., Jacops, E., Kolditz, O., et al. (2023). *State of the art on gas transport in clayey materials – update 2023. Deliverable D6.2 of the HORIZON 2020 project EURAD, work package gas. EC grant agreement*.847593

L'Hostis, V., Amblard, E., Blanc, C., Miserque, F., Paris, C., and Bellot-Gurlet, L. (2011). Passive corrosion of steel in concrete in context of nuclear waste disposal. *Corros. Eng. Sci. Technol.* 46, 177–181. doi:10.1179/1743278210y.0000000013

Li, L., Weetjens, E., Vietor, T., and Hart, J. (2010). Integration of TImoDaZ results within the safety case and recommendations for repository design. *D 14 6th EURATOM Framew. programme Proj. TimoDaZ contract no. FI6W-CT-2007-0364449*.

Liu, C., Wang, J., Zhang, Z., and Han, E.-H. (2017). Studies on corrosion behaviour of low carbon steel canister with and without γ-irradiation in China's HLW disposal repository. *Corros. Eng. Sci. Technol.* 52, 136–140. doi:10.1080/1478422x.2017.1348762

Lombardi, S., and Valentini, G. (1996) "The Dunarobbe forest as natural analogue: analysis of the geoenvironmental factors controlling the wood preservation," in *Sixth EC Natural analogue working group meeting. Proceedings of an international workshop held in Santa Fe*, 16761. New Mexico, USA: EUR.

Lothenbach, B., Kulik, D. A., Matschei, T., Balonis, M., Baquerizo, L., Dilnesa, B., et al. (2019). Cemdata18: a chemical thermodynamic database for hydrated Portland cements and alkali-activated materials. *Cem. Concr. Res.* 115, 472–506. doi:10.1016/j.cemconres.2018.04.018

Lutze, V., Grambow, B., Ewing, R. C., and Jercinovic, M. J. (1987). "Natural analogues in radioactive waste disposal," in *Commission of the European communities - radioactive waste management series*. Editors B. CÔME and N. A CHAPMAN

Ma, B., Fernandez-Martinez, A., Madé, B., Findling, N., Markelova, E., Salas-Colera, E., et al. (2018). XANES-based determination of redox potentials imposed by steel corrosion products in cement-based media. *Environ. Sci. and Technol.* 52, 11931–11940. doi:10.1021/acs.est.8b03236

Ma, B., and Lothenbach, B. (2020a). Synthesis, characterization, and thermodynamic study of selected Na-based zeolites. *Cem. Concr. Res.* 135, 106111. doi:10.1016/j.cemconres.2020.106111

Ma, B., and Lothenbach, B. (2020b). Thermodynamic study of cement/rock interactions using experimentally generated solubility data of zeolites. *Cem. Concr. Res.* 135, 106149. doi:10.1016/j.cemconres.2020.106149

Ma, B., and Lothenbach, B. (2021). Synthesis, characterization, and thermodynamic study of selected K-based zeolites. *Cem. Concr. Res.* 148, 106537. doi:10.1016/j.cemconres.2021.106537

Macdonald, D. D., Urquidi-Macdonald, M., Engelhardt, G. R., Azizi, O., Saleh, A., Almazooqi, A., et al. (2011). Some important issues in electrochemistry of carbon steel in simulated concrete pore water Part 1-theoretical issues. *Corros. Eng. Sci. Technol.* 46, 98–103. doi:10.1179/1743278211y.0000000002

Mäder, U. K., Fierz, T., Frieg, B., Eikenberg, J., Rüthi, M., Albinsson, Y., et al. (2006). Interaction of hyperalkaline fluid with fractured rock: field and laboratory experiments of the HPF project (Grimsel Test Site, Switzerland). *J. Geochem. Explor.* 90, 68–94. doi:10.1016/j.gexplo.2005.09.006

Mäder, U., Jenni, A., Lerouge, C., Gaboreau, S., Miyoshi, S., Kimura, Y., et al. (2017). 5-year chemico-physical evolution of concrete–claystone interfaces, Mont Terri rock laboratory (Switzerland). *Swiss J. Geosciences* 110, 307–327. doi:10.1007/s00015-016-0240-5

Majzlan, J., Grevel, K.-D., and Navrotsky, A. (2003). Thermodynamics of Fe oxides: Part II. Enthalpies of formation and relative stability of goethite (α-FeOOH), lepidocrocite (γ-FeOOH), and maghemite (γ-Fe2O3). *Am. Mineralogist* 88, 855–859. doi:10.2138/am-2003-5-614

Mallinson, L. G., and Davies, I. L. (1987). *A historical examination of concrete*. Commission of the European Communities. Nuclear Science and Technology, EUR 10937.

Marcial, J., Riley, B. J., Kruger, A. A., Lonergan, C. E., and Vienna, J. D. (2024). Hanford low-activity waste vitrification: a review. *J. Hazard. Mater.* 461, 132437. doi:10.1016/j.jhazmat.2023.132437

Marcos, N. (2003). *Bentonite-iron interactions in natural occurrences and in laboratory - the effects of the interactions on the properties of bentonite: a literature survey*. Olkiluoto, Finland: Posiva Oy. Posiva Working Report WR2003-55.

Marsh, G. P., Harker, A. H., and Taylor, K. J. (1989). Corrosion of carbon steel nuclear waste containers in marine sediment. *Corrosion* 45, 579–589. doi:10.5006/1.3577876

Marsh, G. P., Taylor, K. J., Shrland, S. M., and Tasker, P. W. (1986). An approach for evaluating the general and localised corrosion of carbon-steel containers for nuclear waste disposal. *MRS Online Proc. Libr.* 84, 227–238. doi:10.1557/proc-84-227

Martin, C. (2021). "Interface glass – steel," in *Experiments and numerical model studies on interfaces*. Editors G. DEISSMANN, N. AIT MOUHEB, C. MARTIN, M. J. TURRERO, E. TORRES, B. KURSTEN, et al. Final version as of 12.05.2021 of deliverable D2.5 of the HORIZON 2020 project EURAD. EC Grant agreement no: 847593.

Maslehuddin, M. (1994). *The influence of Arabian Gulf environment on mechanisms of reinforcement corrosion*. United Kingdom: University of Aston in Birmingham. PhD thesis.

Maslehuddin, M., Page, C. L., Rasheeduzzafar, A. L., and Mana, A. I. (1996). "Effect of temperature on pore solution chemistry and reinforcement corrosion in contaminated concrete,". *Corrosion of reinforcement in concrete construction*. Editors C. L. PAGE, P. B. BAMFORTH, and J. W. FIGG (United Kingdom: RSC Special Publications), 183, 67–75.

Mccafferty, E. (2010). *Introduction to corrosion science*. Springer.

Mcvay, G. L., and Buckwalter, C. Q. (1983). Effect of iron on waste-glass leaching. *J. Am. Ceram. Soc.* 66, 170–174. doi:10.1111/j.1151-2916.1983.tb10010.x

Metcalfe, R., and Walker, A. (2004). *Proceedings of the international workshop on bentonite-cement interaction in repository environments*. Tokyo. Posiva Working Report WR2004-25, Posiva, Olkiluoto, Finland.

Mibus, J., Diomidis, N., Wieland, E., and Swanton, S. (2018). *Final synthesis report on results from WP2 - D 2.18 from CArbon-14 Source Term project from the European Union's Seventh Framework Programme for research, technological development and demonstration under grant agreement no. 604779*.

Michau, N. (2005). *Ecoclay II: effects of cement on clay barrier performance*. Andra Report C.RP.ASCM.04.0009. Andra, Paris, France.

Michelin, A., Burger, E., Leroy, E., Foy, E., Neff, D., Benzerara, K., et al. (2013a). Effect of iron metal and siderite on the durability of simulated archeological glassy material. *Corros. Sci.* 76, 403–414. doi:10.1016/j.corsci.2013.07.014

Michelin, A., Drouet, E., Foy, E., Dynes, J. J., Neff, D., and Dillmann, P. (2013b). Investigation at the nanometre scale on the corrosion mechanisms of archaeological ferrous artefacts by STXM. *J. Anal. Atomic Spectrom.* 28, 59–66. doi:10.1039/c2ja30250k

Michelin, A., Leroy, E., Neff, D., Dynes, J. J., Dillmann, P., and Gin, S. (2015). Archeological slag from Glinet: an example of silicate glass altered in an anoxic iron-rich environment. *Chem. Geol.* 413, 28–43. doi:10.1016/j.chemgeo.2015.08.007

Mihara, M., Nishimura, T., Wada, R., and Honda, A. (2002). Estimation on gas generation and corrosion rates of carbon steel, stainless steel and zircaloy in alkaline solutions under low oxygen condition. *JNC Tech. Rev.* 15, 91–101. (in Japanese).

Millot, L., Houjeij, H., Matta, G., Ferrandis, J.-Y., Laux, D., and Monsanglant Louvet, C. (2024). Radiolysis of bituminized radioactive waste: a comprehensive review. *EPJ Nucl. Sci. Technol.* 10, 4. doi:10.1051/epjn/2024004

Milodowski, A. E., Alexander, W. R., West, J. M., Shaw, R. P., Mcevoy, F. M., Scheidegger, J. M., et al. (2015) "A catalogue of analogues for radioactive waste management," in *British geological survey commissioned report CR/15/106*. Keyworth, Nottingham, United Kingdom: British Geologcial Survey.

Milodowski, A. E., Cave, M. R., Kemp, S. J., Taylor, H., Green, K., Williams, C. L., et al. (2009). *Mineralogical investigations of the interaction between iron corrosion products and bentonite from the NF-PRO experiments*. Sweden: SKB. SKB Technical Report TR-09-03.

Milodowski, A. E., Norris, S., and Alexander, W. R. (2016). Minimal alteration of montmorillonite following long-term interaction with natural alkaline groundwater: implications for geological disposal of radioactive waste. *Appl. Geochem.* 66, 184–197. doi:10.1016/j.apgeochem.2015.12.016

Mollaali, M., Buchwald, J., Montoya, V., Kolditz, O., and Yoshioka, K. (2023). Clay–rock fracturing risk assessment under high gas pressures in repository systems. *IOP Conf. Ser. Earth Environ. Sci.* 1124, 012120. doi:10.1088/1755-1315/1124/1/012120

Moncouyoux, J., Aure, A., and Ladirat, C. (1991). Investigation of full-scale high-level waste containment glass blocks Task 3 Characterization of radioactive waste forms A series of final reports (1985-89). *No 24, Comm. Eur. Communities Nucl. Sci. Technol. EUR*, 13612.

Montes-H, G., Fritz, B., Clement, A., and Michau, N. (2005). Modeling of transport and reaction in an engineered barrier for radioactive waste confinement. *Appl. Clay Sci.* 29, 155–171. doi:10.1016/j.clay.2005.01.004

Mosser-Ruck, R., Cathelineau, M., Guillaume, D., Charpentier, D., Rousset, D., Barres, O., et al. (2010). Effects of temperature, pH, and iron/clay and liquid/clay ratios on experimental conversion of dioctahedral smectite to berthierine, chlorite, vermiculite, or saponite. *Clays Clay Minerals* 58, 280–291. doi:10.1346/ccmn.2010.0580212

Moyce, E. B. A., Rochelle, C., Morris, K., Milodowski, A. E., Chen, X., Thornton, S., et al. (2014). Rock alteration in alkaline cement waters over 15 years and its relevance to the geological disposal of nuclear waste. *Appl. Geochem.* 50, 91–105. doi:10.1016/j.apgeochem.2014.08.003

Mulcahy, S. R., Jackson, M. D., Chen, H., Li, Y., Cappelletti, P., Wenk, H. R., et al. (2017). Phillipsite and Al-tobermorite mineral cements produced through low-temperature water-rock reactions in roman marine concrete. *Am. Mineralogist* 102, 1435–1450. doi:10.2138/am-2017-5993ccby

Müller-Vonmoos, M., and Kahr, G. (1983) *Mineralogische unterschungen von Wyoming Bentonit MX-80 und montigel*, 83-12. Switzerland: NAGRA Technischer bericht, Nagra.

NAGRA (2002) "Project Opalinus Clay. Models, codes and data for safety assessment. Demonstration of disposal feasibility for spent fuel, vitrified high-level waste and long-lived intermediate-level waste," in *NAGRA technical report 02–06*. Switzerland: Nagra.

Naish, C. C., Balkwill, P. H., O'Brien, T. M., Taylor, K. J., and Marsh, G. P. (1991). The anaerobic corrosion of carbon steel in concrete, Task 3: characterization of waste forms. *A Ser. final Rep. (1985-1989) No 33, Nucl. Sci. Technol. Comm. Eur. Communities EUR13663*.

NDA (2016). *Geological disposal – geosphere status report*. NDA Report no. DSSC/453/01, Nuclear Decommissioning Authority, Harwell, Didcot, United Kingdom.

NEA (2012). Cementitious materials in safety cases for geological repositories for radioactive waste: role, evolution and interactions. *NEA/RWM/R(2012)3/REV*.

Necib, S., Bucur, C., Caes, S., Cochin, F., Cvetković, B. Z., Fulger, M., et al. (2018). Overview OF 14C release from irradiated zircaloys in geological disposal conditions. *Radiocarbon* 60, 1757–1771. doi:10.1017/rdc.2018.137

Necib, S., Diomidis, N., Keech, P., and Nakayama, M. (2017a). Corrosion of carbon steel in clay environments relevant to radioactive waste geological disposals, Mont Terri rock laboratory (Switzerland). *Swiss J. Geosciences* 110, 329–342. doi:10.1007/s00015-016-0259-7

Necib, S., Linard, Y., Crusset, D., Michau, N., Daumas, S., Burger, E., et al. (2016). Corrosion at the carbon steel-clay borehole water and gas interfaces at 85 °C under anoxic and transient acidic conditions. *Corros. Sci.* 111, 242–258. doi:10.1016/j.corsci.2016.04.039

Necib, S., Linard, Y., Crusset, D., Schlegel, M., Daumas, S., and Michau, N. (2017b). Corrosion processes of C-steel in long-term repository conditions. *Corros. Eng. Sci. Technol.* 52, 127–130. doi:10.1080/1478422x.2017.1320155

Necib, S., Schlegel, M. L., Bataillon, C., Daumas, S., Diomidis, N., Keech, P., et al. (2019). Long-term corrosion behaviour of carbon steel and stainless steel in Opalinus clay: influence of stepwise temperature increase. *Corros. Eng. Sci. Technol.* 54, 516–528. doi:10.1080/1478422x.2019.1621456

Neeft, E. A. C. (2018). 14C exposure from disposal of radioactive waste compared to 14C exposure from cosmogenic origin. *Radiocarbon* 60, 1911–1923. doi:10.1017/rdc.2018.141

Neeft, E., Weetjens, E., Vokal, A., Leivo, M., Cochepin, B., Martin, C., et al. (2020). *Treatment of chemical evolution in National Programmes, D 2.4 of the HORIZON 2020 project EURAD*. EC Grant agreement no.847593

Neff, D., Dillmann, P., Descostes, M., and Beranger, G. (2006). Corrosion of iron archaeological artefacts in soil: estimation of the average corrosion rates involving analytical techniques and thermodynamic calculations. *Corros. Sci.* 48, 2947–2970. doi:10.1016/j.corsci.2005.11.013

Neff, D., Reguer, S., Bellot-Gurlet, L., Dillmann, P., and Bertholon, R. (2004). Structural characterization of corrosion products on archaeological iron: an integrated analytical approach to establish corrosion forms. *J. Raman Spectrosc.* 35, 739–745. doi:10.1002/jrs.1130

Neff, D., Saheb, M., Monnier, J., Perrin, S., Descostes, M., L'Hostis, V., et al. (2010). A review of the archaeological analogue approaches to predict the long-term corrosion behaviour of carbon steel overpack and reinforced concrete structures in the French disposal systems. *J. Nucl. Mater.* 402, 196–205. doi:10.1016/j.jnucmat.2010.05.003

NF-PRO (2008). Understanding and physical and numerical modelling of the key processes in the near field and their coupling for different host rocks and repository strategies (NF-pro). *Eur. Comm. Nucl. Sci. Technol. EUR* 23720.

NIROND (2013) "ONDRAF/NIRAS research, development and demonstration (RD&D) plan state-of-the-art report as of december 2012,". NIROND, Belgim.

Norris, S., and Capouet, M. (2018). Overview of CAST project. *Radiocarbon* 60, 1649–1656. doi:10.1017/rdc.2018.142

Ojovan, M. I., and Lee, W. E. (2014). *An introduction to nuclear waste immobilisation*. Elsevier.

Ojovan, M. I., and Yudintsev, S. V. (2023). Glass, ceramic, and glass-crystalline matrices for HLW immobilisation. *Open Ceram.* 14, 100355. doi:10.1016/j.oceram.2023.100355

Osacký, M., Šucha, V., Czímerová, A., and Madejová, J. (2010). Reaction of smectites with iron in a nitrogen atmosphere at 75°C. *Appl. Clay Sci.* 50, 237–244. doi:10.1016/j.clay.2010.08.004

Osacký, M., Šucha, V., Czímerová, A., Pentrák, M., and Madejová, J. (2013). Reaction of smectites with iron in aerobic conditions at 75°C. *Appl. Clay Sci.* 72, 26–36. doi:10.1016/j.clay.2012.12.010

Padovani, C., King, F., Lilja, C., Féron, D., Necib, S., Crusset, D., et al. (2017). The corrosion behaviour of candidate container materials for the disposal of high-level waste and spent fuel - a summary of the state of the art and opportunities for synergies in future R&D. *Corros. Eng. Sci. Technol.* 52, 227–231. doi:10.1080/1478422x.2017.1356973

Pastina, B., Lehikoinen, J., and Puigdomenech, I. 2012. "Safety case approach for a KBS-3 type repository in crystalline rock," in *Cementitious materials in safety cases for geological repositories for radioactive waste: role, evolution and interactions* (France: NEA). *NEA/RWM/R(2012)3/REV*.

Paul, A. (1977). Chemical durability of glasses; a thermodynamic approach. *J. Mater. Sci.* 12, 2246–2268. doi:10.1007/bf00552247

Pelayo, M., García-Romero, E., Labajo, M. A., and Pérez Del Villar, L. (2011). Occurrence of Fe–Mg-rich smectites and corrensite in the Morrón de Mateo bentonite deposit (Cabo de Gata region, Spain): A natural analogue of the bentonite barrier in a radwaste repository. *Appl. Geochem.* 26, 1153–1168. doi:10.1016/j.apgeochem.2011.04.005

Perko, J., Jacques, D., Seetharam, S. C., and Mallants, D. (2010). *Long-term evolution of the near surface disposal facility at Dessel*. Belgium: NIROND-TR 2010–04 E, ONDRAF/NIRAS.

Perko, J., Mayer, K. U., Kosakowski, G., DE Windt, L., Govaerts, J., Jacques, D., et al. (2015). Decalcification of cracked cement structures. *Comput. Geosci.* 19, 673–693. doi:10.1007/s10596-014-9467-2

Pfingsten, W., Paris, B., Soler, J. M., and Mäder, U. K. (2006). Tracer and reactive transport modelling of the interaction between high-pH fluid and fractured rock: field and laboratory experiments. *J. Geochem. Explor.* 90, 95–113. doi:10.1016/j.gexplo.2005.09.009

Philippini, V., Naveau, A., Catalette, H., and Leclercq, S. (2006). Sorption of silicon on magnetite and other corrosion products of iron. *J. Nucl. Mater.* 348, 60–69. doi:10.1016/j.jnucmat.2005.09.002

Philippini, V., Naveau, A., Catalette, H., and Leclercq, S. (2007). Erratum to 'Sorption of silicon on magnetite and other corrosion products of iron' [J. Nucl. Mater. 348 (2006) 60–69]. *J. Nucl. Mater.* 362, 139. doi:10.1016/j.jnucmat.2006.07.006

Pointeau, I., Coreau, N., and Reiller, P. E. (2008) *Uptake of anionic radionuclides onto degraded cement pastes and competing effect of organic ligands*, 96, 367–374.

Pointeau, I., Reiller, P., Macé, N., Landesman, C., and Coreau, N. (2006). Measurement and modeling of the surface potential evolution of hydrated cement pastes as a function of degradation. *J. Colloid Interface Sci.* 300, 33–44. doi:10.1016/j.jcis.2006.03.018

Poyet, S. (2006). The Belgian supercontainer concept: study of the concrete buffer behaviour in service life. *J. De Physique Iv* 136, 167–175. doi:10.1051/jp4:2006136018

Qin, Z., Demko, B., Noël, J., Shoesmith, D., King, F., Worthingham, R., et al. (2004). Localized dissolution of millscale-covered pipeline steel surfaces. *Corrosion* 60, 906–914. doi:10.5006/1.3287824

Rahman, R. O. A., and Ojovan, M. I. (2021). *Sustainability of life cycle management for nuclear cementation-based Technologies*. United Kingdom: Woodhead Publishing.

Rajala, P. (2017). *Microbially-induced corrosion of carbon steel in a geological repository environment*. Finland: VTT Science 155. PhD Thesis.

Rajala, P., Carpén, L., Vepsäläinen, M., Raulio, M., Sohlberg, E., and Bomberg, M. (2015). Microbially induced corrosion of carbon steel in deep groundwater environment. *Front. Microbiol.* 6, 647. doi:10.3389/fmicb.2015.00647

Read, D., Glasser, F. P., Ayora, C., Guardiola, M. T., and Sneyers, A. (2001). Mineralogical and microstructural changes accompanying the interaction of Boom Clay with ordinary Portland cement. *Adv. Cem. Res.* 13, 175–183. doi:10.1680/adcr.2001.13.4.175

Rebiscoul, D., Tormos, V., Godon, N., Mestre, J. P., Cabie, M., Amiard, G., et al. (2015). Reactive transport processes occurring during nuclear glass alteration in presence of magnetite. *Appl. Geochem.* 58, 26–37. doi:10.1016/j.apgeochem.2015.02.018

Reijonen, H. M., and Alexander, W. R. (2015). Bentonite analogue research related to geological disposal of radioactive waste: current status and future outlook. *Swiss J. Geosciences* 108, 101–110. doi:10.1007/s00015-015-0185-0

Reimers, P. (1992). *Quality assurance of radioactive waste packages by computerized tomography Task 3 Characterization of radioactive waste forms A series of final reports (1985-89). No 37, Nuclear Science and Technology*. Commission of the European Communities. EUR13879.

Reiser, J. T., Parruzot, B., Weber, M. H., Ryan, J. V., Mccloy, J. S., and Wall, N. A. (2017). The use of positrons to survey alteration layers on synthetic nuclear waste glasses. *J. Nucl. Mater.* 490, 75–84. doi:10.1016/j.jnucmat.2017.03.007

Reiser, J., Neill, L., Weaver, J., Parruzot, B., Musa, C., Neeway, J., et al. (2005). Glass corrosion in the presence of iron-bearing materials and potential corrosion suppressors. *Mater. Res. Soc. Symposium Proc.* 1744, 139–144. doi:10.1557/opl.2015.503

Ribet, I., Bétrémieux, S., Gin, S., Angeli, F., and Jégu, C. (2009) "Long-term behaviour of vitrified waste packages," in *Proceedings global 2009. Paris.* ogy.

Ribet, I., Gin, S., Godon, N., Jollivet, P., Minet, Y., Grambow, B., et al. (2007). Long-term behaviour of glass: improving the glass source term and substantiating the basic hypotheses. *GLASTAB. Eur. Comm. - Nucl. Sci. Technol.*

Roadcap, G. S., Sanford, R. A., Jin, Q., Pardinas, J. R., and Bethke, C. M. (2006). Extremely alkaline (pH > 12) ground water hosts diverse microbial community. *Ground Water* 44, 511–517. doi:10.1111/j.1745-6584.2006.00199.x

Roosz, C., Vieillard, P., Blanc, P., Gaboreau, S., Gailhanou, H., Braithwaite, D., et al. (2018). Thermodynamic properties of C-S-H, C-A-S-H and M-S-H phases: results from direct measurements and predictive modelling. *Appl. Geochem.* 92, 140–156. doi:10.1016/j.apgeochem.2018.03.004

Sakuragi, T. (2017). *Final Report on Zr alloys corrosion studies at RWMC D 3.19 of the EURATOM seventh framework project CAST grant agreement no. 604779*.

Savage, D. (1998). "Maqarin natural analogue study: phase III," in *Technical report TR-98-04*. Editor J. A. T. SMELLIE (Sweden: SKB), 281–316.

Savage, D. (2009). "A review of experimental evidence for the development and properties of cement bentonite interfaces with implications for gas transport,". *Nagra report NAB 09-30* (Switzerland: Nagra).

Savage, D. (2011). A review of analogues of alkaline alteration with regard to long-term barrier performance. *Mineral. Mag.* 75, 2401–2418. doi:10.1180/minmag.2011.075.4.2401

Savage, D. (2014). *An assessment of the impact of the long term evolution of engineered structures on the safety-relevant functions of the bentonite buffer in a HLW repository*. Switzerland: NAGRA. NAGRA Technical Report TR 13-02.

Savage, D., and Benbow, S. (2007). *Low pH cement. SKI Report 2007:32*. Stockholm, Sweden: Swedish Nuclear Power Inspectorate.

Savage, D., and Cloet, V. (2018) *A review of cement-clay modelling*, 18-24. Switzerland: NAGRA Arbeitsbericht NAB Nagra.

Savage, D., Walker, C., Arthur, R., Rochelle, C., Oda, C., and Takase, H. (2007). Alteration of bentonite by hyperalkaline fluids: a review of the role of secondary minerals. *Phys. Chem. Earth* 32, 287–297. doi:10.1016/j.pce.2005.08.048

Schlegel, M. L., Bataillon, C., Benhamida, K., Blanc, C., Menut, D., and Lacour, J.-L. (2008). Metal corrosion and argillite transformation at the water-saturated, high-temperature iron–clay interface: a microscopic-scale study. *Appl. Geochem.* 23, 2619–2633. doi:10.1016/j.apgeochem.2008.05.019

Schlegel, M. L., Bataillon, C., Brucker, F., Blanc, C., Prêt, D., Foy, E., et al. (2014). Corrosion of metal iron in contact with anoxic clay at 90°C: characterization of the corrosion products after two years of interaction. *Appl. Geochem.* 51, 1–14. doi:10.1016/j.apgeochem.2014.09.002

Schlegel, M. L., Martin, C., Brucker, F., Bataillon, C., Blanc, C., Chorro, M., et al. (2016). Alteration of nuclear glass in contact with iron and claystone at 90 °C under anoxic conditions: characterization of the alteration products after two years of interaction. *Appl. Geochem.* 70, 27–42. doi:10.1016/j.apgeochem.2016.04.009

Scourfield, S. J., Kent, J. E., Wickham, S. M., Nieminen, M., Clarke, S., and Frasca, B. (2020). Thermal treatment for radioactive waste minimisation and hazard reduction: overview and summary of the EC THERAMIN project. *IOP Conf. Ser. Mater. Sci. Eng.* 818, 012001. doi:10.1088/1757-899x/818/1/012001

Sellin, P., and Leupin, O. X. (2013). The use of clay as an engineered barrier in radioactive-waste management a review. *Clays Clay Minerals* 61, 477–498. doi:10.1346/ccmn.2013.0610601

Shade, J. W., Pederson, L. R., and Mcvay, G. L. (1983). "Waste glass-metal interactions in brines," in *Advances in ceramics VIII, nuclear waste management*. Editors G. G. WICKS and W. A. ROSS (American Ceramic Society), 358–367.

Shanggeng, L., Zhaoguang, W. U., and Delu, L. (1995). Study of media effect on glass surface. *Mater. Res. Soc. Symposium Proc.* 353, 63–71. doi:10.1557/proc-353-63

Sidborn, M., Marsic, N., Crawford, J., Joyce, S., Hartley, L., Idiart, A., et al. (2014). Potential alkaline conditions for deposition holes of a repository in Forsmark as a consequence of OPC grouting. *SKB Rep. R-12-17, SKB, Swed*.

Small, J., Nykyri, M., Helin, M., Hovi, U., Sarlin, T., and Vaara, M. (2008). Experimental and modelling investigations of the biogeochemistry of gas production from low and intermediate level radioactive waste. *Appl. Geochem.* 23, 1383–1418. doi:10.1016/j.apgeochem.2007.11.020

Smart, N. R. (2009). Corrosion behavior of carbon steel radioactive waste packages: a summary review of Swedish and U.K. Research. *Corrosion* 65, 195–212. doi:10.5006/1.3319128

Smart, N. R., and Adams, R. (2006). *Natural analogues for expansion due to the anaerobic corrosion of ferrous materials*. Sweden: SKB. SKB Technical Report TR-06-44.

Smart, N. R., Blackwood, D. J., Marsh, G. P., Naish, C. C., O'Brien, T. M., Rance, A. P., et al. (2004). *The anaerobic corrosion of carbon and stainless steels in simulated cementitious repository environments: a summary review of Nirex research*. Harwell, Didcot, United Kingdom: AEA Technology. Report AEAT/ERRA-0313.

Smart, N. R., Blackwood, D. J., and Werme, L. (2001). *The anaerobic corrosion of carbon steel and cast iron in artificial groundwaters*. Sweden: SKB. SKB Technical Report TR-01-22.

Smart, N. R., Carlson, L., Heath, T. G., Hoch, A. R., Hunter, F. M., Karnland, O., et al. (2008a). Interactions between iron corrosion products and bentonite. *NF-PRO Final Rep*. Serco/TAS/MCRL/19801/C001 Issue 2.

Smart, N. R., Rance, A. P., Fennell, P. A. H., Reddy, B., and Padovani, C. 2019. Experimental studies of radiation induced corrosion in support of the Belgian Supercontainer concept. Wood Reference 207022/01, Issue 1.

Smart, N. R., Rance, A. P., Nixon, D. J., Fennell, P. A. H., Reddy, B., and Kursten, B. (2017a). Summary of studies on the anaerobic corrosion of carbon steel in alkaline media in support of the Belgian supercontainer concept. *Corros. Eng. Sci. Technol.* 52, 217–226. doi:10.1080/1478422x.2017.1356981

Smart, N. R., Rance, A. P., and Werme, L. O. (2008b). The effect of radiation on the anaerobic corrosion of steel. *J. Nucl. Mater.* 379, 97–104. doi:10.1016/j.jnucmat.2008.06.007

Smart, N. R., Reddy, B., Rance, A. P., Nixon, D. J., and Diomidis, N. (2017b). The anaerobic corrosion of carbon steel in saturated compacted bentonite in the Swiss repository concept. *Corros. Eng. Sci. Technol.* 52, 113–126. doi:10.1080/1478422x.2017.1316088

Smart, N. R., Reddy, B., Rance, A. P., Nixon, D. J., Frutschi, M., Bernier-Latmani, R., et al. (2017c). The anaerobic corrosion of carbon steel in compacted bentonite exposed to natural Opalinus Clay porewater containing native microbial populations. *Corros. Eng. Sci. Technol.* 52, 101–112. doi:10.1080/1478422x.2017.1315233

Soler, J. M., and Mäder, U. K. (2010). Cement-rock interaction: infiltration of a high-pH solution into a fractured granite core. *Geol. Acta* 8, 221–233.

Soler, J. M., Pfingsten, W., Paris, B., Mäder, U. K., Frieg, B., Neall, F., et al. (2006). *HPF-Experiment: modelling report*. Switzrland: Nagra. NAGRA Technical Report NTB–05-01.

Soler, J. M., Vuorio, M., and Hautojarvi, A. (2011). Reactive transport modeling of the interaction between water and a cementitious grout in a fractured rock. Application to ONKALO (Finland). *Appl. Geochem.* 26, 1115–1129. doi:10.1016/j.apgeochem.2011.04.001

Somervuori, M., and Carpen, L. (2021). "Interface "steel/iron – granite"," in *Experiments and numerical model studies on interfaces*. Editors G. DEISSMANN, N. AIT MOUHEB, C. MARTIN, M. J. TURRERO, E. TORRES, B. KURSTEN, et al. *Final version as of 12.05.2021 of deliverable D2.5 of the HORIZON 2020 project EURAD. EC Grant agreement no: 847593*.

Souza, R. F., Brandão, P. R. G., and Paulo, J. B. A. (2012). Effect of chemical composition on the ζ-potential of chromite. *Miner. Eng.* 36-38, 65–74. doi:10.1016/j.mineng.2012.02.012

Stein, M. (2014) "Erläuterungen zur Verpackung radioaktiver Abfälle im Endlagerbehälter," in *NAGRA arbeitsbericht NAB 14-04*. Switzerland: Nagra.

Stroes-Gascoyne, S., Hamon, C. J., Dixon, D. A., Kohle, C. L., and Maak, P. (2007). The effects of dry density and porewater salinity on the physical and microbiological characteristics of compacted 100% bentonite. *Sci. Basis Nucl. Waste Manag. XXX* 985, 505. doi:10.1557/proc-985-0985-nn13-02

Stroes-Gascoyne, S., Hamon, C. J., and Maak, P. (2011). Limits to the use of highly compacted bentonite as a deterrent for microbiologically influenced corrosion in a nuclear fuel waste repository. *Phys. Chem. Earth* 36, 1630–1638. doi:10.1016/j.pce.2011.07.085

Stroes-Gascoyne, S., Hamon, C. J., Maak, P., and Russell, S. (2010). The effects of the physical properties of highly compacted smectitic clay (bentonite) on the culturability of indigenous microorganisms. *Appl. Clay Sci.* 47, 155–162. doi:10.1016/j.clay.2008.06.010

Stroes-Gascoyne, S., and West, J. M. (1997). Microbial studies in the Canadian nuclear fuel waste management program. *Fed. Eur. Microbiol. Soc. (FEMS) Microbiol. Rev.* 20, 573–590. doi:10.1016/s0168-6445(97)00035-1

Swanson, J. S., Cherkouk, A., Arnold, T., Meleshyn, A., and Reed, D. T. (2018) "Microbial influence on the performance of subsurface, salt-based radioactive waste repositories. An evaluation based on microbial ecology," in *Bioenergetics and projected repository conditions*. NEA No. 7387.

Szabó-Krausz, Z., Aradi, L. E., Király, C., Kónya, P., Török, P., Szabó, C., et al. (2021). Signs of *in-situ* geochemical interactions at the granite–concrete interface of a radioactive waste disposal. *Appl. Geochem.* 126, 104881. doi:10.1016/j.apgeochem.2021.104881

Taniguchi, N., Kawasaki, M., and Kawakami, S. K. M. (2004). "Corrosion behaviour of carbon steel in contact with bentonite under anaerobic condition," in *Proceedings of the 2nd international workshop "prediction of long term corrosion behaviour in nuclear waste systems", science and Technology series*.

Taylor, H. F. W. (1997). *Cement chemistry*. 2nd edition. London: Thomas Telford Publishing.

Techer, I. P. M., Bartier, D., Tinseau, E., Devol-Brown, I., Boulvais, P., and Suchorski, K. (2012b) "Engineered analogues of cement/clay interactions in the Tournemire experimental platform (France): a couple mineralogical and geochemical approach to track tiny disturbances," in *NEA, 2012. Cementitious materials in safety cases for geological repositories for radioactive waste: role, evolution and interactions, NEA/RWM/R(2012)3/REV*. France.

Techer, I., Bartier, D., Boulvais, P., Tinseau, E., Suchorski, K., Cabrera, J., et al. (2012a). Tracing interactions between natural argillites and hyper-alkaline fluids from engineered cement paste and concrete: chemical and isotopic monitoring of a 15-years old deep-disposal analogue. *Appl. Geochem.* 27, 1384–1402. doi:10.1016/j.apgeochem.2011.08.013

Thorpe, C. L., Neeway, J. J., Pearce, C. I., Hand, R. J., Fisher, A. J., Walling, S. A., et al. (2021). Forty years of durability assessment of nuclear waste glass by standard methods. *npj Mater. Degrad.* 5, 61. doi:10.1038/s41529-021-00210-4

Tinseau, E., Bartier, D., Hassouta, L., Devol-Brown, I., and Stammose, D. (2006). Mineralogical characterization of the Tournemire argillite after *in situ* interaction with concretes. *Waste Manag.* 26, 789–800. doi:10.1016/j.wasman.2006.01.024

Torres, E. (2011). *Geochemical processes at the C-steel/bentonite interface in a deep geological repository: experimental approach and modeling*. Spain: Universidad Complutense de Madrid.

Torres, E., Escribano, A., Baldonedo, J. L., Turrero, M. J., Martín, P. L., Peña, J., et al. (2009). Evolution of the geochemical conditions in the bentonite barrier and its influence on the corrosion of the carbon steel canister. *Sci. Basis Nucl. Waste Manag. XXXII* 1124, 301–306.

Torres, E., Turrero, M. J., Escribano, A., and Martín, P. L. (2014). *Formation of iron oxide and oxyhydroxides under different environmental conditions. Iron/bentonite interaction*. PEBS Project. Deliverable D2.3-6-2.

Torres, E., Turrero, M. J., Peña, J., Martín, P. L., Escribano, A., Alonso, U., et al. (2007). Interaction iron-compacted bentonite: corrosion products and changes in the properties of the bentonite. *Final Rep. NF-PRO_Deliverable D2.3.2 Compon. 2*.

Trinchero, P., Molinero, J., Ebrahimi, H., Puigdomenech, I., Gylling, B., Svensson, U., et al. (2018). Simulating oxygen intrusion into highly heterogeneous fractured media using High Performance Computing. *Math. Geosci.* 50, 549–567. doi:10.1007/s11004-017-9718-6

Trinchero, P., Puigdomenech, I., Molinero, J., Ebrahimi, H., Gylling, B., Svensson, U., et al. (2017). Continuum-based DFN-consistent numerical framework for the simulation of oxygen infiltration into fractured crystalline rocks. *J. Contam. Hydrology* 200, 60–69. doi:10.1016/j.jconhyd.2017.04.001

Tsivilis, S., Sotiriadis, K., and Skaropoulou, A. (2007). Thaumasite form of sulfate attack (TSA) in limestone cement pastes. *J. Eur. Ceram. Soc.* 27, 1711–1714. doi:10.1016/j.jeurceramsoc.2006.05.048

Tunturi, P. J. (1988). *Korroosiokäsikirja, suomen korroosioyhdistys, hangon kirjapaino*.

Turrero, M. J., and Cloet, V. (2017). *FeBEX-DP concrete ageing, concrete/bentonite and concrete/rock interaction analysis*. Switzerland: NAGRA. NAB 16-018.

Turrero, M. J., Torres, E., Cuevas, J., Samper, J., and Montenegro, L. (2021). "Interface "steel/iron – bentonite," in *Experiments and numerical model studies on interfaces*. Editors G. DEISSMANN, N. AIT MOUHEB, C. MARTIN, M. J. TURRERO, E. TORRES, B. KURSTEN, et al. *Final version as of 12.05.2021 of deliverable D2.5 of the HORIZON 2020 project EURAD. EC Grant agreement no: 847593*.

Tuutti, K. (1982). *Corrosion of steel in concrete*. Stockholm, Sweden: Swedish Cement and Concrete Research Institute. Report no. 4 82.

Uras, S., Zovini, C., Paratore, A., Tits, J., Pfingsten, W., Dahn, R., et al. (2021). State of the art in packaging, storage, and monitoring of cemented wastes (Deliverable 7.1 of the Predis project). *EC Grant Agreem. No. No*, 945098.

Utton, C. A., Hand, R. J., Bingham, P. A., Hyatt, N. C., Swanton, S. W., and Williams, S. J. (2013). Dissolution of vitrified wastes in a high-pH calcium-rich solution. *J. Nucl. Mater.* 435, 112–122. doi:10.1016/j.jnucmat.2012.12.032

Utton, C. A., Swanton, S. W., Schofield, J., Hand, R. J., Clacher, A., and Hyatt, N. C. (2012). Chemical durability of vitrified wasteforms: effects of pH and solution composition. *Mineral. Mag.* 76, 2919–2930. doi:10.1180/minmag.2012.076.8.07

Vahlund, F., and Andersson, E. (2015). *Safety analysis for SFR Long-term safety Main report for the safety assessment SR-PSU*. Sweden: SKB TR-14-01, SKB.

Van Eijk, R. J., and Brouwers, H. J. H. (2000). Prediction of hydroxyl concentrations in cement pore water using a numerical cement hydration model. *Cem. Concr. Res.* 30, 1801–1806. doi:10.1016/s0008-8846(00)00413-0

Van Iseghem, P., Berghman, K., Lemmens, K., Timmermans, W., and Wang, L. (1992) *Laboratory and* in-situ *interaction between simulated waste glasses and clay Task 3 Characterization of radioactive waste forms A series of final reports (1985-89) No 21*, 13607. Commission of the European Communities - Nuclear science and technology, EUR.

Van Iseghem, P., Lemmens, K., Aertsens, M., Gin, S., Ribet, I., Grambow, B., et al. (2006). Chemical durability of high-level waste glass in repository environment: main conclusions and remaining uncertainties from the GLASTAB and GLAMOR projects. *Mater. Res. Soc. Symposium Proc.* 932, 95.1–304. doi:10.1557/proc-932-95.1

Van Loon, L. R., and Hummel, W. (1995). *The radiolytic and chemical degradation of organic ion exchange resins under alkaline conditions: effect on radionuclide speciation*. Switserland: Nagra. NAGRA Technical Report 95-08.

Vehmas, T., and Itälä, A. (2019) "Compositional parameters for solid solution C-S-H and the applicability to thermodynamic modelling," in *KIT scientific reports 7752: proceedings of the second workshop of the Horizon 2020 Cebama project*, 293–300.

Vehmas, T., Montoya, V., Alonso, M. C., Vašíček, R., Rastrick, E., Gaboreau, S., et al. (2020). Characterization of Cebama low-pH reference concrete and assessment of its alteration with representative waters in radioactive waste repositories. *Appl. Geochem.* 121, 104703. doi:10.1016/j.apgeochem.2020.104703

Verhoef, E. V., Neeft, E. A. C., Deissmann, G., Filby, A., Wiegers, R. B., and Kers, D. A. (2016). *Waste families in OPERA. OPERA-PU-COV023*. Netherlands: COVRA.

Vernaz, E., Grambow, B., Lutze, W., Lemmens, K., and Van Iseghem, P. (1996). "Assessment of the long-term durability of radioactive waste glass,". *European commission*. Editor T. MCMENAMIN (Luxembourg: EUR), 17543.

Vienna, J. D., Ryan, J. V., Gin, S., and Inagaki, Y. (2013). Current understanding and remaining challenges in modeling long-term degradation of borosilicate nuclear waste glasses. *Int. J. Appl. Glass Sci.* 4, 283–294. doi:10.1111/ijag.12050

Vieno, T., Lehikoinen, J., Löfman, J., Nordman, H., and Mészáros, F. (2003). *Assessment of disturbances caused by construction and operation of ONKALO*. Posiva, Finland. Posiva 2003-06.

Virpiranta, H., Taskila, S., Leiviskä, T., Rämö, J., and Tanskanen, J. (2019). Development of a process for microbial sulfate reduction in cold mining waters - cold acclimation of bacterial consortia from an Arctic mining district. *Environ. Pollut.* 252, 281–288. doi:10.1016/j.envpol.2019.05.087

Wanner, H., Albinsson, Y., and Wieland, E. (1983). Project Caesium–An ion exchange model for the prediction of distribution coefficients of caesium in bentonite. *SKB Tech. Rep.* 94.

Watson, C., Savage, D., and Wilson, J. (2017). Geochemical modelling of the LCS experiment. *Quintessa Rep. QRS-1523D-2, Quintessa, Henley-on-Thames, U. K.*

Weetjens, E., Sillen, X., and Van Geet, M. (2006). *NF-PRO deliverable 5.1.2: mass and energy balance calculations: contribution from SCK●CEN under contract FI6W-CT-2003-02389*.

Werme, L., Björner, I. K., Bart, G., Zwicky, U., Grambow, B., Lutze, W., et al. (1990). Chemical corrosion of highly radioactive borosilicate nuclear waste glass under simulated repository conditions. *J. Mater. Res.* 5, 1130–1146. doi:10.1557/jmr.1990.1130

Wersin, P., Johnson, L. H., Schwyn, B., Berner, U., and Curti, E. (2003) "Redox conditions in the near field of a repository for SF/HLW and ILW in Opalinus Clay," in *NAGRA technical report NTB 02-13*. Switzerland: Nagra.

Wersin, P., and Kober, F. E. (2017) "FEBEX-DP. Metal corrosion and iron-bentonite interaction studies," in *NAGRA arbeitsbericht report NAB*, 16-16. Switzerland: Nagra.

Williams, S. J., and Scourse, E. M. (2015). Carbon-14 Source term in geological disposal; the EC project CAST. *J. Nucl. Res. Dev.* 10, 8–12.

Wilson, J. C. (2017). FEBEX-DP: geochemical modelling of iron-bentonite interactions. *Quintessa Rep. QRS-1713A-R3, Quitessa, Henley-on-Thames, U. K.*

Wilson, J. C., Benbow, S., Sasamoto, H., Savage, D., and Watson, C. (2015). Thermodynamic and fully-coupled reactive transport models of a steel–bentonite interface. *Appl. Geochem.* 61, 10–28. doi:10.1016/j.apgeochem.2015.05.005

Wilson, J., Cressey, G., Cressey, B., Cuadros, J., Ragnarsdottir, K. V., Savage, D., et al. (2006a). The effect of iron on montmorillonite stability. (II) Experimental investigation. *Geochimica Cosmochimica Acta* 70, 323–336. doi:10.1016/j.gca.2005.09.023

Wilson, J., Savage, D., Cuadros, J., Shibata, M., and Ragnarsdottir, K. V. (2006b). The effect of iron on montmorillonite stability. (I) Background and thermodynamic considerations. *Geochimica Cosmochimica Acta* 70, 306–322. doi:10.1016/j.gca.2005.10.003

Wittebroodt, C., Goethals, J., DE Windt, L., Fabian, M., Miron, G. D., Zajec, B., et al. (2023). *Final technical report on the steel/cement material interactions. Final version of deliverable D2.9 of the HORIZON 2020 project EURAD*. EC Grant agreement no.847593

Wittebroodt, C., Turrero, M. J., Torres, E., Gómez, P., Garralón, A., Notario, B., et al. (2024). *Final technical report on the steel/clay material interactions. Final version of deliverable D2.7 of the HORIZON 2020 project EURAD*. EC Grant agreement.847593

Wouters, K., Janssen, P., Moors, H., and Leys, N. (2016). Geochemical performance of the EBS: translation and orientation of existing knowledge towards the Boom clay in The Netherlands (GePeTO). *OPERA-PU-SCK515, COVRA, Netheraldns*.

Wouters, K., Moors, H., Boven, P., and Leys, N. (2013). Evidence and characteristics of a diverse and metabolically active microbial community in deep subsurface clay borehole water. *Fems Microbiol. Ecol.* 86, 458–473. doi:10.1111/1574-6941.12171

Yamaguchi, T., Sakamoto, Y., Akai, M., Takazawa, M., Iida, Y., Tanaka, T., et al. (2007). Experimental and modeling study on long-term alteration of compacted bentonite with alkaline groundwater. *Phys. Chem. Earth* 32, 298–310. doi:10.1016/j.pce.2005.10.003

Yoshikawa, H., Gunji, E., and Tokuda, M. (2008). Long term stability of iron for more than 1500 years indicated by archaeological samples from the Yamato 6th tumulus. *J. Nucl. Mater.* 379, 112–117. doi:10.1016/j.jnucmat.2008.06.009

Zhang, J. Y., Qian, S. Y., and Baldock, B. (2009). *Laboratory study of corrosion performance of different reinforcing steels for use in concrete structures*. Ottawa, Ontario, Canada: National Research Council Canada. (NRCC).

Živica, V. (2002). Significance and influence of the ambient temperature as a rate factor of steel reinforcement corrosion. *Bull. Mater. Sci.* 25, 375–379. doi:10.1007/bf02708013